Technische Universität München
TUM School of Computation, Information and Technology

User cooperation for resource-efficient URLLC in mesh networks

Tapisha Soni, M.Sc.

Vollständiger Abdruck der von der TUM School of Computation, Information and Technology der Technischen Universität München zur Erlangung einer

Doktorin der Ingenieurwissenschaften (Dr.-Ing.)

genehmigten Dissertation.

Vorsitz: Prof. Dr. Florian Matthes

Prüfer der Dissertation:

1. Prof. Dr.-Ing. habil. Alois C. Knoll
2. Prof. Dr.-Ing. Robert Schober

Die Dissertation wurde am 22. März 2024 bei der Technischen Universität München eingereicht und durch die TUM School of Computation, Information and Technology am 16.01.2025 angenommen.

Abstract

Advanced fifth-generation (5G) wireless networks will play a crucial role in the digitization of factories and connected vehicles, relying on highly reliable communication demanding ultra-reliable low-latency communication (URLLC) services to ensure a defect-free uninterrupted system. In these scenarios, the high density of devices allows independent device-to-device (D2D) communication links via so-called sidelink (SL) that can form densely-populated mesh networks. The reliability of a wireless connection can be improved substantially in a resource-efficient manner if a significant degree of diversity can be exploited. The diversity offered by the D2D links between the user equipments (UEs) in the vicinity can be made available by user cooperation. To this aim, we propose a SL-assisted *Cooperative Retransmission Scheme* called *CoRe*, in which the neighboring UEs assist an error-prone downlink (DL) transmission by retransmitting unsuccessful DL packets to the target UE via SL. The cooperative scheme realized by independently fading D2D links is evaluated firstly using theoretical analysis by link-level evaluation, followed by a system-level evaluation considering two example scenarios: vehicle-to-everything (V2X) communication, where the focus is on road scenarios with wirelessly connected vehicles, and industrial internet-of-things (IoT) communication, where the focus is on factories with devices and controllers connected wirelessly. Analysis has revealed that the attainable gains in outage probability scale up to one order of magnitude per cooperating user. Considering the degradation due to path-loss effects, appropriate user grouping should be applied for the cooperative retransmissions. System-level analysis has indicated a reliable transmission facilitated by our SL-aided retransmissions via D2D links that attains a larger Signal-to-Interference-Noise Ratio (SINR) for the retransmissions, yielding reduced latency thanks to a lower number of required retransmissions. Our evaluations show that CoRe allows saving one retransmission for attaining the URLLC reliability target of 99.999% and significantly reducing the queuing delays compared to the conventional DL retransmissions. Further, we extend the CoRe scheme with an optimal power control (PC) scheme, which gradually increments the power with every retransmission, mainly to keep the power expense low and mitigate interference at the base station (BS). As a result, compelling benefits in terms of low transmit power consumption for SL-assisted retransmissions have been observed. Inspired by this outcome, we propose a novel radio resource management scheme named *Flipped-Underlay* and develop the *Flipped-Underlay Resource Allocation (FURA)* algorithm, realized by underlay communication, which enables communication of both uplink (UL) and SL transmission in the same resource by underlaying the D2D signal for retransmission below the UL signal. While in conventional underlay, a D2D communication with small transmit power is assigned to resources already allocated for UL and thus underlaid, in our scheme, the D2D resources are allocated firstly, and hence we call it *flipped-underlay*. The reuse of resources by the flipped-underlay scheme substantially reduces the total amount of resources the system occupies.

This thesis reveals four-fold gains from the CoRe scheme: (1) showing benefits of diversity by user cooperation using distinct user grouping, (2) a significant reduction in the total number of SL-assisted retransmissions compared to conventional retransmissions via DL while maintaining the desired reliability and latency performance, (3) reduced transmit power consumption thanks to optimal power allocation for retransmissions, and finally yet importantly, (4) improved resource usage efficiency by reuse of resources using flipped-underlay algorithm. Consequently, the results prove the proposed CoRe scheme, with added extensions in terms of PC and resource management, to be an efficient tool to guarantee the quality-of-service (QoS) requirements of URLLC at low costs of resources.

Zusammenfassung

Die fünfte Generation des Mobilfunks (5G) spielt eine entscheidende Rolle bei der drahtlosen Vernetzung zwischen Geräten in Fabriken sowie zwischen Fahrzeugen. Um eine fehlerfreie und unterbrechungsfreie Kommunikation zu gewährleisten, ist eine hochzuverlässige Datenübertragung mit geringer Latenz erforderlich (Ultra reliable low latency communication, URLLC). In den genannten Anwendungsgebieten, also Vernetzung der Industrie sowie von Fahrzeugen, liegt eine hohe Gerätedichte vor, die eine unabhängige Device-to-Device (D2D) Kommunikation über sogenannte sidelinks (SL) erlaubt, wodurch ein hochverdichtetes Mesh-Netzwerk gebildet werden kann. In solch einem Netzwerk, welches die verschiedenen Geräte bilden, besteht eine große Anzahl an Möglichkeiten, wie sich die verschiedenen Geräte miteinander verbinden können. Durch diese Flexibilität kann die Zuverlässigkeit einer drahtlosen Kommunikation ressourcenschonend erheblich verbessert werden. Die Vielfalt an möglichen Links, welche die D2D Verbindungen zwischen den benachbarten Nutzergeräten bietet, kann durch Kooperation zwischen den Nutzern verfügbar gemacht werden. Zu diesem Zweck schlagen wir ein SL-unterstütztes kooperatives Verfahren für die Sendewiederholung vor, welches wir *CoRe (Cooperative Retransmission)* nennen. Hierbei unterstützen die benachbarten Nutzergeräte eine fehleranfälligen Downlink (DL) Übertragung, indem sie fehlerhaft übertragene DL-Pakete zu den Ziel-Nutzergeräten über den SL erneut übertragen. Das kooperative Verfahren, welches auf statistisch unabhängigen D2D Verbindungen basiert, wird zunächst theoretisch analysiert, um zu einer Bewertung auf Link-Ebene zu kommen, gefolgt von einer vollständigen Bewertung auf System-Ebene. Hierbei stehen zwei Szenarien im Fokus: Einerseits die Vernetzung im Straßenverkehr (”vehicle-to-everything - V2X)”, bei welcher Fahrzeuge drahtlos miteinander kommunizieren, und andererseits die Vernetzung in Fabriken (”Industrial Internet of Things - IIoT)”, bei der alle Geräte in einer Fabrik drahtlos miteinander verbunden sind. Die Untersuchung zeigt, dass sich Gewinne in der Ausfallwahrscheinlichkeit von bis zu einer Größenordnung pro zusätzlichem kooperierenden Benutzer erzielen lassen. Bei Berücksichtigung von Pfadverlust-Effekten sollten geeignete Nutzergruppierungen innerhalb der kooperativen Sendewiederholungen angewendet werden. Die Analyse auf Systemebene zeigt, dass eine zuverlässige Übertragung mit Hilfe von D2D Verbindungen zu einem höheren Signal-zu-Interferenz-und-Rausch-Verhältnis bei den Sendewiederholungen führt. Dies verursacht eine geringere Latenz, dank der dadurch reduzierten Zahl an erforderlichen Sendewiederholungen. Unsere Bewertung zeigt, dass CoRe, verglichen mit dem konventionellen Verfahren für Sendewiederholungen im DL, eine Sendewiederholung weniger benötigt, um die für URLLC geforderte Zuverlässigkeit von 99,999% zu erreichen, sowie die Warteschlangen (queuing delays) signifikant

reduziert. Des Weiteren haben wir das CoRe-Verfahren um eine optimale Leistungssteuerung (Power Control - PC) erweitert, welche die Leistung graduell für jede Sendewiederholung erhöht. Hierdurch ist es möglich, den Energieaufwand seitens der Terminals gering zu halten und die Interferenz an der Basisstation zu minimieren. Tatsächlich konnte in unserer Untersuchung mit diesem Verfahren ein deutlich geringerer Energieverbrauch für SL-gestützte Sendewiederholungen beobachtet werden. Inspiriert durch dieses Ergebnis, haben wir ein neuartiges Radioressourcenmanagement-Schema namens *Flipped-Underlay* sowie den *Flipped-Underlay Resource Allocation (FURA)* Algorithmus entwickelt, welcher auf "underlay" Datenübertragung beruht. Der Algorithmus ermöglicht die gleichzeitige Datenübertragung, sowohl von uplink (UL) und SL in derselben Ressource, indem das D2D-Signal dem UL-Signals unterlagert wird. Im konventionellen "underlay"-Verfahren wird ein D2D-Signal mit geringer Sendeleistung einer Ressource zugeordnet, die bereits für ein UL Signal zugeteilt worden ist - das D2D Signal wird also unterlagert. Dahingegen wird in unserem Verfahren die Ressource zuerst der D2D-Verbindung zugeteilt, weswegen wir sie als *flipped-underlay* bezeichnen. Die Wiederverwendung von Ressourcen durch das flipped-underlay-Schema reduziert die vom System benötigten Ressourcen insgesamt erheblich.

Die vorliegende Dissertation zeigt den vierfachen Nutzen des CoRe-Verfahrens: Sie zeigt (1) den Vorteil der Flexibilität durch Nutzerkooperation basierend auf festgelegter Nutzergruppierung, (2) eine signifikante Reduktion der Gesamtanzahl an SL-unterstützten Sendewiederholungen verglichen mit konventionellen Sendewiederholungen im DL unter Beibehaltung der gewünschten Zuverlässigkeit und Latenz, (3) eine reduzierte Übertragungsleistung dank optimaler Leistungssteuerung der D2D-Übertragungen und schließlich (4) eine verbesserte Ressourceneffizienz durch Wiederverwendung von Ressourcen mit Hilfe des FURA Algorithmus. Folglich belegen die Resultate der vorliegenden Dissertation, dass das vorgeschlagene CoRe-Verfahren mit der Erweiterung um Leistungssteuerung und Ressourcenmanagement ein effizientes Tool ist, das die durch URLLC gestellten Anforderungen an die Servicequalität zu geringen Kosten garantieren kann.

Acknowledgement

I would like to express my sincere gratitude to my supervisor Prof. Alois Knoll for his support and guidance during my thesis. I would like to extend my sincere thanks to Prof. Robert Schober, for kindly accepting the role as the advisor and providing valuable feedback. I am deeply indebted to Prof. Florian Matthes, my defense chairman, for his consistent support and encouragement throughout the defense and submission process. Importantly, I am extremely grateful to have been mentored by Dr. Malte Schellmann, his enthusiasm for the topic and expertise in the field have made this an inspiring experience for me. I am thankful to him for his aspiring assistance and collaboration in the past years. I am also thankful to my manager Joseph Eichinger, who provided me with this research opportunity to pursue my interests and excel in the field. It has been a great pleasure working with one of the best research teams at the Huawei Munich Research Center, Germany. This competitive yet friendly work environment has prepared me for the challenges ahead. I would like to thank all my colleagues for the invaluable technical/non-technical discussions. I would also like to acknowledge the Technical University of Munich for the academic exposure to pursue this doctoral project and Huawei Munich Research Center for the financial support.

Getting through my dissertation required more than academic support, I am profoundly thankful to my parents from the bottom of my heart, who set me off on the road to this journey a long time ago and for always having faith in me. The values and resilience they instilled in me have helped me rise as a research professional and more importantly a better human. Special thanks to my brother, Tushar, and my best friend, Madhuri, for keeping me sane throughout this period. Finally, I would like to express my heartfelt thanks to my husband, Dennis, for being there unconditionally every step of the way and for his unwavering encouragement and emotional strength. This achievement would not have been possible without their steadfast support.

Munich, March 22, 2024 *Tapisha Soni*

Contents

1

Introduction

This chapter gives an introduction to the problem statement, motivation, and the research questions addressed in this dissertation. It highlights the key contributions, solution approach, and benefits of the proposed solution.

1.1 Motivation

In the past years, only a few technologies have impacted our civilization as much as wireless technology. Wireless technology revolutionized the way of access to information and communication. It has been gradually impacting different parts of life over decades, and the upcoming generation of wireless technology will drastically influence the way of living. In today's era of technologies, seamless internet connection is no longer limited to mobile communication among humans. An essential need for wireless communication arises from various sectors, such as traffic, autonomous vehicles, industry, healthcare, media, public safety, etc. In these modern digital ecosystems, different components interact, like vehicles in traffic, machines in industrial manufacturing, sensors in smart cities, and medical devices in healthcare [93, 55]. For a seamless functioning of these applications, wireless connectivity is considered essential to ensure rapid and smooth interaction between components. Therefore, wireless technology - being a popular, agile, and innovative field of research, has gained significant attention in both academia and industry. Efforts in research and development have resulted in 5G/5G advanced, the fifth generation of wireless technology [92, 98]. Compared to 4G networks [115], 5G promises a multitude of benefits in terms of a faster and more reliable connection, larger connection density, higher capacity, and larger bandwidth.

The development of 5G and beyond primarily aims to drive global digitization, with substantial benefits as a result. For instance, in traffic, vehicles can be wirelessly connected to other vehicles, networks, pedestrians, and infrastructure (V2X: vehicles-to-everything [70]). The wireless communication of cars with their surrounding will enhance traffic safety, improve traffic efficiency, and ultimately enable autonomous driving [89]. Moreover, in an industrial production line or logistics, the direct connection between machines like automated guided vehicles (AGVs) can enable the exchange of information (IIoT: industrial internet-of-things [104]). The fourth industrial revolution, Industry 4.0, aims at an intelligent, automated, and interconnected production system. This revolutionary development of IIoT will transform today's industry into smart factories [117].

However, to fully harness the benefits of V2X and IIoT, wireless communication must satisfy stringent performance requirements. V2X and IIoT type of applications require an uninterrupted high-speed information exchange for real-time communications among a large number of devices. Most challenging is to achieve the quantitative requirements for transmission reliability and latency defined in the 3GPP standard [92, 98]. Ultra-reliable communication with a reliability of 99.999% within a latency budget of $1-10$ ms is required. The 5G service category that supports these challenging requirements is known as ultra-reliable low-latency communication (URLLC) [92, 84, 88]. In recent years, different methods have been developed to improve reliability and reduce latency. However, many existing solutions that meet URLLC requirements inherently involve a fundamental trade-off between reliability, latency, and throughput, which is further exacerbated by the scarcity of radio resources.

For application scenarios like V2X and IIoT, further challenges arise from the fact that information must be exchanged among many mobile devices simultaneously. In such a densely populated mesh network, larger devices can block the transmission links of other devices and obstruct ongoing URLLC transmissions. This indicates that such mesh networks are error-prone, making the latency-critical reliability requirements particularly challenging for real-time use cases.

Further, when a large number of devices are transmitting simultaneously in such mesh networks, the likelihood of signals from different devices interfering is notably higher. High interference in the network reduces the received signal quality. Several approaches exist to mitigate mutual interference among users [109, 91, 58, 30]. For instance, research has shown that transmit power control (PC) is one of the useful means to alleviate interference in the network [30, 33]. However, it is challenging to minimize the power allocation to users while striking a balance between URLLC quality-of-service (QoS) and power savings.

Furthermore, supporting seamless communication among a large number of devices introduces additional challenges that must be addressed. In mesh networks, simultaneous interaction among the devices is necessary to guarantee an uninterrupted system. However, this concurrent establishment of numerous URLLC transmission links demands more radio resources to fulfill desired URLLC requirements. Due to the scarcity of spectrum resources, communication services that demand higher resource usage incur greater costs for network operators [92]. Thus, radio access technologies aimed at improving resource efficiency have long been of interest to both the wireless industry and researchers [111, 56, 88, 113]. The ultimate goal is to support reliable transmission within the latency budget for numerous transmission links simultaneously in a resource-efficient manner. Several radio resource management techniques have been investigated. However, the need for optimized resource management grows with the increasing demands of new 5G service classes [92].

Motivated by emerging technological opportunities and the growing demand in the industry, we investigate approaches to enable URLLC in mesh networks in this thesis. We chose vehicle-to-everything (V2X) and industrial internet-of-things (IIoT) scenarios as representative use cases of densely populated mesh networks, as they are among the most promising yet highly challenging applications [117, 93].

In particular, our guiding research questions are:

- ***How can reliability be increased and latency reduced simultaneously for URLLC services in highly populated mesh networks?***
- ***How can link diversity be efficiently exploited through user cooperation in a cost-efficient manner to enhance reliability?***
- ***How can transmit power allocation be optimized in densely populated mesh networks to efficiently manage interference among devices?***
- ***How can resource efficiency be enhanced while ensuring ultra-high reliability and low latency for a large number of devices in V2X and IIoT applications?***

1.2 Key Contributions

The objective of this thesis is to facilitate the 5G new service class: ultra-reliable low-latency communication (URLLC), which demands an ultra-high reliability of 99.999% within a latency target of $1-10$ ms for a wirelessly connected automation system in sectors like vehicle-to-everything (V2X) and industrial internet-of-things (IIoT) [92, 117]. Despite the broad research on URLLC, the state-of-the-art schemes fail to provide a comprehensive resource-efficient solution for flawless URLLC applications in error-prone densely populated mesh networks. In this thesis, we present multiple scientific contributions aimed at addressing the research questions outlined in the preceding section.

- **Design of a user cooperation model (*CoRe*) for URLLC:**
  The major challenge is to achieve high reliability of 99.999% within strict latency constraints for a large number of transmission links in a resource-efficient manner. The existing solutions suggest various ways to improve transmission reliability and reduce latency. While many of these promising approaches satisfy URLLC requirements, they are highly resource-intensive and result in the common quality of service (QoS) trade-off among latency, reliability, and throughput.

  To circumvent this challenge of a resource-efficient URLLC network, we develop a new fundamental approach built on the underlying relay concept. In Chapter-3, this novel Cooperative Retransmission model, which we name *CoRe* [96], is introduced and described in detail. The guiding idea of our model is to establish simultaneous retransmissions via device-to-device (D2D) links by selecting the appropriate users in the vicinity and, importantly, using resources efficiently for all consecutive retransmissions. The key mechanism of CoRe is to exploit available users from the surroundings to assist erroneous transmission, which can provide an additional degree of diversity in each retransmission attempt. Conventionally, retransmissions are performed via the original transmission link, for instance, downlink (DL) hybrid automatic repeat request (HARQ) retransmissions, which we use as a benchmark. The main difference from state-of-the-art solutions lies in retransmissions through dynamic selection and grouping of users available in the surrounding, combined with the application of transmit diversity schemes for optimal resource utilization. Unlike the existing approaches, exploiting the users present in the surroundings and using a transmit diversity scheme for retransmission makes CoRe a flexible and resource-efficient solution. Our crucial assumption is that CoRe outperforms traditional DL HARQ retransmissions due to the higher degree of diversity made available by user cooperation.

We evaluate this assumption using analytical methods and realistic system-level evaluations. The analytical results show that the reliability performance improves with every additional user added for cooperation, compared to the conventional single frequency network (SFN) scheme. Benefits of the proposed user cooperation model have been highlighted in terms of URLLC reliability in Rayleigh fading as well as Ricean fading channels. Additionally, system-level simulation results validate the analytical performance, showing that our user cooperation strategy can successfully achieve the URLLC reliability target of 10^{-5}. Further, latency performance for the desired reliability target of 99.999% is evaluated in Chapter-4, using system-level simulation. Our results highlight that the probability for higher latency is reduced by CoRe compared to the traditional DL retransmissions while fulfilling the URLLC target, thanks to the reduction in the number of retransmissions. Using CoRe, the reliability of 99.999% is achieved already after two retransmission attempts instead of three retransmissions, as in the traditional DL HARQ. Hence, one retransmission is saved, eventually reducing the overall system latency. As a result, the URLLC reliability requirement of 10^{-5} within a latency budget of $1-10$ ms can be accomplished by CoRe while improving resource efficiency through the transmit diversity scheme.

To conclude, we design a resource-efficient scheme based on an innovative cooperative retransmission approach, which improves reliability and latency compared to the state-of-the-art benchmark. This is prime for implementing automated wireless systems like connected-cars [70] and connected-factory [117, 104], for which URLLC QoS is mandatory. The contribution of our novel approach may serve the community as an inspiration and catalyze the research for further improvements in URLLC service.

- **Power Saving scheme for the user cooperative model of URLLC:**
  For application scenarios like V2X and IIoT, information needs to be exchanged between a large number of mobile devices. In so-called densely populated networks, interference between the devices is highly likely, which leads to a decline in reliability and an increase in latency, which is crucial for URLLC. Research has indicated the importance of transmit power control (PC) to mitigate interference. Power, one of the most costly resources in wireless communication, makes it essential to moderate the transmit power used by devices. In literature, several power-saving mechanisms have been suggested using the standard DL path-loss measurements [47, 30, 33]. The PC in sidelink (SL) for D2D transmissions based on the SL path-loss measure, has gained more attention recently [72, 60]. However, aiming at efficient power allocation for multiple D2D users in our CoRe model requires further enhancements in the existing PC schemes.

  For investigating the effect of interference and power consumption for CoRe, we use extensive system-level simulations to analyze the impact of PC, focusing on realistic V2X and industrial factory scenarios (Chapter-4 and Chapter-5). Upon examining the state-of-the-art PC schemes based on DL path-loss and SL path-loss measure, we identify the following trade-off: URLLC performance can be achieved at the cost of higher transmit power using DL-based PC or transmit power can be reduced at the expense of URLLC performance using SL-based PC.

To overcome this dilemma, we develop an optimal PC scheme for CoRe that aims to meet the SINR target in error-prone DL transmissions by extending the PC mechanism for single D2D transmissions [110], inspired by [100]. In Chapter-4, our PC scheme is described in detail, along with its performance evaluation. The fundamental idea of the PC approach is to boost the transmit power with each retransmission attempt gradually. Since all the assisting users in CoRe can be located at varying distances from the target user, we consider their individual SL path-loss measurements for PC. The results highlight that, with our PC scheme, the power consumption for retransmissions is substantially reduced when two users (dual-user) cooperate in retransmission. Notably, the URLLC performance is guaranteed while keeping the transmit power consumption to a minimum. Significant power savings of at least 10 dB are achieved with the proposed scheme compared to the traditional DL-based PC scheme.

As a key contribution, our optimal PC methodology for dual-user retransmissions can be validated as a balanced approach that reduces power consumption while meeting URLLC requirements. Thus, our CoRe model for error-prone DL transmissions with the proposed optimal PC allows to mitigate the interference among different user transmissions. This indicates that the optimal PC scheme facilitates reduced power consumption in error-prone mesh networks, representing a core contribution to the advancement of future applications such as connected-cars and connected-factories.

- **Radio Resource management technique using underlay for URLLC user cooperation:**
Scarcity of spectrum resources is a well-known and extensively studied issue that still requires further improvements due to the growing demand for new service classes, particularly URLLC. These highly demanding services require a large number of radio resources to fulfill their QoS requirements: reliability of 99.999% within $1-10$ ms latency. Therefore, the resource utilization in our CoRe model must be efficiently managed to further enhance resource efficiency.

To address the challenge of radio resources scarcity and inspired by the potential for resource sharing enabled by the benefits of our PC mechanism, we propose a new radio resource management scheme, called *Flipped-Underlay* [116], which is presented and evaluated in Chapter-5. Flipped-underlay, as the name implies, is an inverted mechanism that distinguishes it as a unique approach for underlay communication between D2D and UL users. Simply stated, it allows the radio resources allocated to D2D users to be reused by UL transmissions. Existing underlay solutions typically treat D2D users as secondary users [37, 105, 40], making them unsuitable for our CoRe model, where D2D users must be prioritized as they assist the retransmissions. In our flipped-underlay approach, we design a flipped-underlay resource allocation (FURA) algorithm [116] as the central decision-making entity, which opts for resource allocation using underlay and non-underlay (orthogonal) mode.

We analyze resource usage by using system-level simulations for an industrial factory scenario. The flipped-underlay scheme with our proposed FURA algorithm is developed in the NS3 network simulator. Comparative analysis of flipped-underlay to traditional orthogonal resource allocation represents significant resource savings, amounting up to 27%. Hence, additional users can be served with the same number of resources when the flipped-underlay scheme with optimal PC is applied to CoRe. This increases radio resource-efficiency substantially. The coexistence of services can be improved further as more UL users will be capable of serving low-priority services such as enhanced mobile broadband (eMBB). Consequently, the overall system capacity can be profoundly improved, which is crucial for densely populated V2X and IIoT network scenarios.

To conclude, our overall contributions are briefly summarized. A user cooperation model (*CoRe*) is developed that has been proven to facilitate URLLC service in mesh networks, which outperforms state-of-the-art benchmarks as a result of gains in improved reliability and latency with a reduced number of retransmissions. Next, an optimal PC for dual-user CoRe is proposed, which substantially reduces power consumption without compromising quality of service (QoS). Finally, a resource management underlay scheme (*Flipped-underlay*) is implemented, which achieves a notable reduction in overall resource consumption and a corresponding enhancement in system capacity. CoRe, along with its extensions, can be regarded as a comprehensive low-power resource-efficient solution for ultra-reliable and low-latency data transmission.

1.3 Outline of the Thesis

This thesis consists of six chapters in total, including the introduction and conclusion of the thesis. The overall structure of the thesis is presented below in Figure 1.1.

The remainder of this thesis is structured as follows: Chapter-2 demonstrates the related background and the state-of-the-art solutions relevant to this work. In Chapter-3, we propose the design of our novel cooperative retransmission scheme called *CoRe* and the analytical performance evaluation of CoRe for the target reliability of URLLC. The results presented in Chapter-3 are the baseline to highlight the fundamental benefits of CoRe. The performance evaluation of CoRe is further validated for reliability and latency, by system-level simulations using the NS3 network simulator in the forthcoming chapters. In Chapter-4, CoRe is investigated for a realistic V2X communication scenario: user selection and grouping methods for CoRe are studied, and an optimal PC scheme is introduced for CoRe. Thus, inspired by the achievements, we further investigate CoRe and its extensions for industrial factory automation scenarios. With the aim to improve radio resource-efficiency, in Chapter-5, we develop a new radio resource management technique for resource reuse using underlay communication. The proposed resource allocation algorithm is implemented in NS3 and evaluated using system-level simulations. Lastly, Chapter-6 concludes this thesis and presents the main contributions and achievements of this research.

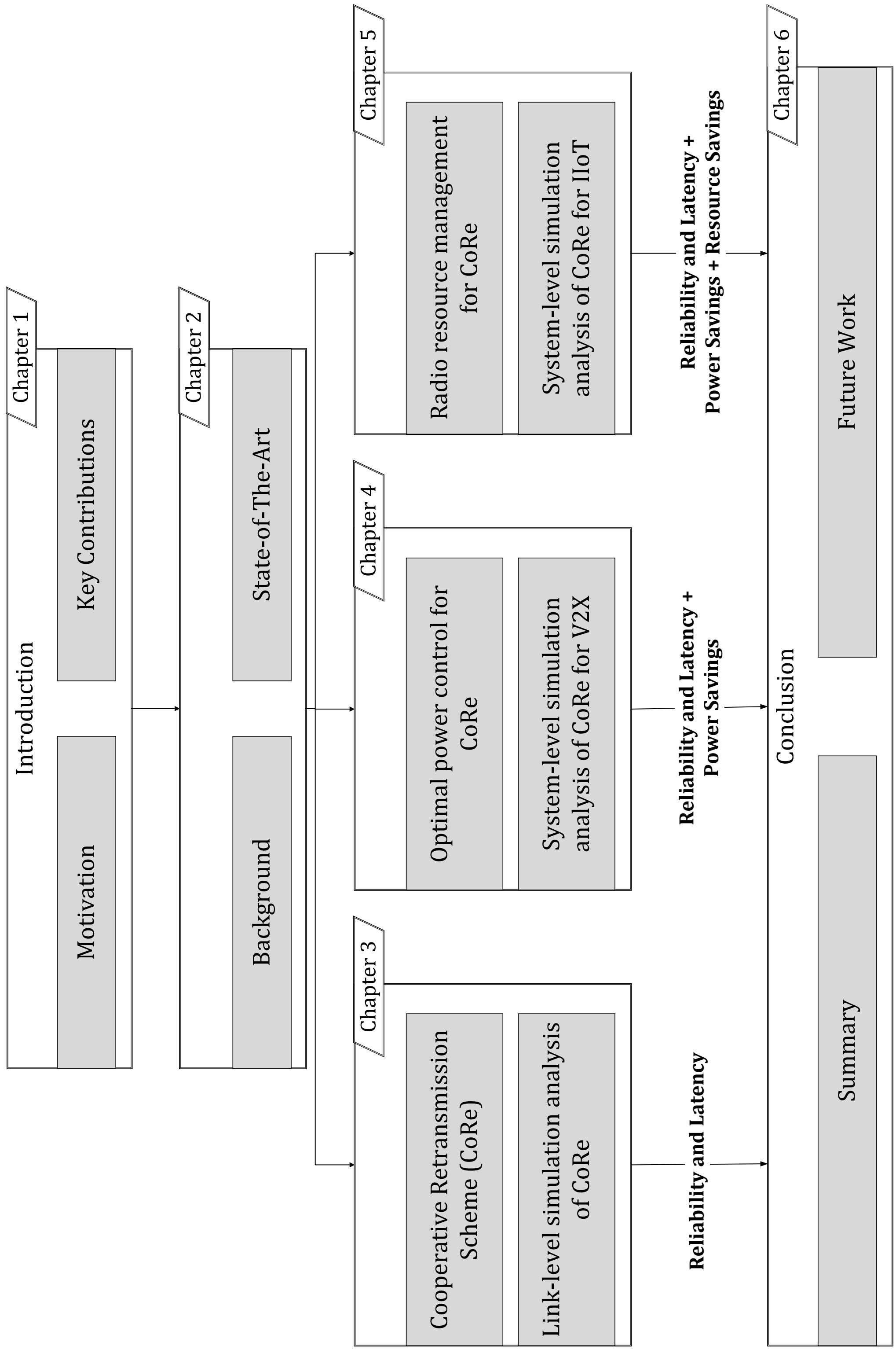

Figure 1.1: Structural overview of the thesis

2

Background and State-of-the-art

This chapter gives an overview of the background and state-of-the-art solutions relevant to the research questions defined in the first chapter. The literature overview highlights 5G key performance indicators (KPIs), requirements and challenges of URLLC, and importantly, potential mechanisms beneficial for accomplishing the URLLC service requirements.

2.1 Services in 5G

The evolution of the 5G New Radio (NR) [52, 84] has broadened the horizon of services that can be supported by wireless communication. It has brought us a set of services with diverse requirements, illustrated in Figure 2.1 [55], representing the 5G services and their use cases. It has been envisioned as a network that will support a diverse set of performance and service requirements and help create connectivity for a wide range of industry verticals such as public safety, e-health, smart cities, automotive, media, manufacturing, etc.

The emergence of rapid technological advances in the contemporary wireless industry led to the establishment of a wide range of critical applications and services that have to be addressed. High-resolution video streaming, massive IoT connectivity, virtual reality (VR), autonomous vehicles, and artificial intelligence (AI) based services are some of these categories. Aiming to facilitate diversified applications, the International Telecommunication Union (ITU) [55] has classified 5G-NR services into three categories: eMBB, URLLC, and mMTC, as stated earlier, highlighted in Figure 2.1.

The most common service type supported by the previous generation of wireless technology, mobile broadband (MBB), needs an upgrade to meet the requirements of eMBB. Applications served by eMBB service demand high data rates, such as ultra-high definition video streaming, augmented reality, and virtual reality. Additionally, one of the main challenges imposed by eMBB is in terms of overall system throughput improvement. Different technologies, such as massive multiple-input multiple-output (MIMO), carrier aggregation, millimeter wave communication, higher order modulation, coding schemes, etc., have been introduced to enhance the system throughput and to improve data rate.

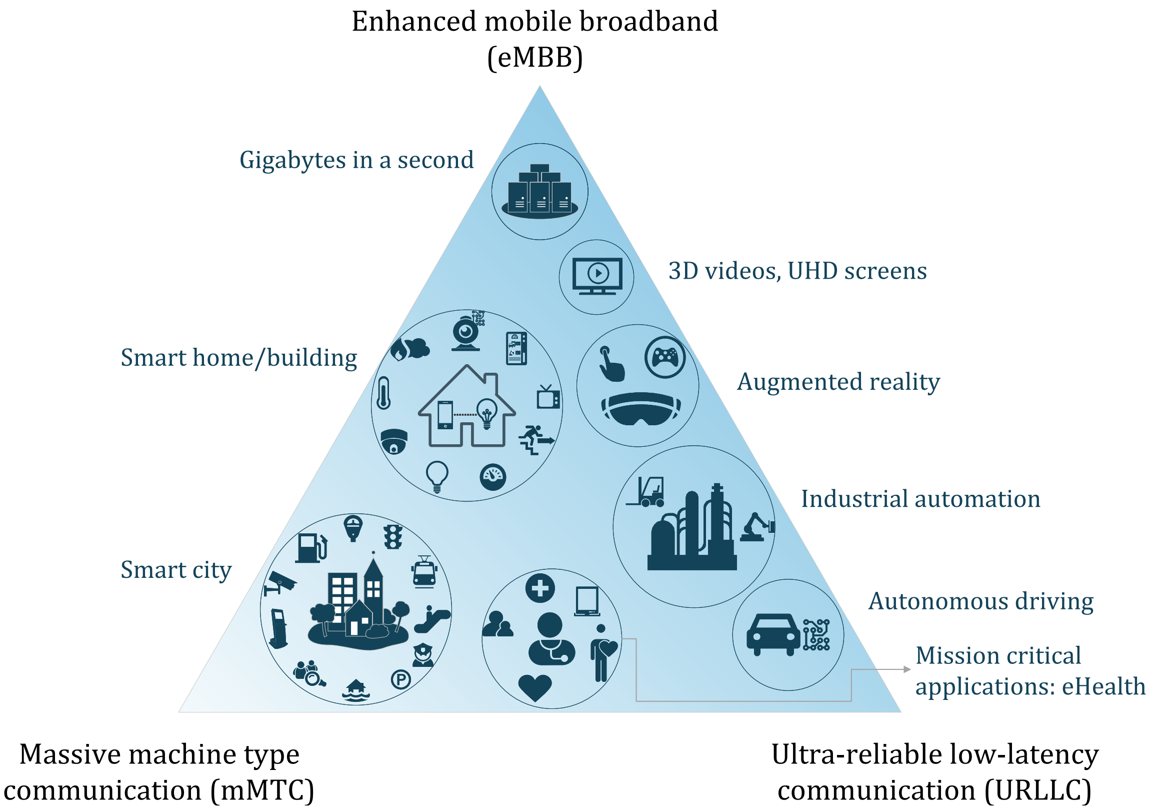

Figure 2.1: 5G Use-cases [55]

mMTC, the new service type, is introduced to support radio access to a large number of machine-type devices. Applications using IoT, such as smart cities, smart agriculture, and smart factories, are expected to be supported by mMTC service. Service requirements of high connection densities, a large volume of data transfers, and energy efficiency are the core of mMTC type of service. Data collection and processing using a massive amount of sensors is the most important aspect of mMTC communications.

The third service category, URLLC, is capable of performing control tasks via the wireless network. It aims to support latency-critical ultra-reliable services such as autonomous driving, mission-critical applications, factory automation, and tactile internet [55]. Since the time it takes for the human reaction is on the order of tens of milliseconds, the packet transmission time for mission-critical applications needs to be on the order of tens to hundreds of microseconds [117]. On the other hand, human perception is extremely fast; therefore, we need tactile internet with delays as low as 1 ms and below. In 4G LTE networks, the latency was significantly improved compared to 3G systems; the end-to-end latency has still been in the range of $10-100$ ms. This is because the backbone network typically uses the best-effort delivery mechanism and hence is not optimized for latency-critical service. To reduce the end-to-end latency, therefore, there should be fundamental changes in both the wireless link and backbone network, which have been introduced with 5G systems.

2.1.1 5G Key Performance Indicators (KPIs)

The development of 5G is targeted to improve the data rates compared to LTE while at the same time supporting diverse applications through radio communication. Figure 2.2 [93] represents the well-known 5G KPIs [54, 52] compared to the existing KPIs defined in the scope of LTE, which have been grouped into three categories coupled with the three 5G service types.

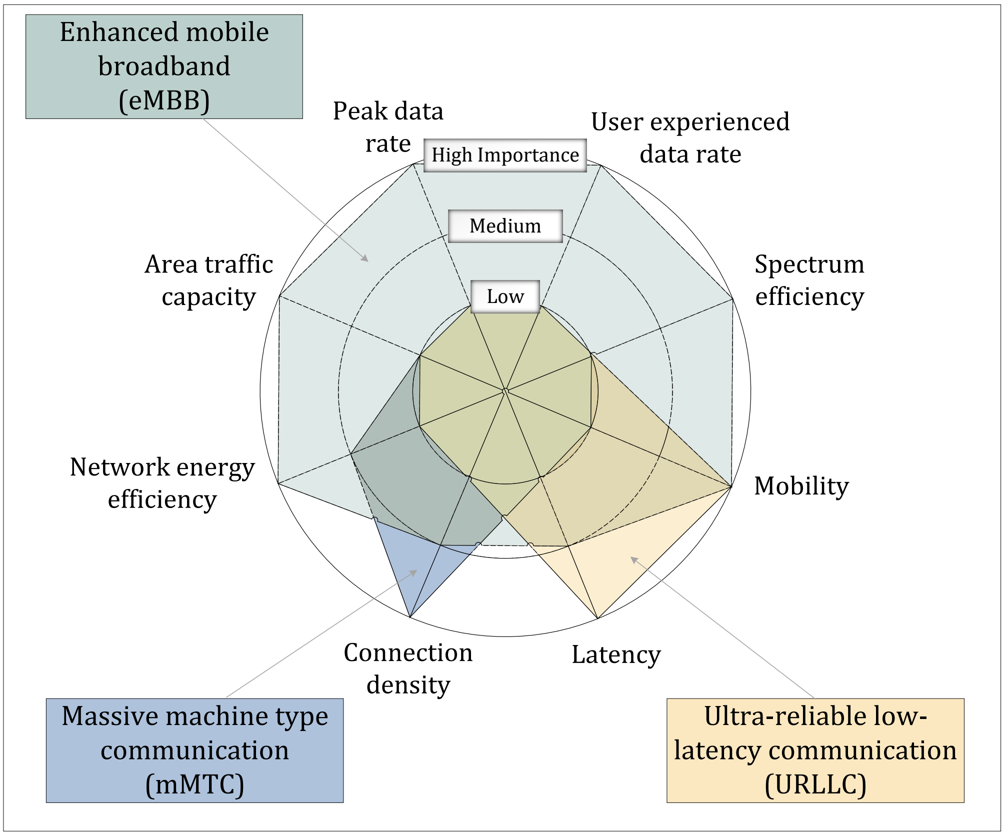

Figure 2.2: 5G Service-based KPIs [55]

The target KPIs for 5G, specified by the ITU [55], are summarized in Figure 2.3 [93]. Considering the eMBB service, a peak data rate of 20 Gbps and 10 Gbps and spectral efficiency of 30 bits/Hz and 15 bits/Hz in DL and UL, respectively, are targeted. Further, a higher network energy efficiency with ten times lower energy consumption and improved connection density by 100 times more connected devices to support mMTC service. Lastly and importantly, mobility as high as 500 Kmph, low latency down to 1 ms, and reliability of orders of magnitude higher are some of the essential performance measures.

Keeping in mind the expectations, there have been major advancements in the physical layer procedures as well as radio access network protocols. Reliability, latency, throughput, and network coverage requirements are distinct for these novel applications and services. In the previous generations of wireless systems, a common network configuration is applied for all the users present in the network. While, with the development of current 5G systems supporting a diverse set of services, one for all configuration leads to either an imbalanced resource consumption or unfulfilled user requirements. Hence, targeting such a diverse set of service demands with efficient bandwidth utilization is one of the pillars of 5G networks.

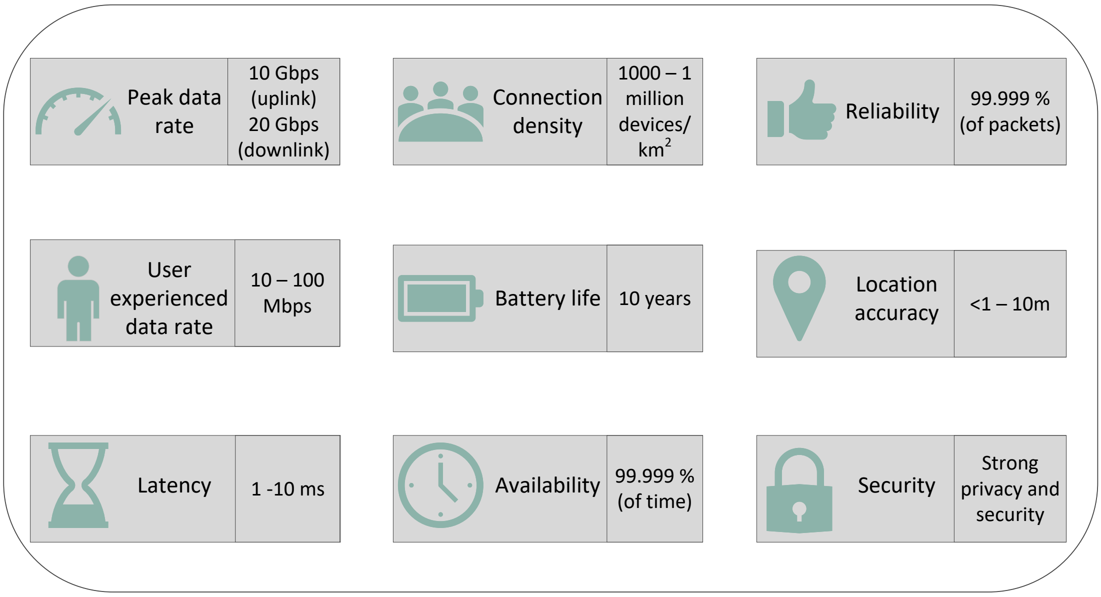

Figure 2.3: 5G Key Performance Indicators (KPIs) according to ITU-R [55] [93]

2.2 Requirements and Challenges of URLLC

URLLC being one of the key services, has emerged to be the most challenging, as higher QoS demands are becoming increasingly important with the widespread use of applications based on the new service types. Unlike the traditional systems, it imposes additional challenges in order to support machine-type communications requiring haptic interactions such as applications for V2X, industrial factory automation, remote control, and tactile internet. In the 3GPP standard, the stringent QoS requirement for URLLC is set to 1 ms latency and reliability of 99.999%, deemed hard to attain for a large number of links with the existing wireless systems due to high system costs. While in practice, applications served by URLLC differ in their QoS requirements, for which the reliability demand can range from 10^{-7} to 10^{-3}, and the latency requirement can range from 0.5 ms to 10 ms [114]. This implies that URLLC service can be tailored for any desired reliability and latency target, which keeps the system costs under control since more stringent constraints come at higher resources and system costs.

2.2.1 Reliability and Latency

How can these stringent QoS requirements for URLLC be attained? Different technologies and solutions have been suggested in the past years considering various factors and target applications for URLLC. Approaches such as transmit/receive diversity schemes, large-scale antenna systems, multi-hop relaying, HARQ transmissions, packet duplication, etc., have been recommended to improve reliability performance. Research suggests boosting antenna diversity in the system as an intuitive yet one of the most effective solutions to improve communication reliability [66, 61]. However, antenna diversity to meet the coverage area of the network comes at a cost and restrictions in terms of the size and design of the antennas. Cooperative communication among different nodes in the network via relays has been widely studied as a means to achieve such ultra-high reliability targets [59].

On the other hand, the end-to-end latency critical requirement means that a packet transmission that cannot be successfully decoded within a deadline is discarded, thus translating to a loss of reliability. Packets are potentially dropped due to erroneous delivery, synchronization failures, or overflowing transmission queues. It consists of different delay components dependent on the communication scenario, such as transmission delay, processing delay, queuing delay, routing delay, and propagation delay. TTI shortening is one of the commonly proposed state-of-the-art solutions in order to reduce the end-to-end transmission delay for URLLC [97, 82], as it reduces the round trip time (RTT) of data transmission. It can be possible to meet the low latency demand by allocating more resources which could reduce the block error rate of transmissions, yet this has a direct unfavorable impact on the system capacity and the spectral efficiency.

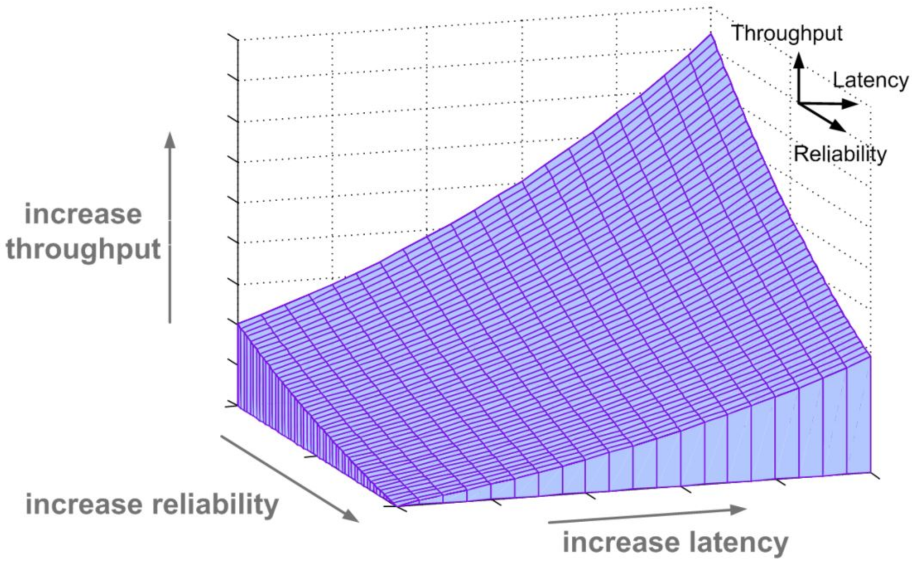

Figure 2.4: Fundamental trade-off between latency, reliability and throughput [53]

Consequently, solutions like these have been manifested to attain performance improvements at the expense of a large number of radio resources [85]. However, radio resources are usually limited; hence, it is vital to strike a balance between resource consumption and performance improvement. The reliability and throughput can be improved by increasing the number of retransmissions or by applying the opportunistic channel-aware scheduling at the cost of higher latency, as illustrated in Figure 2.4 [53]. Thus, due to this common QoS trade-off among latency, reliability, and throughput [53], it is challenging to attain a high reliability and low latency performance simultaneously [52, 108, 85].

2.2.2 Impact on System Design

Keeping in mind the URLLC constraints, the 5G system-level design has been adapted to suit the requirements with a new flexible OFDMA frame structure [71, 54, 77] [111] using flexible numerology [90]. Adaptable numerology allows changing the subcarrier spacing based on demand, and thus the symbol length reduces with an increase in numerology, in turn modifying the slot duration. As stated above, the radio resource format with traditional slot structure, each of 1ms slot duration upgraded to mini-slot level radio resources of 0.125 – 0.250 ms slot duration [68], allows shorter RTT for latency critical services. A flexible frame structure offers the possibility of prioritizing service-dependent performance measures. Unlike traditional eMBB traffic, URLLC traffic is most commonly composed of very small packets generating traffic for machine-to-machine communication, which causes a large signaling overhead leading to low spectrum efficiency. Analytical investigations by Durisi et al. [64] studied the protocols for short packet transmission among a pair of nodes in a broadcast scenario, where they state principles to adapt the wireless system design. Their investigation suggests adjustment in packet length and coding rate to be beneficial to attain high reliability. However, this study does not consider the overhead due to the control information and optimization for resource usage. While another detailed study by Popovski et al. [87] on communication theoretic principles of URLLC covers different aspects of the system design, such as the network topology, access protocols, framing for URLLC small packet size, the failure probability of URLLC transmissions, the channel state information (CSI), and packet header overheads. Additionally, investigations [73] have shown the effect of physical layer waveforms, error correction techniques, convolution codes, and adaptive numerology [90] on URLLC network capacity and reliability.

2.2.3 Role of Retransmission Schemes

Retransmission schemes such as ARQ [3] and HARQ [20] have been well-known to improve communication reliability and spectral efficiency. The ARQ and HARQ mechanisms are presented in Figures 2.5 and 2.6, respectively. As shown in the figures, feedback in the form of Acknowledgment (ACK) and negative acknowledgment (NACK) is sent to the receiver upon unsuccessful reception of the data. In the ARQ scheme, the data packets are discarded until the successful reception of data; for instance, data packets 1 and 3 in Figure 2.5. In contrast, the HARQ scheme stores the unsuccessfully received data packets in a buffer, which are combined with the consecutive retransmissions; as illustrated in Figure 2.6, where data packet 1 is buffered and combined.

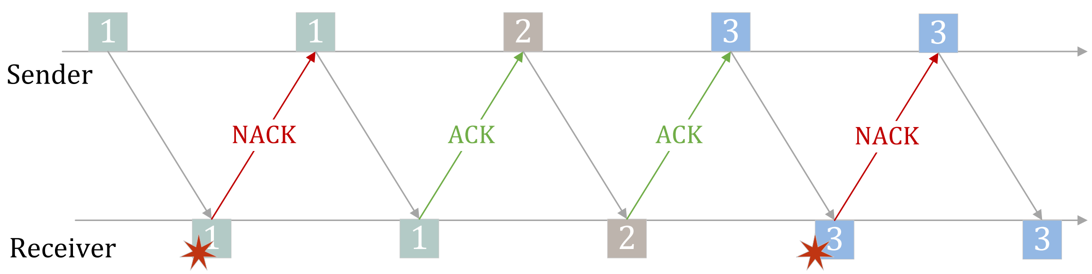

Figure 2.5: Automatic Repeat Request (ARQ) scheme [3]

Authors in [83] show benefits in terms of reliability using ARQ/HARQ at the cost of latency. Thus, indicating that the trade-off between reliability and latency [87] weighs down most of the existing solutions for URLLC type of traffic. Further, the authors in [67] recommend different enhancement aspects to adapt the 5G HARQ protocols, whereas other researchers [74] take into account the support of sidelink in order to enable successful reception of the packets. In [83], the authors propose a hybrid retransmission scheme by studying the NACK-only retransmissions and blind retransmissions, focusing on the trade-off between spectral efficiency and URLLC performance. Further, their study compares incremental redundancy (IR) and chase combining (CC), showing that both soft-combining schemes perform similarly in terms of signal-to-noise ratio (SNR) in a deep-fade scenario. Thus, it can be concluded that CC is preferable due to its simplicity and implementation compared to IR soft combining. The line of work [57] on HARQ design and optimization for ultra-reliable communication studies the effectiveness of spatial diversity and HARQ transmissions. They conclude that gains in link quality are obtained by spatial diversity, while the efficiency of radio resource utilization is improved by the HARQ method.

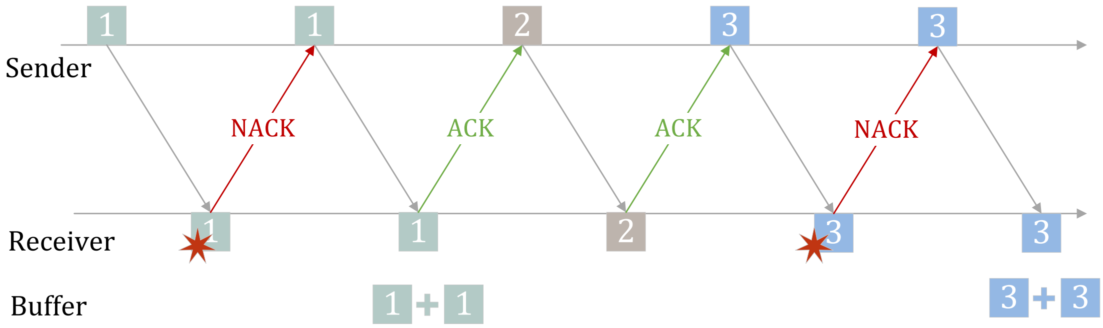

Figure 2.6: Hybrid Automatic Repeat Request (ARQ) scheme [20]

2.2.4 Multiplexing Services with URLLC

Further, multiplexing other services with URLLC has been gaining attention recently to support diverse services in a resource-efficient manner [81, 112]. Most commonly applied to the two critical and highly demanded services, i.e., eMBB and URLLC [95]. Authors in [9] highlight different resource sharing methods among URLLC and other service types. In contrast to URLLC QoS constraint of high reliability and low latency, eMBB services demand higher data rates [97, 111]. The coexistence of eMBB and URLLC services is addressed in recent literature. The resource allocation of both services simultaneously is very challenging due to their QoS trade-off. To this aim, studies addressing multiplexing of URLLC and eMBB traffic recommend the superimposition of eMBB traffic and shared wideband resource allocation for both service types in comparison to dedicated service-based resource allocation [77, 82]. Prioritization helps further enhance the service-based performance, especially for URLLC service, which can be allowed to preempt an ongoing eMBB transmission. Several research articles focus on physical layer aspects, such as link adaptation, modulation and coding schemes, and fading analysis, to improve the system design for URLLC traffic [64, 62, 69].

Further, in order to facilitate flexibility for different service types, slicing is one of the most imminent technologies of 5G, where one physical network is split into multiple logical networks called slices. There has been tremendous research on slicing and different technologies, such as network function virtualization (NFV), software-defined networks (SDN), and cloud computing, to support slicing. However, it still brings us to the usual yet essential concern of scarcity of resources to fulfill the QoS requirements using these advanced technologies.

At the same time, the common solution approaches can be trivial for URLLC, given the scarcity of spectrum resources for wireless communications. Given that URLLC is resource-expensive, demand for a large number of URLLC connections is likely to become incredibly expensive. Due to stringent QoS requirements, the resource allocation for URLLC is inevitably conservative, and hence the bandwidth usage efficiency for URLLC must be handled carefully.

2.3 Diversity Schemes

As the name suggests, diversity means the transmission of redundant signals over independent channel realizations with relevant combining at the receiver. It can be attained via different domains, such as time, frequency, and space. Time diversity and frequency diversity benefit at the cost of transmission delay and bandwidth, respectively. Whereas spatial diversity has proved to be one of the most prominent diversity schemes for achieving high data rates using multiple transmit and receiver antennas. However, utilizing diversity for reliability improvements always translates to a rate loss since additional resources in time/frequency/space are used for transmitting a single message.

2.3.1 Spatial Diversity in point-to-point MIMO

One of the renowned techniques in wireless communication standards, multiple input multiple output (MIMO) using multiple antennas, has been shown to increase the system capacity [5, 6]. Maximum diversity of M*N can be obtained, assuming Rayleigh distributed fading coefficients for M transmit antennas and N receive antennas. MIMO has been extensively researched and applied in different solutions to improve wireless systems by providing gains in reliability using diversity or rate improvement via spatial multiplexing. The diversity gains scale in proportion to the number of transmit and receive antennas [17]. However, it is crucial to install, such a large number of antennas at the UEs, unlike the BS, given the space limitations. Hence, the solution to overcome this limitation has brought us to cooperative diversity [11, 16]: the benefits of transmit/receive antenna diversity can be attained similarly by exploiting the nodes present in the network, especially when considering scenarios like indoor factory automation or V2X.

2.3.2 Cooperative Diversity (Distributed MIMO)

The groundbreaking research by van der Meulen [2] introduced the concept of cooperative communication via a relay channel. A broadcast transmission is considered, which can be overheard by other nodes in the network. The simplest relay channel model consists of three nodes: source, destination, and relay, where the relay channel can assist transmission from the source to the destination only via a single relay. Following this innovation, extensive investigation by Cover and Gamal [4] and Laneman et al. [11, 16] on the relay channel model (refer Figure 2.7) led to the discovery of principal relaying protocols such as Decode and Forward (DF), Amplify and Forward (AF) [15], Estimate and Forward (EF), and Compress and Forward (CF), called as repetition based cooperative diversity algorithms. DF relay technique detects and decodes the signal data and re-encodes the data, which is then transmitted to the destination node. Whereas EF relaying works essentially similar to DF relaying but differs in the coding procedure, where the relay can estimate the decoding outcome by measuring the received SNR. In CF relaying, the data is decoded, and then a compressed version of the observation by the source is forwarded to the destination. Furthermore, Lanemann et al. [15, 16] proposed the AF technique based on amplified repeaters [9], suitable for relays with low computation power, where the received data is only amplified without decoding at the relay before transmitting it to the destination. Although AF relaying can attain high data rates, it comes with certain drawbacks in terms of noise amplification, latency, and scalability to larger networks [21, 13, 19].

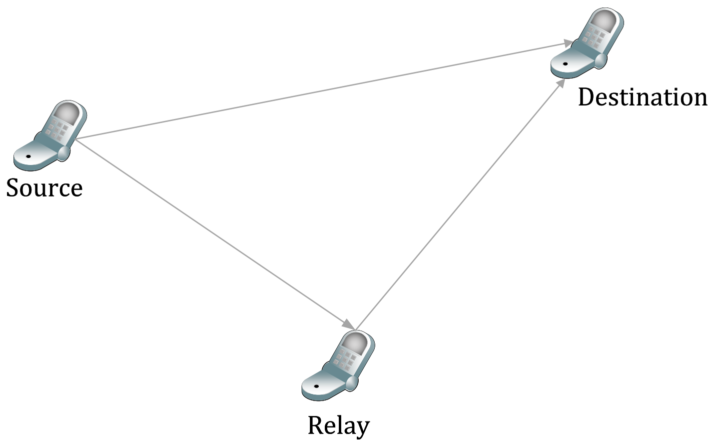

Figure 2.7: Fundamental relaying mechanism [2]

The repetition-based cooperative techniques stated above, where the relays transmit data on orthogonal subchannels, cost excess resources to realize the diversity gains. While the well-known distributed space-time block codes (STBC) were originally introduced by Laneman and Wornell [15] as a bandwidth-efficient solution designed based on space-time codes to enable simultaneous transmission on the same subchannel by multiple relays. Initially, the scheme targeted networks with a large number of single antenna relays, assuming frequency non-selective channels with negligible Doppler spread [27]. It was further extended for a realistic environment with mobility rendering frequency-selective and time-varying channels, resulting in a combination of STBC and OFDM [12], as the infamous OFDM technique can convert the frequency-selective channel into multiple flat-fading subchannels. The STBC-OFDM codes the data symbols over multiple space and time periods considering the channels remain constant over certain symbol periods (depending on the space-time coded matrix) [16, 27, 12, 48]. In orthogonal STBCs, each relay transmits using a different column of the STBC matrix, with N_c as the total number of columns. Assuming the total number of relays N to be active nodes, a full diversity order of $d = N$ can be achieved if $N < N_c$ for $N_c >= 2$. Thus, it is very critical to maintain these gains for networks with a large number of relays such that $N > N_c$, since each node cannot be assigned a unique column of the STBC matrix; hence, the overlap degrades the diversity order. In contrast to the orthogonal STBC, which requires channel estimation, a differential distributed STBC scheme was proposed [18], which has been shown to gain full diversity for $N = 2$ relay nodes without requiring channel estimation.

Inspired by those findings, diversity via relaying has been extensively researched, leading to a wide range of solutions. Cooperative relaying has been deeply studied in the past decades focusing on measures such as relay selection, energy efficiency, fading channels, and different types of wireless systems. The exploitation of link diversity and its impact on communication reliability has been analytically investigated in [31], highlighting a fundamental improvement in the efficiency of resource usage. The research work in [49] aims at multi-hop AF networks over generalized fading channels. They propose expressions for outage probability and symbol-error rate when selection combining or maximal ratio combining (MRC) is applied at the receiver. Additionally, they also derive the cumulative density function of the SNRs at the MRC receiver. Similarly, authors in [44] study the dual-hop relaying system employed with MRC and provide closed-form expressions for outage probability and symbol-error rate, while the selected relay performs fixed gain forwarding by performing only fixed amplification to the received signal. Cooperative relay has been proven to perform better in terms of sample-error-rate on the order of relays than single relay [103] for AF system in Nakagami-m and Rayleigh fading environments.

Relay selection is essential to the efficient functioning of the cooperative transmissions, as additional relays increase the complexity of the system. Selection schemes for DF, such as opportunistic relaying [24], where a single best relay is selected with the strongest source-relay-destination path among several potential relays in a distributed fashion using instantaneous channel measurements, and selection-cooperation [23], which restricts relaying to only one node per source based on the best relay-destination channel, have been proposed. This selection-cooperation scheme has been shown to outperform the distributed STBC at the cost of some detrimental effect on overall throughput due to the additional overhead in relay selection. Considering mobility in wireless networks, authors in [22] studied a HARQ-based intra-cluster geographic relaying, i.e., HARQ with opportunistic relaying, where the relays content to take part in the HARQ transmissions. Here, they show improvements in throughput and indicate that the selection of relay nodes based on the average SNR measure is more effective than the instantaneous SNR measure. Another study [29] proposed a scheme in which the source node is considered as well in the relay selection, called incremental transmission relay selection highlighting gains in diversity-multiplexing trade-off. An incremental transmission scheme with relay selection applicable to AF or DF has been derived by Tannious and Nosratinia [34], where the relay retransmits the packet to the source while the protocol is limited to a maximum of one retransmission. Their scheme enables a feedback loop from the destination node to validate the need for cooperation, assuming perfect channel state information (CSI) at the nodes. Individually each node evaluates its own eligibility based on the decision threshold and supports cooperation if applicable.

Along with the benefits of cooperative relaying systems, such systems can impose additional challenges as well in terms of complex schedulers, increased interference, increased overhead in designing coding matrix, and higher end-to-end latency if multi-hop relays are considered, if not designed crucially and maintained well.

3

Cooperative Retransmission (CoRe) Model: Concept and Link-level Analysis

Facilitating URLLC service simultaneously for a massive number of transmission links demands a robust mechanism. Given the challenges of high reliability and low latency, this chapter describes the fundamental solution for enabling a resource-efficient URLLC provisioning, thereby supporting a high number of links. First, we present the concept and design of our Cooperative Retransmission Scheme (CoRe) and its fundamental principles. Further, CoRe is theoretically analyzed, and the respective findings are discussed.

We consider densely populated scenarios where the devices, such as vehicles in V2X or AGVs in a factory, are usually mobile. In this thesis, such devices present in various use cases are generalized as smart devices/nodes/users. Given the high user density, it is likely that some of the larger devices can become obstacles to other devices. This is one of the most common causes of interruption in data transmission in such scenarios.

We illustrate this problem in Figure 3.1, representing a snapshot of a single-cell from a multi-cell network for URLLC communication. In this network scenario, a cell consists of a base station (BS) and different smart devices connected to the BS and the neighboring devices. In our example, the target device named *Node-A* is the device of interest. It is surrounded by other neighbor devices, to which it communicates through D2D transmission via the sidelink (SL). We examine a downlink URLLC multicast transmission from the BS to the target device (Node-A). The nature of multicast transmissions allows all the devices in the vicinity to overhear the packet transmission intended for Node-A. The figure shows that an obstacle between the BS and Node-A blocks the downlink transmission. Similarly, different URLLC transmissions can be interrupted simultaneously due to other larger mobile devices, e.g., a bypassing trailer on a highway or a larger AGV in the factory. Such obstruction may cause link failure and loss of data, which can be critical for a URLLC service, primarily to fulfill the high-reliability requirement within a short latency budget. Therefore, we focus in particular on this service interruption problem when the URLLC service is likely to be disturbed due to the transmission link blockage.

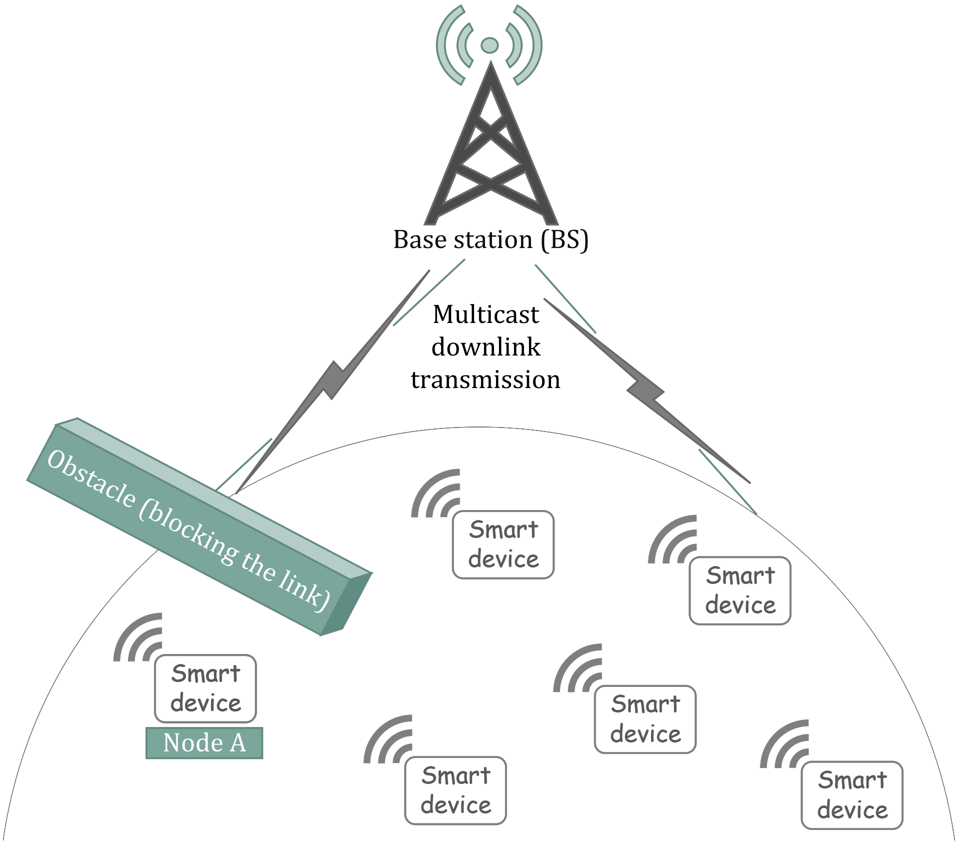

Figure 3.1: Sidelink (SL)-assisted cooperative retransmissions

3.1 Sidelink-assisted Cooperative Retransmission Scheme (CoRe)

As exemplified above, one of the main challenges arises when the URLLC transmission link is obstructed, which causes a loss of URLLC data packets. To resolve this issue, considering the quality of service (QoS) demands of URLLC, we design and implement a unique Cooperative Retransmission Scheme called *CoRe*, inspired by the study on SL-assisted retransmissions [74]. The objective of CoRe is to achieve the stringent reliability of 99.999% and latency of $1-10$ ms at the minimum cost of resources.

Our fundamental CoRe scheme consists of two stages, which are instantiated in Figure 3.2. When the target device (Node-A) experiences a link failure leading to unsuccessful reception of the URLLC packet from the BS, a retransmission request is triggered (stage-I: Retransmission request). In this stage, shown in the top part of Figure 3.2, Node-A sends a request to its neighbors, asking for their assistance. Next, after receiving the retransmission request, retransmission is carried out by different neighbor users (stage II), shown in the bottom part of Figure 3.2)).

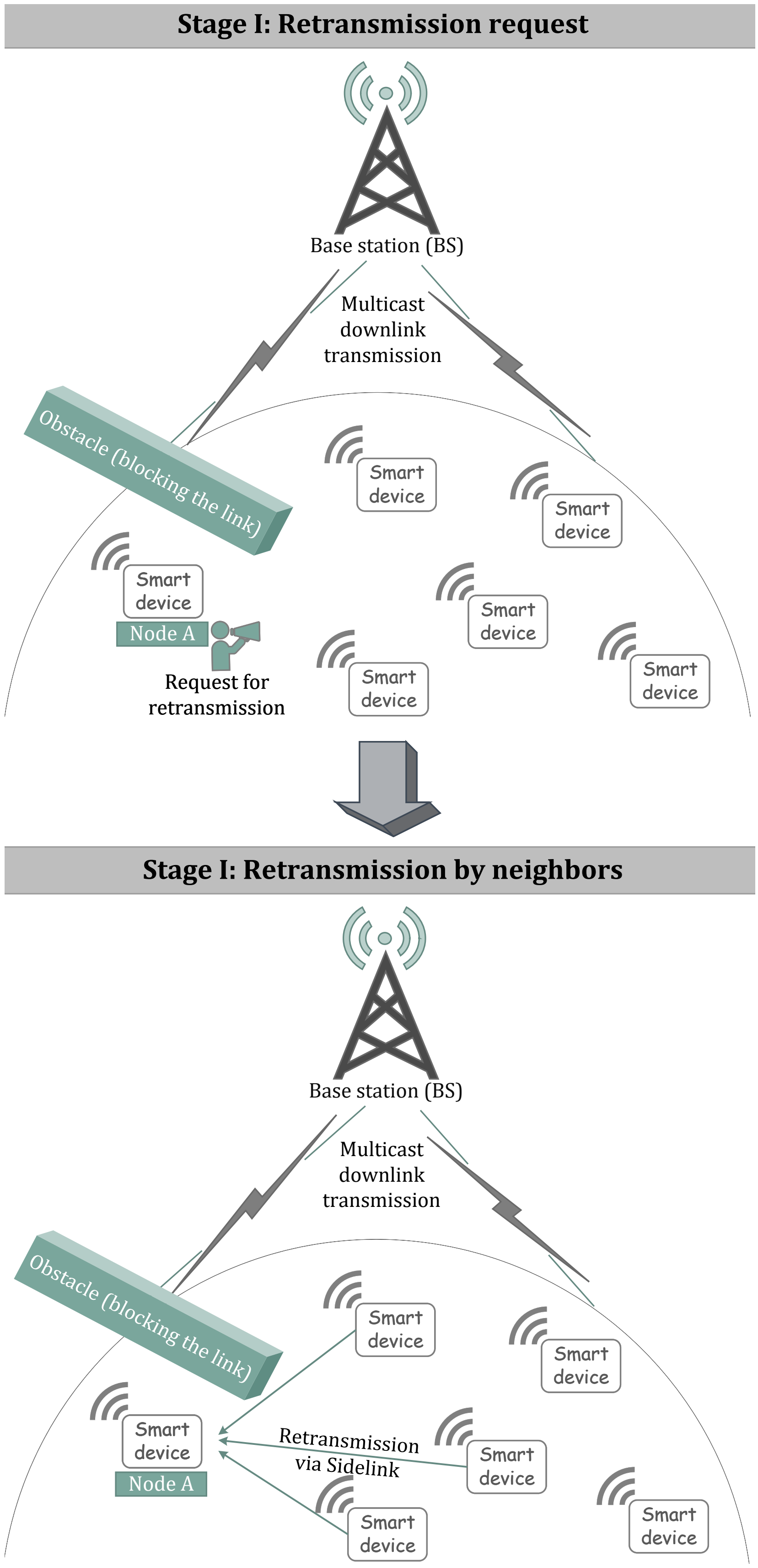

Figure 3.2: Sidelink (SL)-assisted cooperative retransmissions (CoRe) fundamental mechanism

In this thesis, *Cooperation* in CoRe means multiple users transmit the same signal simultaneously using the same resource to assist a neighbor. These device-to-device (D2D) links between the neighbors and Node-A are assumed to be independently fading. Aiming for a resource-efficient solution for URLLC, we enable the retransmissions via these D2D links using transmit diversity schemes [7] in a distributed fashion, exemplified below in Section 3.1.2.

Neighbor users in a predefined group containing all eligible users for retransmissions can be the potential assisting nodes to support Node-A. The user eligibility depends on the successful reception of the DL multicast packet by the neighbor users themselves. This implies that the neighbor users can only assist the URLLC transmission to Node-A if they have successfully received the original downlink transmission from the BS. To enable neighbor users to overhear URLLC data communication, it is necessary that the BS transmits URLLC packets in a multicast fashion to the whole group of neighbor users (including Node-A). If the neighbor nodes have overheard the URLLC packets dedicated to Node-A, they can support the downlink URLLC transmission by retransmitting those packets via the sidelink to Node-A. We call these neighbors that participate in retransmission assisting nodes/assisting users. Since mesh networks can be formed in scenarios such as industrial automation or V2X, which are densely populated by devices, at least a few neighbors can be expected to receive the DL packet successfully. A complete synchronization among the users present in the proximity is assumed for the CoRe scheme, while the users are aware of their neighbors that can support the transmission.

3.1.1 CoRe Scheme: Group-based HARQ retransmissions

We extend the baseline SL-assisted CoRe presented above to a group-based CoRe scheme, demonstrated in Figure 3.3, to realize maximum gains from user diversity. Considering the problem of disrupted URLLC link to Node-A elaborated above (Figure 3.1), followed by an unsuccessful reception from the BS, the target device (Node-A) requests a retransmission to its neighbors in stage-I of baseline CoRe (Figure 3.2). In order to exploit diversity gains to the fullest and if the delay budget allows, we allow more than one retransmission by the assisting nodes. We enable the selection of different user groups for consecutive retransmissions in our CoRe model.

We illustrate the CoRe scheme with group-based enhancement considering two (dual) consecutive retransmissions in Figure 3.3. Stage-II of baseline CoRe is divided into two substages to realize the group retransmissions, as demonstrated in Figure 3.3. Two distinct user groups are selected from the set of eligible users for retransmissions. In Stage II-A, the first group (group 1), consisting of assisting node-1 and assisting node-2, retransmits the same packet to Node-A in the first time-slot. While the first group retransmits, the other neighbor users can overhear this first retransmission to Node-A. This increases the probability of successful reception by users in the second group (group 2). Next, in Stage II-B, the second group consisting of assisting node-3 and assisting node-4 retransmits the same packet to Node-A in the next time slot.

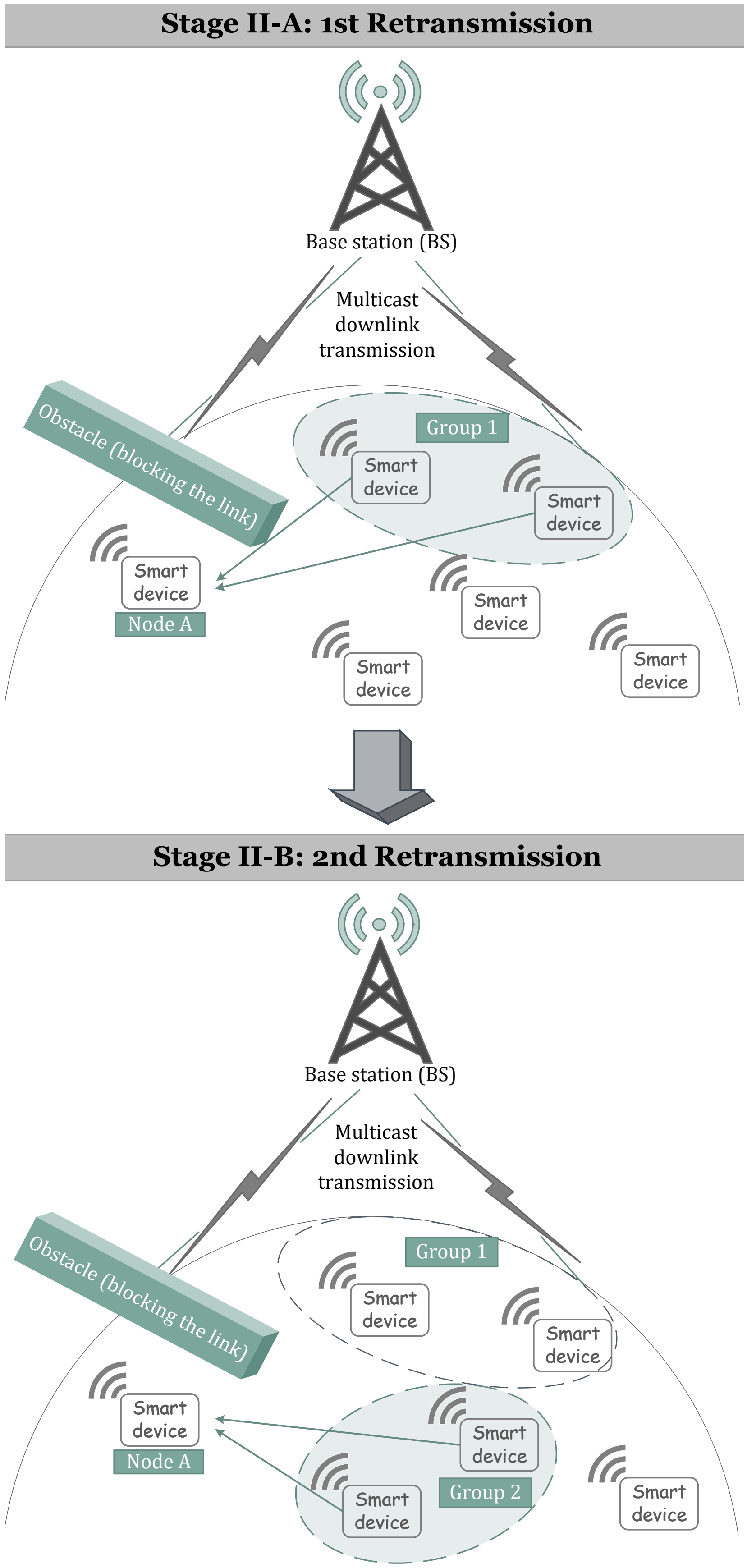

Figure 3.3: Sidelink (SL)-assisted cooperative retransmissions (CoRe): Group-based cooperative retransmissions

We apply the Chase Combining (CC) HARQ scheme [25, 20] to the dual retransmissions of group-based CoRe. It enables the two groups of assisting nodes to send the same coded information in different retransmission attempts without decoding and re-encoding the original data packet, supporting the tight delay constraint. Unlike the incremental redundancy HARQ scheme [25], CC HARQ receives duplicate data packets in different retransmission attempts. At the receiver, all received packets are combined using the maximum ratio combining (MRC) technique described in detail in the next section.

All the users present in a mesh network are directly connected to each other via sidelink, thus enabling them to exchange information without the BS. The elementary aim of CoRe is to exploit these multiple D2D links present in the network to support a downlink transmission from the BS. As the literature research has shown the promising benefits of diversity in wireless systems, we benefit from these large number of nodes present in scenarios that can form mesh networks. As stated above, gains from multiple neighbor nodes are realized by the transmit diversity schemes explained in detail in the following.

3.1.2 Transmit Diversity Scheme and Combining for CoRe

Transmit diversity schemes, such as distributed space-time block codes (STBC) [15, 27] or cyclic delay diversity (CDD) [10], enable a constructive addition of the same signal propagated via different paths. Figure 3.4 shows the STBC coding matrix on the left, with rows as time slots and columns as transmit antennas. The entries of the matrix s_{ij} represent the modulated symbol for i^{th} time slot and j^{th} transmit antenna, for T total time slots. Each column of the STBC matrix provides an orthogonal coding sequence.

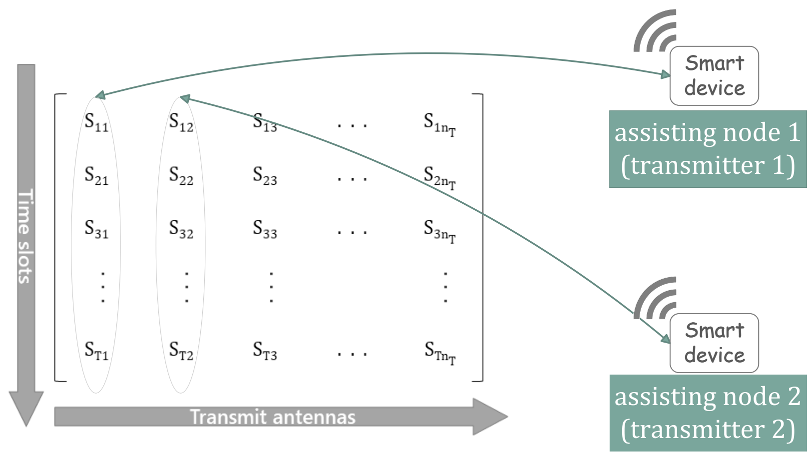

Figure 3.4: Mapping of Space-time block code (STBC) matrix to assisting nodes of CoRe

As described above, our CoRe model uses multiple neighbor users simultaneously to assist a downlink transmission. To enable cooperation in CoRe in a resource-efficient manner, we apply the transmit diversity scheme - STBC, to retransmissions in stage II (Figure 3.2). All neighbor nodes which cooperatively retransmit are allocated one column each of the STBC coding matrix. Thus, each assisting node uses a unique coding sequence for encoding the data in space and time. This allows the transmission by multiple assisting nodes via different D2D paths simultaneously in the same resource. Since each of these D2D links experiences different small-scale fading and shadow fading caused by bypassing larger mobile devices, the constructively added signal at the receiver benefits from the diversity of these independent channels.

The design complexity of the STBC matrix increases with an increase in the order of STBC. It is critical to attain full diversity gains without sacrificing the data rate for higher-order STBC. The only orthogonal STBC that does not come at an effective rate loss is the famous case of STBC called Alamouti's code [7]. It has been proven to be a rate-1 code and is valid only for two transmit antennas. The Alamouti coding matrix adapted for CoRe is as follows given by Figure 3.5 ($*$ denotes the complex conjugate).

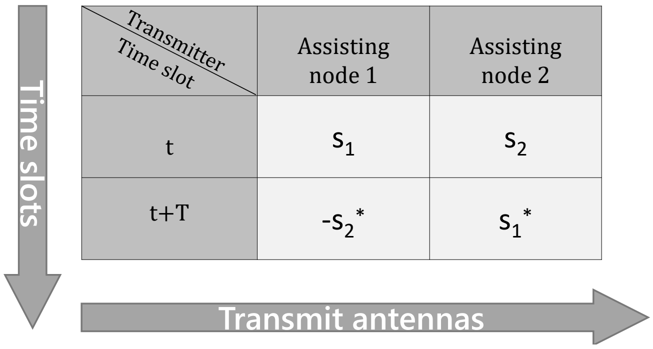

Figure 3.5: Alamouti Space-time block code (STBC) coding matrix for CoRe (reproduced from [7])

STBC Combining for CoRe

The well-known combining scheme for STBC is applied at the receiver [7, 48, 12]. This combining aims to benefit from the diversity gain and thus maximizes the SNR of the combined received signal. Figure 3.6 represents the STBC for two-branch transmit diversity with one receiver for our CoRe scheme; the two assisting nodes (assisting node-1 and assisting node-2) transmit the same signal simultaneously to Node-A using STBC.

As depicted in Figure 3.6, the signal transmitted from assisting node-1 is denoted by s_1 and from assisting node-2 by s_2. The channel between the assisting node-1 and the target device (Node-A) is denoted by h_1, and between assisting node-2 and the target device (Node-A) is denoted by h_2, modeled by a complex multiplicative distortion. Assuming constant fading across the two time-slots, the channel is expressed as

$$\begin{aligned} h_1(t) = h_1(t+T) &= h_1 = \alpha_1 e^{j\theta_1} \\ h_2(t) = h_2(t+T) &= h_2 = \alpha_2 e^{j\theta_2} \end{aligned} \tag{3.1}$$

Noise and interference as the complex random variables, n_1 and n_2, are added for the reception in two successive time slots. Using the STBC coding sequence from Figure 3.5, the received signals y_1 and y_2 at time t and $t+T$ are given by,

$$\begin{aligned} y_1 &= h_1 s_1 + h_2 s_2 + n_1 \\ y_2 &= -h_1 s_2^* + h_2 s_1^* + n_2 \end{aligned} \tag{3.2}$$

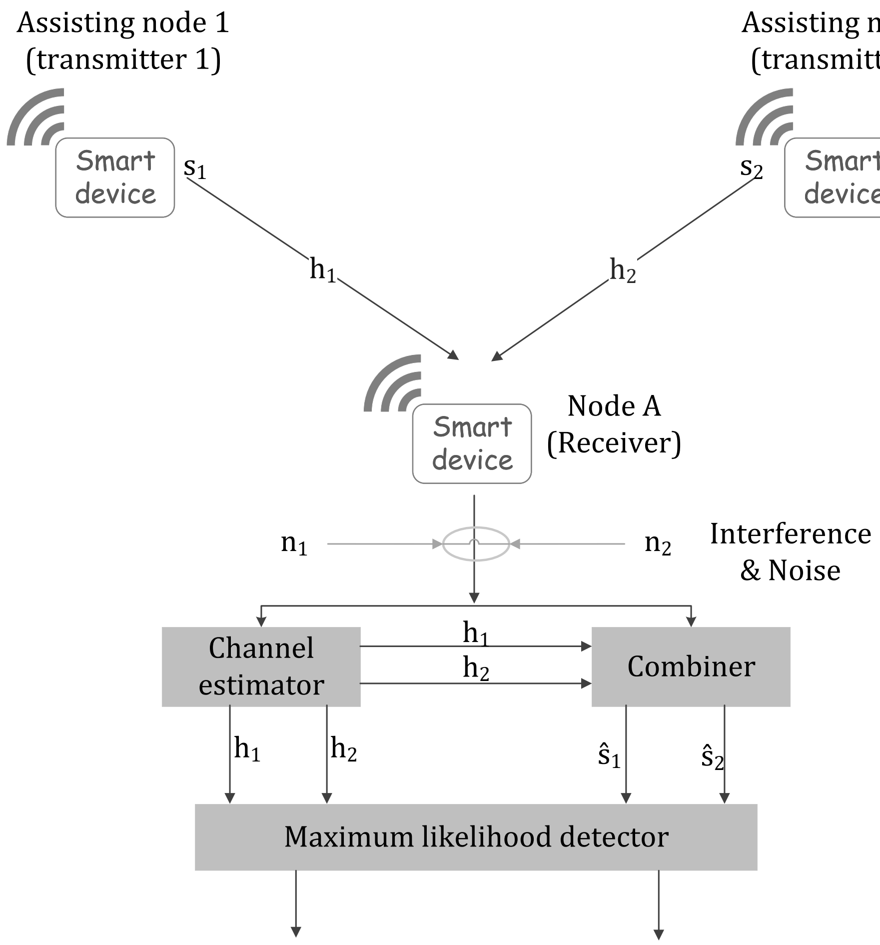

Figure 3.6: Distributed transmit diversity scheme applied to CoRe

The combiner shown in Figure 3.6, generates the following two combined signals.

$$\begin{aligned} \hat{s}_1 &= h_1^* y_1 + h_2 y_2^* \\ \hat{s}_2 &= h_2^* y_1 - h_1 y_2^* \end{aligned} \tag{3.3}$$

The combined signals using Eq. (3.1) and (3.2) can be written as

$$\begin{aligned} \hat{s}_1 &= (\alpha_1^2 + \alpha_2^2)s_1 + h_1^* n_1 + h_2 n_2^* \\ \hat{s}_2 &= (\alpha_1^2 + \alpha_2^2)s_2 - h_1^* n_2^* + h_2^* n_1 \end{aligned} \tag{3.4}$$

These combined signals $\hat{s}_1$ and $\hat{s}_2$ are then sent to the maximum likelihood detector. Although the combining scheme is different from the standard Maximum Ratio Combining (MRC), the combined signal from the resulting diversity order from two transmit antennas is equivalent to the MRC scheme. Thus, the CoRe scheme enables a constructive addition of the powers of the channel coefficients from all these individual D2D links of the assisting nodes, as enabled by the STBC combining at the receiver (Node-A).

3.2 Analytical Evaluation

At first, we evaluate the performance of the SL-assisted CoRe scheme using analytical methods. To validate the fundamental idea of CoRe, it is essential to study the impact of diversity when a different number of users from the neighborhood transmit simultaneously. We analyze the reliability gains in the form of channel outage by several neighbor users cooperatively transmitting the packet via D2D channel (SL). In realistic scenarios such as an industrial factory or V2X, the users will likely experience direct line-of-sight (LOS) paths to other users in close vicinity. However, due to the continuous movement of devices in these scenarios, it is probable that other moving devices can block the direct LOS paths. Therefore, we perform the initial investigation considering two cases: D2D channels of the assisting users modeled as Rayleigh fading [14, 28], where no direct LOS path exists, and D2D channels of the assisting users modeled as Ricean fading channels [8], where the direct LOS component is the dominant path.

The investigation on SL-assisted retransmission by a single relay node [74] shows the impact on system reliability and latency, characterized in terms of the block error rate and the number of required retransmissions, respectively. Taking this work as the baseline, we have reused parts of its analytical framework to investigate our resource-efficient CoRe scheme for mesh networks containing many nodes, aiming at high reliability that we measure in terms of the outage probability. In particular, we analyze the impact of the number of cooperating users (UEs) on the communication reliability attainable in a 5G-URLLC network and the further improvement yield by additional retransmission based on HARQ/ARQ schemes. For the analysis, we assume that the diversity gains from different D2D links can be made fully available, realized by distributed transmit diversity schemes [15, 27, 10], as explained in the previous section.

3.2.1 D2D Channels Modeled as Rayleigh Fading

The Rayleigh distribution is commonly used to describe the statistical time-varying nature of the received envelope of a flat fading signal or the envelope of an individual multipath component [14, 28]. All D2D channels are assumed to be independently Rayleigh fading with equal average power of unity. In essence, the assumption of Rayleigh fading condition implies no presence of any LOS component. The transmissions in SL from different users are assumed to be fully synchronous on the symbol level. Here, the transmit power is shared equally among all the assisting nodes, cooperatively retransmitting simultaneously.

The power yield by the constructive addition of independent Rayleigh fading D2D channel coefficients can be characterized by the Gamma distribution as $\Gamma(k, \Theta)$.

$$f_x(x) = \Gamma(k, \Theta) \tag{3.5}$$

where: k = the *shape* parameter
Θ = the *scale* parameter

While the shape parameter k reflects the number of complex Rayleigh fading variables stemming from statistically independent links, Θ reflects the inverse of the scaling factor used to scale the transmit power per link. Thus, the power scaling is reflected in the denominator of the scale parameter Θ.

Assuming k users are transmitting the same signal using a spatial diversity transmission scheme with equal power sharing and a constant sum power of unity, the distribution of the accumulated channel gain can be characterized by $\Gamma(k,k)$.

$$f_x(x) = \Gamma(k,k) \tag{3.6}$$

Let the probability distribution function (pdf) of the Gamma distribution be given as

$$f(x;k,\Theta) \tag{3.7}$$

Then the probability of the accumulated channel gain to lie below a target value ρ is given by the cumulative distribution function (CDF)

$$\begin{aligned} F(x;k,\Theta) &= \int_0^{\rho} f(x;k,\Theta)dx \\ &= \int_0^{\Theta\rho} f(x;k,1)dx \\ &=: q_k(x \leq \Theta\rho) \end{aligned} \tag{3.8}$$

Since the parameter Θ scales the overall distribution of x, it may also be used to scale the target value ρ while using the unscaled Gamma function $f(x;k,1)$ instead, as shown above in Eq. (3.8). The probability expressed by the CDF is denoted as $q_k(x \leq \Theta\rho)$, representing the measure of channel outage.

The channel outage for k cooperatively transmitting users sharing a total power of unity equally yields:

$$\text{Channel outage for k users} = q_k(x \leq k\rho) \tag{3.9}$$

Figure 3.7 presents the CDF of channel outage probability using Eq. (3.9) for $k \in \{1,\ldots,8\}$ cooperating users and the channel gain ρ given in dB (normalized to the average channel gain). It represents the behavior of channel outage when the diversity order is increased. We use outage probability as a measure of reliability. Thus, the outcome indicates that exploiting user diversity in cooperative retransmissions gradually reduces the outage probability.

Further, we represent in Figure 3.8 the same channel outage performance as above (Figure 3.7), in detail, using a logarithmic scale for $k = 1$ to $k = 6$ users. As we aim at high reliability, the BS should choose a coding scheme yielding a low bit error rate. Hence, we set $p_0 = 0.95$ for the probability that the nodes successfully receive the downlink multicast packet from the BS. The bit error rate relates to the channel outage, and from Figure 3.8, we observe that an outage of 5% translates to a channel gain of $\rho = -13$ dB for a single user. Thus, we correspondingly select $\rho = -13$ dB as the operation point for this evaluation. We interpret the probability of channel outage by analyzing the derived operation point of $\rho = -13$ dB channel gain in Figure 3.8. Considering $k = 1$ to $k = 6$ cooperatively transmitting users, it can be observed that the outage probability decreases by one order of magnitude per user added to the cooperation cluster. Overall, every additional user highlights an improvement in outage probability.

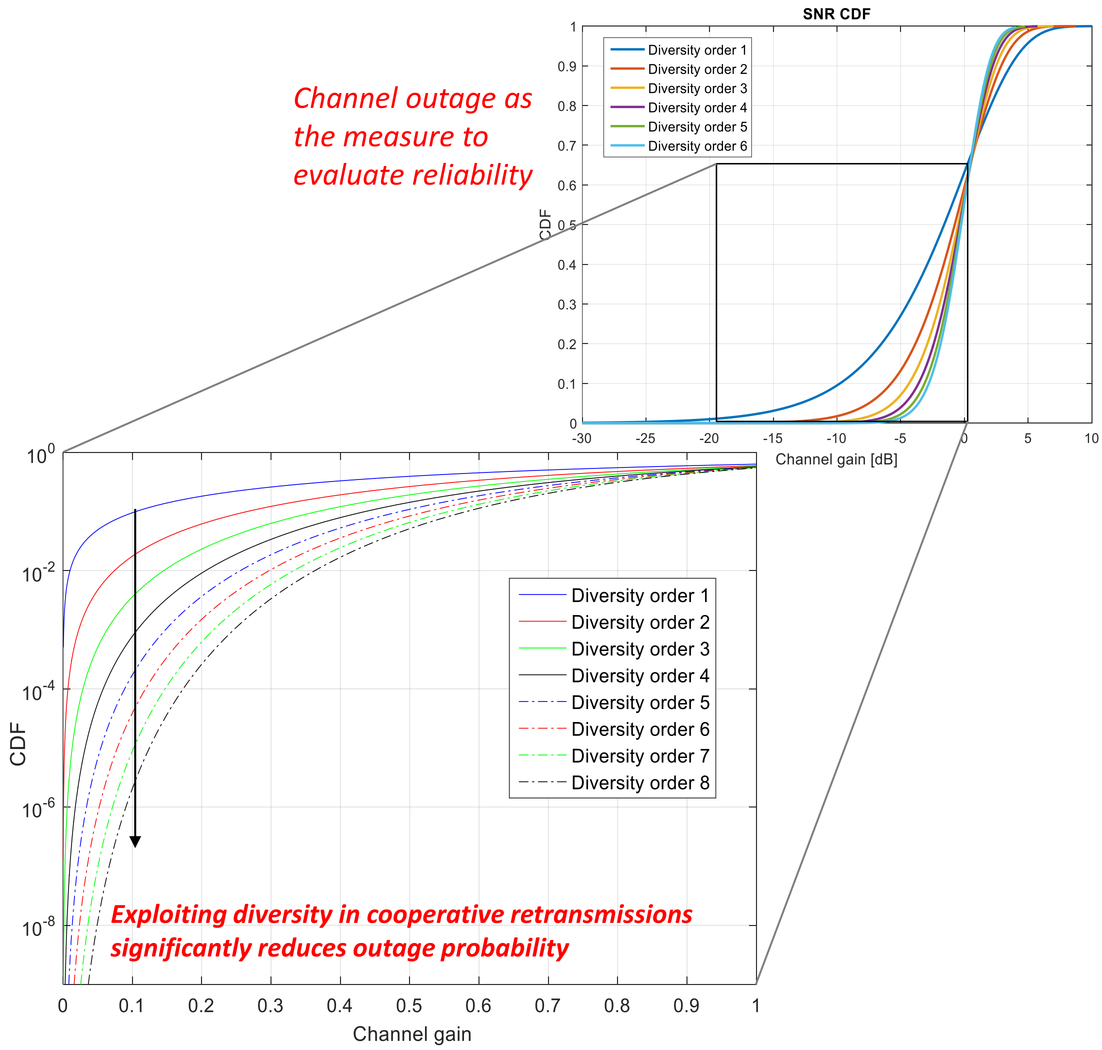

Figure 3.7: CDF of the channel gain representing the channel outage as a measure of reliability (Rayleigh fading)

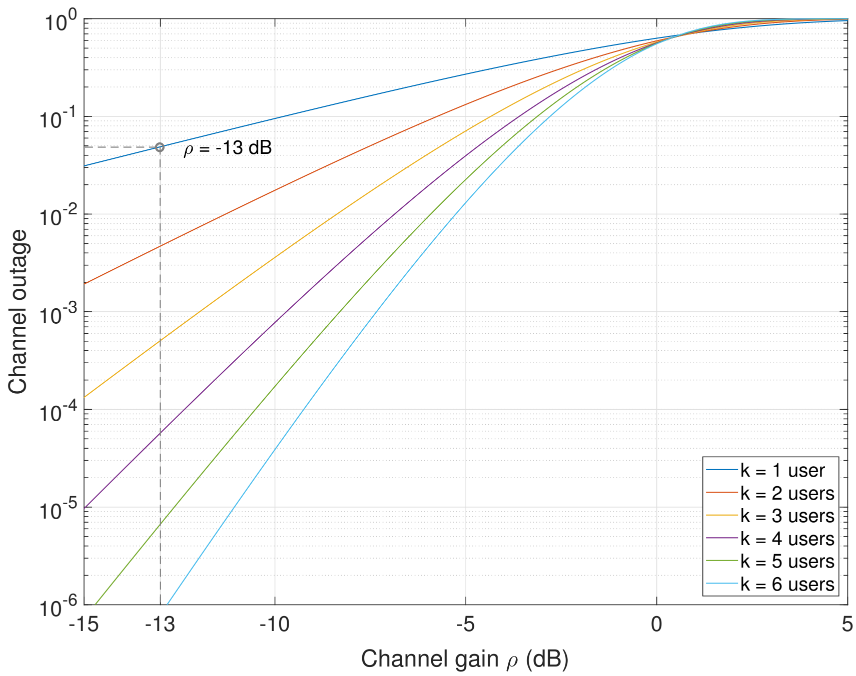

Figure 3.8: CDF of the channel gain representing the channel outage for up to six cooperating users (Rayleigh fading)

Furthermore, we investigate the dependence of the accumulated channel gain ρ on the number of cooperatively transmitting users k for a fixed channel outage probability q_k. Results are shown in Figure 3.9 for up to $k = 8$ cooperatively transmitting users and outage probabilities q_k spanning five orders of magnitude (as indicated in the legend). It can be observed that for a channel gain $\rho = -13$ dB, i.e., a factor of 20 below the total average power of the channel, the outage probability scales by one order of magnitude with every additional user cooperating, as discussed above. Moreover, for a small number of cooperating users, $k \leq 3$, there is a distance of 3 dB between curves representing outage probabilities that differ by one order of magnitude. From this analysis, we can conclude that adding 3 dB power gives the same outage improvement as including an additional user to the cooperation cluster while maintaining the total power constraint. Thus, highlighting the improved resource-efficiency when user cooperation is applied. The distance between the curves decreases with an increasing number of cooperating users, such that the difference of 3 dB translates to a jump of two orders of magnitude for $k \geq 7$ cooperating users. If more than four users are cooperatively transmitting, then adding 3 dB to the total transmit power decreases the outage probability by more than one order of magnitude. This observation leads to the conclusion that when $k \geq 4$ users cooperate, it can be more reasonable to increase the power instead of adding another user to improve the reliability.

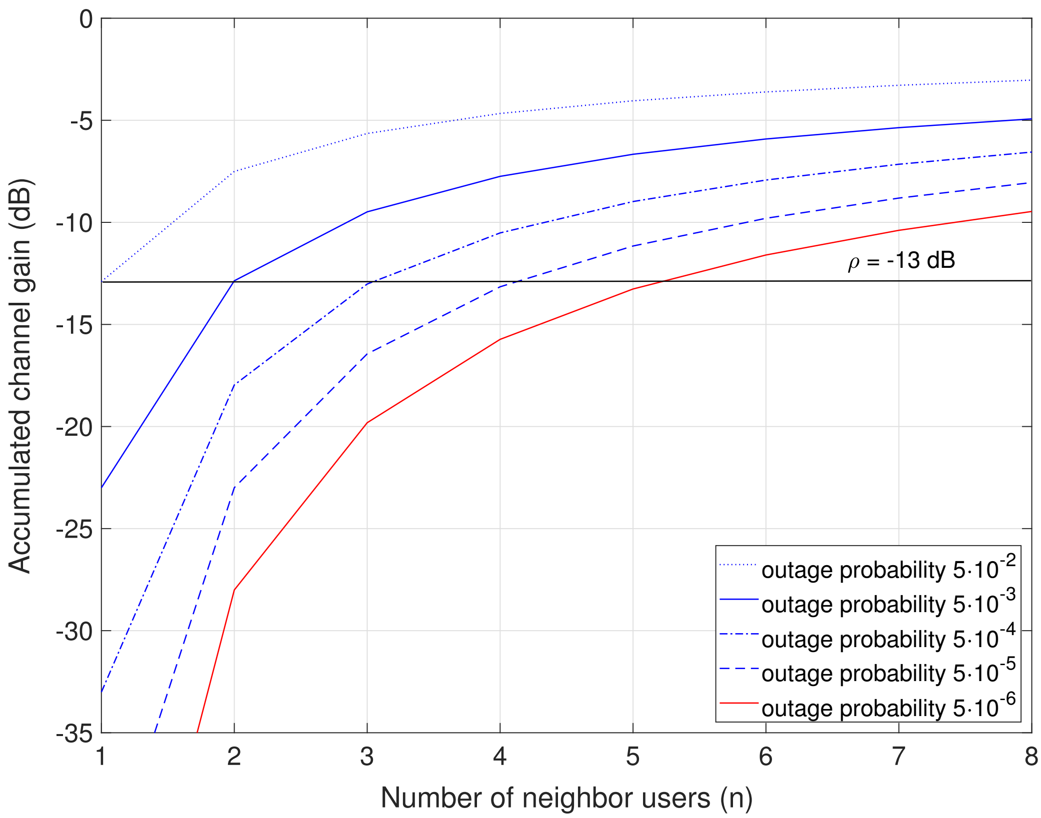

Figure 3.9: Channel outage over the number of neighbor users for Rayleigh fading

3.2.2 D2D Channels Modeled as Ricean Fading

Typical D2D channels will likely exhibit a strong line-of-sight (LOS) component and may be subject to rich scattering. While the previous analysis assumes all D2D channels to be Rayleigh fading, next, we evaluate the impact of direct LOS path between the transmitter and receiver, taking Ricean fading [8] into account, for different degrees of diversity (k). The Ricean distribution is modeled in terms of the K-factor expressed in decibels.

$$\text{K-factor} = 10 * \log_{10}\left(\frac{a_0^2}{\sigma^2}\right) \tag{3.10}$$

where: K-factor = strength of LOS component [dB]
a_0^2 = the signal power of the direct LOS paths [dB]
σ^2 = the signal power of the indirect paths [dB]

The quantity K-factor is the measure of the strength of the LOS component, which is defined as the ratio of the signal power of the direct LOS path and the signal power of the indirect non-line-of-sight (NLOS) paths. We assume the indirect NLOS paths are modeled as complex Gaussian distribution with total power σ^2. When K-factor = 0, implying the absence of the LOS component, then this leads to Rayleigh fading, whereas fading in the channel declines with an increase in the value of the K-factor.

The power yield by the constructive addition of Ricean fading channel coefficients can be characterized by the non-central Gamma distribution $\Gamma(k,\Theta,\delta)$, with k denoting the *shape*, Θ the *scale* parameter, and δ as the non-centrality parameter. While the shape parameter k reflects the degrees of freedom from statistically independent links, and Θ reflects the inverse of the scaling factor used to scale the transmit power per each link, the non-centrality parameter δ has a direct relation to K-factor (Eq. (3.10)). This implies that for an unscaled distribution $\theta = 1$, the non-centrality parameter δ is equal to K-factor.

We apply the outage probability analysis for D2D links modeled as Ricean fading channels, similarly, as illustrated above, for Rayleigh fading D2D channels. The probability distribution function (pdf) of the non-central Gamma distribution is given as

$$f(x;k,\Theta,\delta) \tag{3.11}$$

Thus, the probability of the accumulated channel gain to lie below a target value ρ is given by the cumulative distribution function (CDF) as

$$\int_0^\rho f(x;k,\Theta,\delta)dx =: q_k(x \leq \Theta\rho) \tag{3.12}$$

The probability expressed by the CDF in Figure 3.10 is denoted as $q_k(x \leq \Theta\rho)$, representing the measure of channel outage for Ricean fading channel distribution. Similar to the analysis for Rayleigh fading channels derived in the previous section, we repeat the outage probability analysis now considering Ricean fading channels with K-factors $\{1,5\}$. The channel outage probability considering the two cases of Ricean fading channels is presented in Figure 3.10a and 3.10b, respectively. Recalling our assumption for the success rate of reception, the probability that the nodes successfully receive the multicast packet from the BS is set to $p_0 = 0.95$. Thus, reading from Figure 3.10, a channel outage of 5% for a single user translates to a channel gain of $\rho = -11.5$ dB for K-factor=1 and $\rho = -6$ dB for K-factor=5.

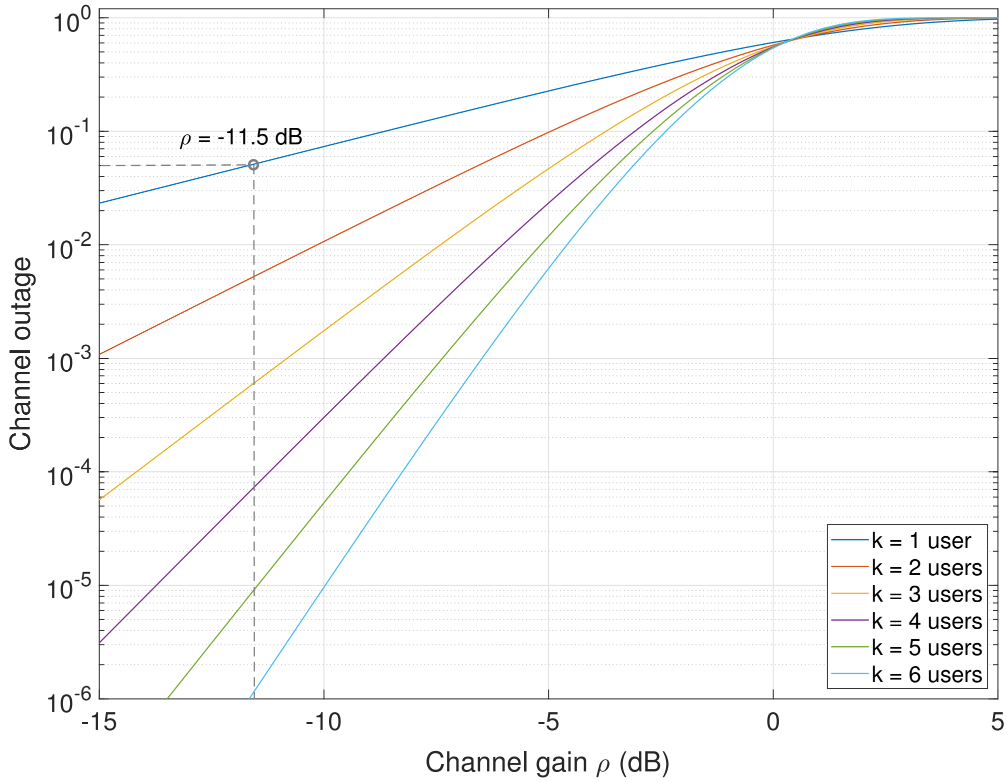

(a) Ricean fading K-factor=1

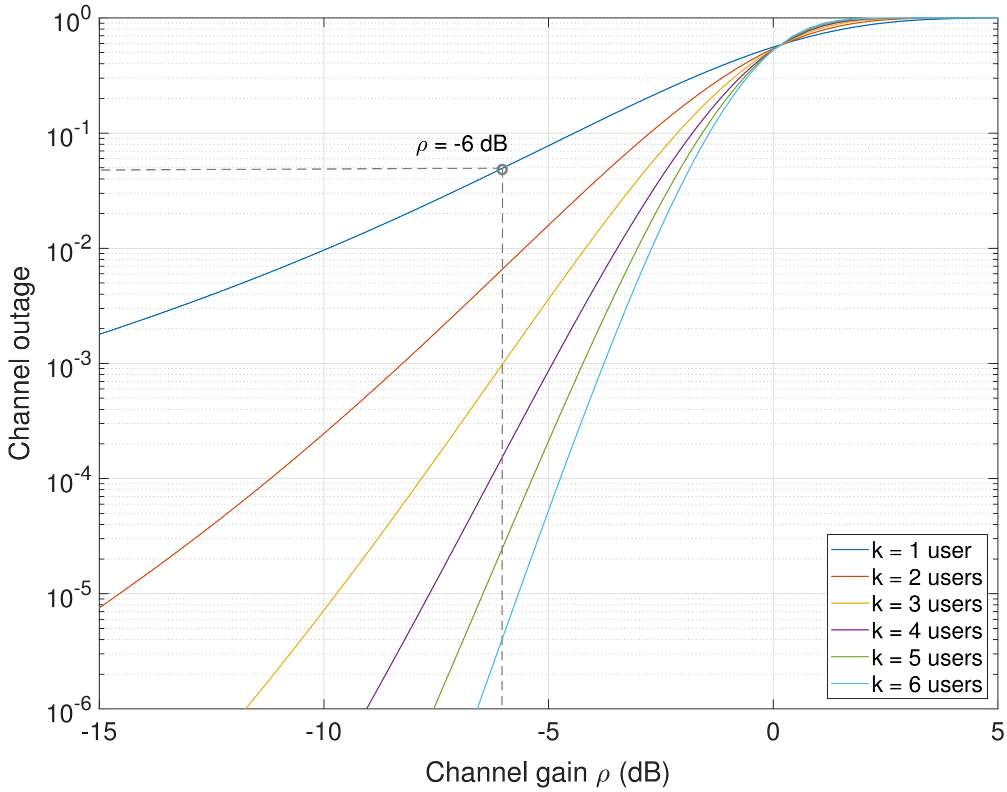

(b) Ricean fading K-factor=5

Figure 3.10: CDF of the channel gain representing the channel outage for up to six cooperating users for Ricean fading with K-factor=1 and K-factor=5

It can be observed from Figure 3.10a that, for a relatively low strength of the LOS component, K-factor =1, the outage probability decreases by one order of magnitude per user added to the cooperation cluster for the operation point $\rho = -11.5$ dB. Compared to the performance for Rayleigh fading channels (Figure 3.8), the overall channel outage behavior for Ricean fading (K-factor=1) does not change significantly, except the operation point drops slightly. Next, considering a stronger LOS component for Ricean fading with K-factor = 5, in Figure 3.10b, at the operation point $\rho = -6$ dB, a gradual decrease in outage probability is observed as well. It is important to note that the operation point for a channel outage of 5% increases with Ricean K-factor, showing that the required margin above the average channel gain reduces. This can be attributed to the fact that the Ricean distribution gets smaller with an increase in the K-factor.

Further, we compare the outage performance for Ricean fading channels with different K-factors in detail for $k = 1$ and $k = 2$ cooperating users, in Figure 3.11. The blue curves represent the channel outage for a single user, and the red curves represent the channel outage for two users. At operation point $\rho = -11.5$ dB, for the single user ($k = 1$ user), a difference of one order of magnitude is clearly visible when moving to stronger LOS from K-factor=1 to K-factor=5. When increasing the number of cooperating users to two ($k = 2$ users), the difference increases by two orders of magnitude comparing the Ricean K-factor=1 and K-factor=5. This reduction in channel outage occurs as the distribution gets narrower with increasing K-factor. Thus, highlighting the impact of stronger LOS components

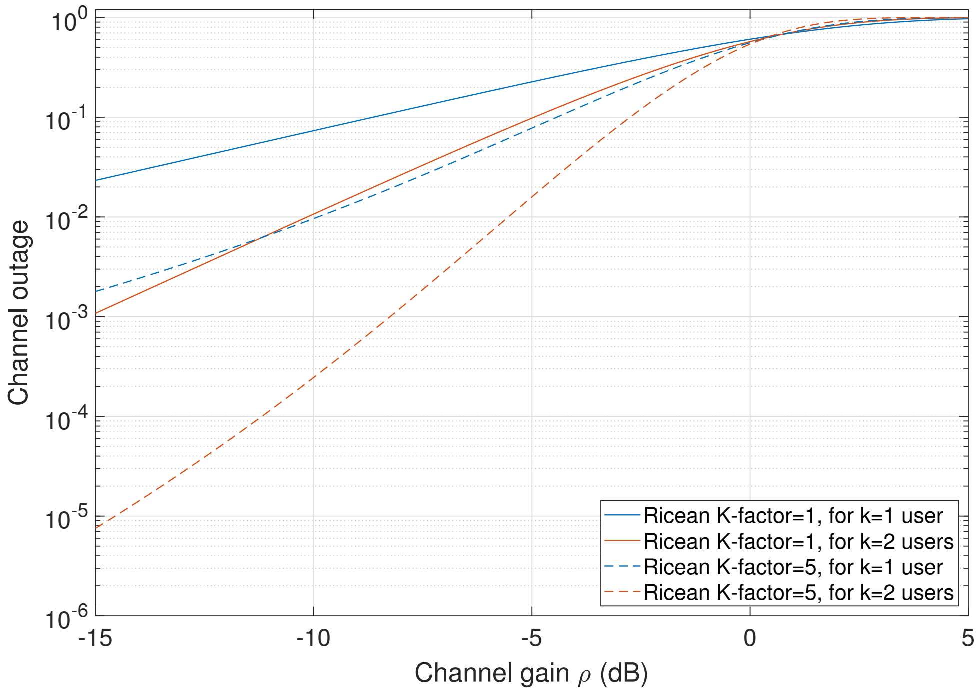

Figure 3.11: Comparison of channel gain representing the channel outage for up to six cooperating users for Ricean fading with K-factor = 1 and Ricean fading with K-factor = 5

as the influence of indirect path is reduced, which enables the Ricean fading channels to perform better than Rayleigh fading channels. In practice, LOS channels may be obstructed frequently; hence we can expect a mix of LOS and NLOS paths. While this hints at Ricean fading, neighboring devices can be expected to experience independently fading channels if they are spaced more than half a wavelength apart from each other. The assumption of independent fading also holds for Ricean channels with a moderate K-factor. This motivates us to use Rayleigh fading as a worst-case assumption, providing an upper bound, and thus, a reference case to model the D2D channels in CoRe model.

3.2.3 Reliability of Cooperative Retransmission Scheme (CoRe)

We now turn the focus on the mesh network scenario of CoRe via the SL illustrated in Section 3.1. In this section, we analyze the attainable reliability depending on the number of cooperating users.

Let p_0 be the probability that a candidate user equipment (UE) for cooperative retransmission has successfully received the packet dedicated to target UE (Node-A) through multicast transmission from the BS, and let $\bar{p}_0 = 1 - p_0$ be the probability for the opposite event (i.e., multicast packet not received). We use the error event, i.e., the negated reliability, to derive the reliability analysis for CoRe. The probability of the packet not being successfully received by Node-A via any of the cooperating links can arise due to one of the two possibilities (Figure 3.12):

1. Failure in successful reception of the original DL multicast packet by any cooperating nodes.
2. All the cooperating nodes that participate in retransmission experience channel outages.

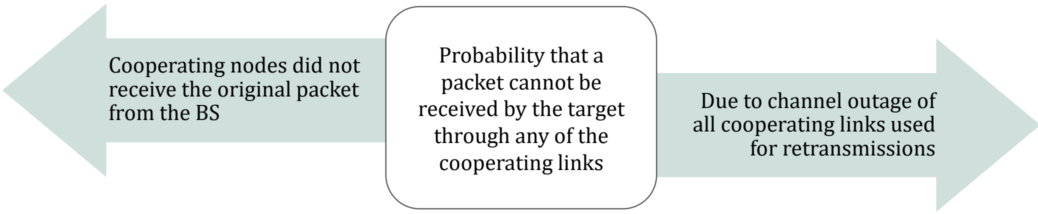

Figure 3.12: Factors affecting the reliability at the target node

Reliability Analysis with single retransmission

Assuming that the probability p_0 is equal for all candidate UEs, the error event (as a measure of reliability) for a single-shot cooperative transmission of n users can be calculated as:

$$q_{1tx}(n) = (\bar{p}_0)^n + \sum_{k=1}^{n} (p_0)^k (\bar{p}_0)^{n-k} \binom{n}{k} \cdot q_k(x \leq n\rho) \tag{3.13}$$

where:
- n = total number of users
- k = number of users that retransmit
- p_0 = probability of successful reception of the original packet
- $\bar{p}_0$ = probability of failure in the reception of the original packet
- ρ = target channel gain
- $q(x \leq n\rho)$ = channel outage probability
- q_{1tx} = error probability with first retransmissions

Note that each of the n users is assigned a constant transmit power for cooperative transmission, reflected by the power scaling factor $1/n$, but transmits only if it has successfully received the packet from the BS. Hence, for reliability, all possible user combinations for $k \in \{0, \ldots, n\}$ simultaneously transmitting users need to be considered. While the first term in Eq. (3.13) represents the case that none of the n users have successfully received the multicast packet from the BS ($k = 0$), the sum term reflects all other cases $k \geq 1$. The probability term q_k in the sum depends on k, the number of actually transmitting users, but not the evaluation point $x \leq n\rho$, which only depends on the scaling factor $1/n$.

Reliability Analysis with two retransmissions

If the latency budget allows supporting more than one retransmission via SL, ARQ and HARQ mechanisms can be applied. Using these, we allow to group the UEs into different sets and let them perform their cooperative retransmissions successively. In the ARQ scheme, a reception signal from a single retransmission that cannot be decoded is discarded until successful reception of the signal. While in the HARQ scheme, signals received in different retransmission attempts are stored and combined such that the overall diversity contained in all the retransmissions can be utilized. We maintain equal power allocation per UE for all the users retransmitting simultaneously in CoRe. The second retransmission has a new power budget now, which allows for increasing the total power spent for the transmission.

We divide the n users into two disjoint subsets with sizes n_1 and n_2, respectively. Here n_1 is the number of users doing the first retransmission, while n_2 is the number of users doing the second retransmission. Then the probability of a channel outage amounts to

For ARQ,

$$q_{n_1}\left(x \leq \frac{n}{2}\rho\right) \cdot q_{n_2}\left(x \leq \frac{n}{2}\rho\right)$$

For HARQ,

$$q_{n_1+n_2}\left(x \leq \frac{n}{2}\rho\right) \tag{3.14}$$

where: n = total number of users
n_1 = number of users in the first subset (1st retransmission)
n_2 = number of users in the second subset (2nd retransmission)
$q_{n_1}(x \leq \frac{n}{2}\rho)$ = channel outage probability for n_1 users
$q_{n_2}(x \leq \frac{n}{2}\rho)$ = channel outage probability for n_2 users
$q_{n_1+n_2}(x \leq \frac{n}{2}\rho)$ = channel outage probability for HARQ from n_1 users in 1st retransmission and n_2 users in 2nd retransmission

Since we consider two retransmissions now, the total available power is accumulated over two time-slots, and thus the equal power allocation yields a scaling factor of $2/n$ per UE. To determine the overall reliability for two retransmissions with ARQ and HARQ scheme, we should consider that the UEs in the second set n_2 can listen to the UEs in the first set n_1 during the first retransmission, and hence they can improve their probability of having received the original packet for Node-A.

Given that k UEs retransmitted the packet in the first retransmission attempt and accounting for this "listening during retransmission," the probability of successful reception of the original packet by the n_2 UEs in the second set is given as

$$p_1(k) = (1-\bar{p}_0)\cdot q_k\left(x \leq \frac{n}{2}\rho\right) \tag{3.15}$$

and accordingly, the probability of unsuccessful reception of the original packet by the n_2 UEs in the second set is

$$\bar{p}_1 = 1 - p_1$$

The probability that the packet cannot be decoded after the second retransmission then yields

For ARQ,

$$p_{arq} = (\bar{p}_1)^{n_2} + \sum_{r=1}^{n_2}(p_1)^r(\bar{p}_1)^{n_2-r}\binom{n_2}{r}\cdot q_r\left(x \leq \frac{n}{2}\rho\right) \tag{3.16}$$

For HARQ,

$$\begin{aligned} p_{harq}(k) &= (\bar{p}_1)^{n_2}\cdot q_k\left(x \leq \frac{n}{2}\rho\right) \\ &+ \sum_{r=1}^{n_2}(p_1)^r(\bar{p}_1)^{n_2-r}\binom{n_2}{r}\cdot q_{r+k}\left(x \leq \frac{n}{2}\rho\right) \end{aligned} \tag{3.17}$$

where:
- n = number of total users
- n_2 = number of users in second subset
- k = number of users cooperating in first subset $k \in n_1$
- r = number of users cooperating in second subset $r \in n_2$
- ρ = target channel gain
- p_1 = probability of successful reception, after the 1st retransmission
- $\bar{p}_1$ = probability of failure in reception, after the 1st retransmission
- $q_r(x \leq \frac{n}{2}\rho)$ = channel outage probability for r users transmitting
- $q_k(x \leq \frac{n}{2}\rho)$ = channel outage probability for k users transmitting
- $q_{r+k}(x \leq \frac{n}{2}\rho)$ = channel outage probability for k users and r users transmitting in 1st and 2nd retransmission attempt, respectively

These two expressions follow the structure of Eq. (3.13). For HARQ, though, it additionally considers in the first term (representing the case that no transmission is carried out during the time slot reserved for the second retransmission) the outage during the first retransmission carried out by the k UEs.

In case there was no first retransmission at all (i.e., $k = 0$), the probability that the packet cannot be decoded after the second retransmission can be calculated similarly to

$$p_{k=0} = (\bar{p}_0)^{n_2} + \sum_{r=1}^{n_2} (p_0)^r (\bar{p}_0)^{n_2-r} \binom{n_2}{r} \cdot q_r \left(x \leq \frac{n}{2}\rho \right) \tag{3.18}$$

With these expressions, we can finally calculate the overall error event for cooperative retransmissions of n UEs by building the sum over all cases of $k \in [0, \ldots, n_1]$ UEs transmitting in the time slot reserved for the first retransmission as

$$q_{2tx} = (\bar{p}_0)^{n_1} p_{k=0} + \sum_{k=1}^{n_1} (p_0)^k (\bar{p}_0)^{n_1-k} \binom{n_1}{k} q_{tot} \tag{3.19}$$

$$q_{tot} = \begin{cases} q_k \left(x \leq \frac{n}{2}\rho \right) \cdot p_{arq} & \text{for ARQ} \\ p_{harq}(k) & \text{for HARQ} \end{cases}$$

Next, we present the single frequency network (SFN) transmission mode and derive its reliability analysis in the following.

Reference System: SFN

We use the SFN transmission mode as a reference system, commonly used in broadcast transmissions. In this mode, the UEs transmit the identical signal in the same resource with equal power allocation. Since there is no further preprocessing of the transmit signals, signals from different UEs add up incoherently at the receiver, so there are no diversity gains due to the lack of cooperation between the UEs. The SFN scheme thus cannot attain a high performance but is yet simple. Note that the performance differences compared to transmit diversity schemes have been investigated in terms of the block error rate in [26]. Following a similar analysis as above, we can obtain the corresponding analytical expressions for the SFN case.

While maintaining the assumption of Rayleigh fading conditions for all channels in the SFN mode, the effective channel for n simultaneously transmitting UEs seen from the receiver maintains its Rayleigh fading characteristics, but the degree of diversity (reflected in the shape parameter of the Gamma distribution) remains constant to 1, independent of the number of users actually transmitting. This happens due to the random and non-constructive addition of channel coefficients. The reliability for a single retransmission via sidelink thus amounts to

$$q_{1tx}(n) = (\bar{p}_0)^n + \sum_{k=1}^{n} p_0^k (\bar{p}_0)^{n-k} \binom{n}{k} \cdot q_1 \left(x \leq \frac{n}{k}\rho \right) \tag{3.20}$$

Note that the different number of simultaneously transmitting UEs now only scales the power at the receiver, yielding an evaluation point of $\frac{n}{k}\rho$, but does not affect the shape of the corresponding Gamma distribution.

With these considerations, Eq. (3.15) and Eq. (3.17) can be updated for the SFN case as follows

$$p_1(k) = 1-\bar{p}_0 \cdot q_1\left(x \leq \frac{n}{2k}\rho\right) \tag{3.21}$$

$$p_{arq} = (\bar{p}_1)^{n_2} + \sum_{r=1}^{n_2} p_1^r (\bar{p}_1)^{n_2-r}\binom{n_2}{r}\cdot q_1\left(x \leq \frac{n}{2r}\rho\right)$$

$$p_{harq}(k) = (\bar{p}_1)^{n_2}\cdot q_1\left(x \leq \frac{n}{2k}\rho\right) + \sum_{r=1}^{n_2} p_1^r(\bar{p}_1)^{n_2-r}\binom{n_2}{r}\cdot q_2\left(x \leq \frac{n}{r+k}\rho\right) \tag{3.22}$$

Note that for the HARQ case, a degree of diversity of two can be realized, thanks to the combination of the signals from successive retransmissions propagating via independent paths. In $p_{harq}(k)$, the shape parameter $k = 2$ contributes as a factor to the mean value of the distribution of $q_2(x)$, and hence the factor 2 in the denominator of the scaling parameter (Θ in Gamma distribution) is dropped compared to the ARQ case.

Equation (3.18) is updated similarly to

$$p_{k=0} = (\bar{p}_0)^{n_2} + \sum_{r=1}^{n_2} p_0^r(\bar{p}_0)^{n_2-r}\binom{n_2}{r}\cdot q_1\left(x \leq \frac{n}{2r}\rho\right) \tag{3.23}$$

The equations to determine the overall reliability for SFN for the ARQ and HARQ cases finally yield

$$q_{2tx} = (\bar{p}_0)^{n_1} p_{k=0} + \sum_{k=1}^{n_1} p_0^k(\bar{p}_0)^{n_1-k}\binom{n_1}{k} q_{tot} \tag{3.24}$$

$$q_{tot} = \begin{cases} q_1\left(x \leq \frac{n}{2k}\rho\right)\cdot p_{arq} & \text{for ARQ} \\ p_{harq}(k) & \text{for HARQ} \end{cases}$$

3.2.4 Reliability Performance Evaluation

D2D Rayleigh Fading Channels

As we aim at high reliability, the BS should choose a coding scheme yielding a low bit error rate, and hence we set $p_0 = 0.95$ for the probability that the UEs successfully receive the multicast packet from the BS. The bit error rate relates to the channel outage, and from Figure 3.8, we observe that an outage of 5% translates to a channel gain of $\rho = -13$ dB for a single user, which we correspondingly select as the operation point for evaluation. Figure 3.13 shows the evaluation of the error event for one and two retransmissions according to Eq. (3.13) and Eq. (3.19), respectively, and for the SFN reference case described above.

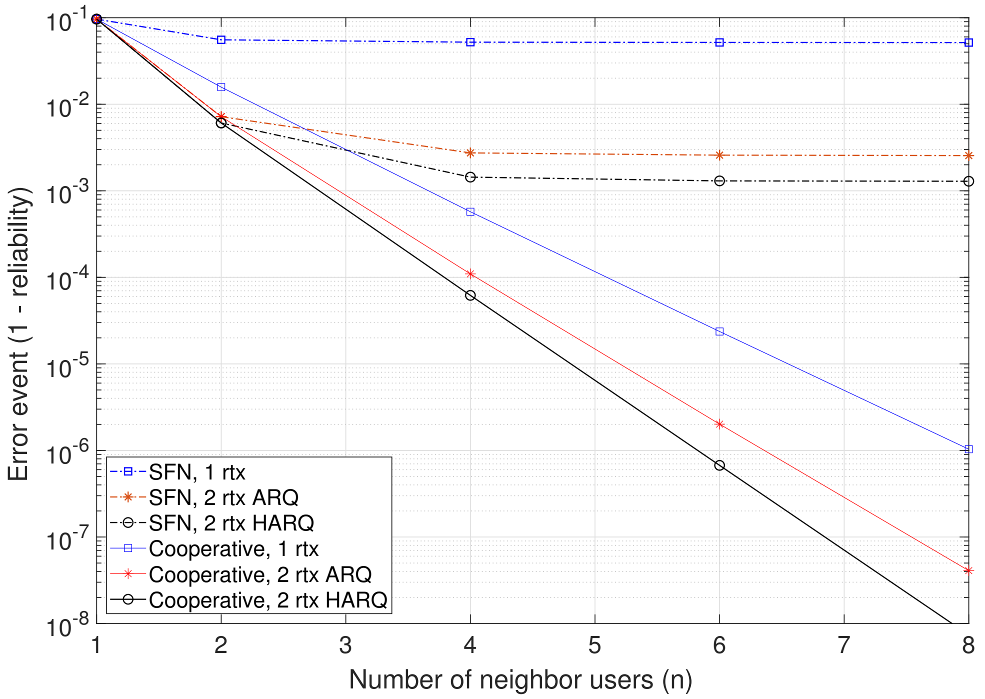

Figure 3.13: Improvement of the reliability by cooperative transmission of neighbor UEs for one and two retransmissions (rtx).

We observe from the figure that the SFN reference system shows a clear saturation behavior since the available degree of diversity is constant to 1 and 2 for one and two retransmissions, respectively. While the reliability for single retransmission is poor, as the error event settles slightly below 10^{-1}, HARQ can improve it down to slightly above 10^{-3}. The cooperative scheme, however, shows that the error event continuously scales with the number of cooperating users n, achieving one order of magnitude per user for the HARQ case. The curve for ARQ exhibits a slope that is less steep than that of HARQ, which reflects the reduced diversity order realized by ARQ compared to HARQ. Hence, the difference between both schemes is minor for a small number of users but becomes more prominent with increasing n. Compared to a single retransmission (rtx), 2 rtx HARQ provides a gain of one order of magnitude for $n = 4$ users, which increases to nearly two orders of magnitude for $n = 7$ users.

D2D Ricean Fading compared to Rayleigh Fading

The reliability performance considering D2D channels to be independently Rayleigh fading is investigated in the previous section. As stated earlier, scenarios with a large number of devices are likely to experience LOS conditions with the neighbor devices. Therefore, we extend our reliability analysis considering D2D channels as Ricean fading channels. The reliability performance for these two scenarios with respect to the number of cooperating users is evaluated and discussed in this section. The derivation of error probability representing reliability for ARQ and HARQ schemes shown in Eq. (3.13) - (3.19) is reused here to assess the performance of cooperating users with channels experiencing Ricean fading conditions.

Figures 3.14a and 3.14b present the evaluation of the error event (1-reliability) for one and two retransmissions for the two cases of Ricean fading, with K-factor $\{1, 5\}$, respectively. As elaborated above in Section 3.2.2, the Ricean K-factor is the measure of the strength of the LOS component.

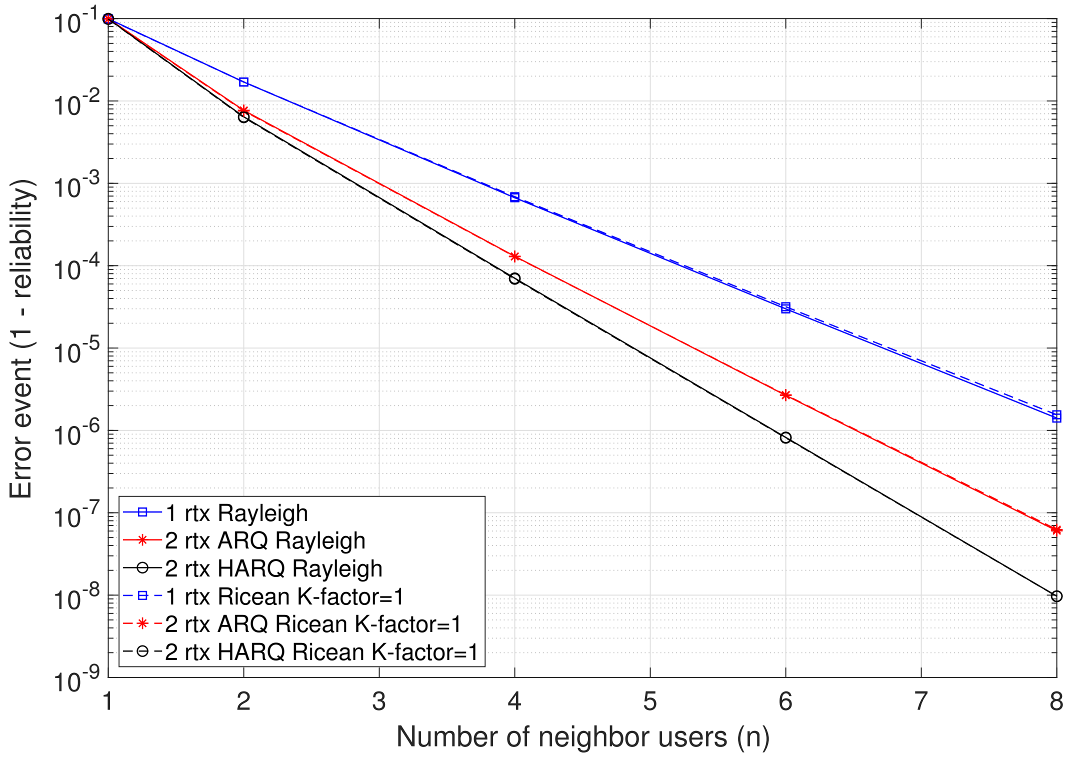

(a) Ricean fading K-factor=1

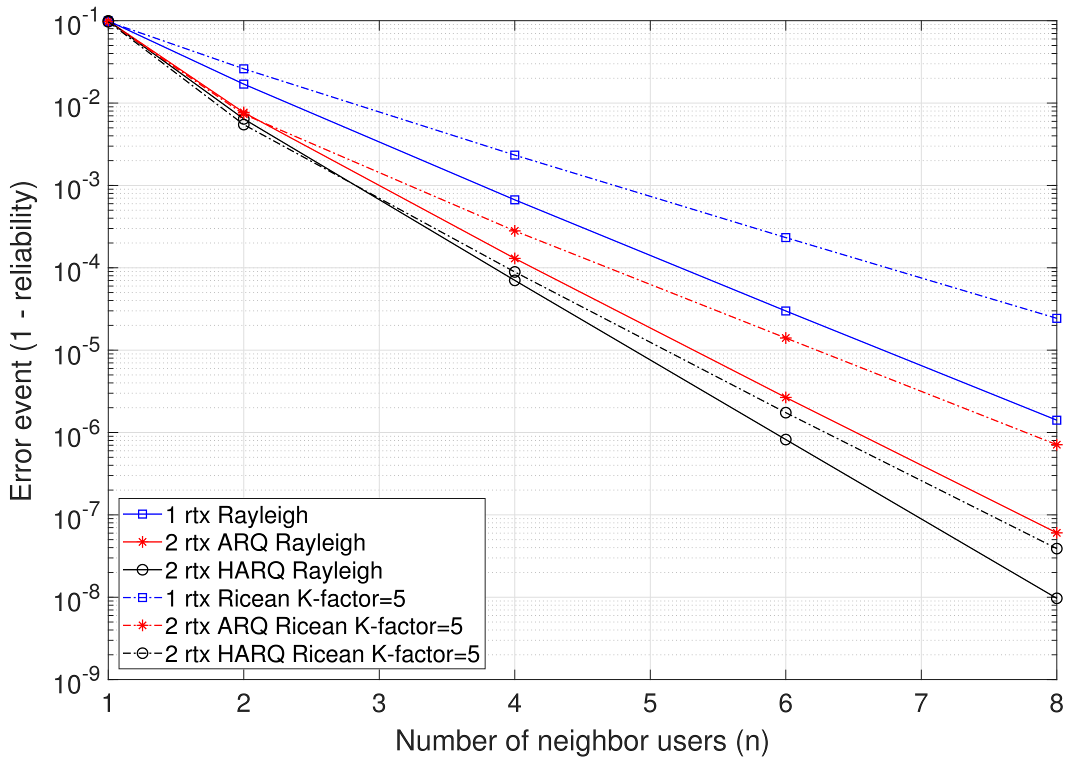

(b) Ricean fading K-factor=5

Figure 3.14: Comparison of reliability by cooperative transmission for Rayleigh fading and Ricean Fading with K-factor = {1,5}

For evaluation, we consider the success rate of reception of the multicast packet to be $p_0 = 0.95$, translating to a channel outage of 5%. Recalling from our previous analysis on channel outage, we obtain an operation point of $\rho = -13$ dB for Rayleigh fading channels, an operation point of $\rho = -11.5$ dB for Ricean K-factor=1 and $\rho = -6$ dB for Ricean K-factor=5, from Figures 3.8 and 3.11 respectively. The Rayleigh fading can be considered the worst-case scenario since the highest power margin is required for a chosen channel outage compared to Ricean fading cases.

In Figure 3.14a, the reliability performance of Ricean fading channels with K-factor = 1 (dashed curves) is compared to the performance of ARQ and HARQ retransmissions when Rayleigh fading (solid curves) for D2D channels is assumed. Considering the respective operation points, we observe that the attainable reliability for a given number of neighbor UEs coincides with the performance attained for Rayleigh fading channels. The Ricean K-factor=1 determines a weak LOS component; therefore, we achieve improvement only in power margin while gaining similar performance as for Rayleigh fading.

The effect of much stronger LOS components realized by a higher value of K-factor (=5) is shown in Figure 3.14b. The performance is evaluated for Ricean fading K-factor=5 at the operation point $\rho = -6$ dB and Rayleigh fading at $\rho = -13$ dB. A consistent increase in reliability can be observed with an increasing number of cooperating users with strong LOS components (Ricean K-factor=5) as well. The narrower shape of the Ricean distribution results in a lower power margin for our chosen channel outage of 5%, as discussed above. For the selected operation point, the gains with increasing the number of users are smaller than one order or magnitude. Hence, the slope of the curves becomes less steep with an increase in K-factor as the smaller power margin leads to a different operation point. Whereas, in Rayleigh fading, we observe that reliability improvement is faster due to the broader distribution and the higher power margin, which is exploited by the indirect paths. We can conclude that user cooperation is undoubtedly beneficial in any case, highlighting more significant quantifiable gains for the Rayleigh fading worst-case scenario while the gains in terms of reduced power margin are realized for Ricean fading. A clear trade-off between the power margin and the number of cooperating users can be observed. Henceforth, the reliability can be improved either by (1) benefiting from the user cooperation when sufficient users are available in the neighborhood or (2) increasing the transmit power when the required number of cooperating users to fulfill the reliability target cannot be made available.

To evaluate this trade-off, we investigate the case when a higher power margin can be utilized to realize maximum gains. To this aim, we now consider the highest power margin derived for the Rayleigh fading operation point, $\rho = -13$ dB, for all three cases: (1) Rayleigh fading, (2) Ricean fading with K-factor=1, and (3) Ricean fading with K-factor=5. In Figure 3.15, an evident shift in the curves can be noted when moving from Rayleigh to Ricean fading channel conditions, thus showing the effect as the LOS components get stronger. These observations are well aligned with the channel outage performance, which indicated reduced channel outage for Ricean fading that reduces further with an increase in K-factor. These larger reliability gains per added user (refer Figure 3.10) at the operation point translates to a steeper slope. Hence, we conclude that the selection of the operation point and thus the power margin impacts the slope of the curves. From our analysis, two alternatives can be recommended: either the same operating point can be selected implying the curves start at the same origin, or the same power margin can be selected to improve the slope of the curves.

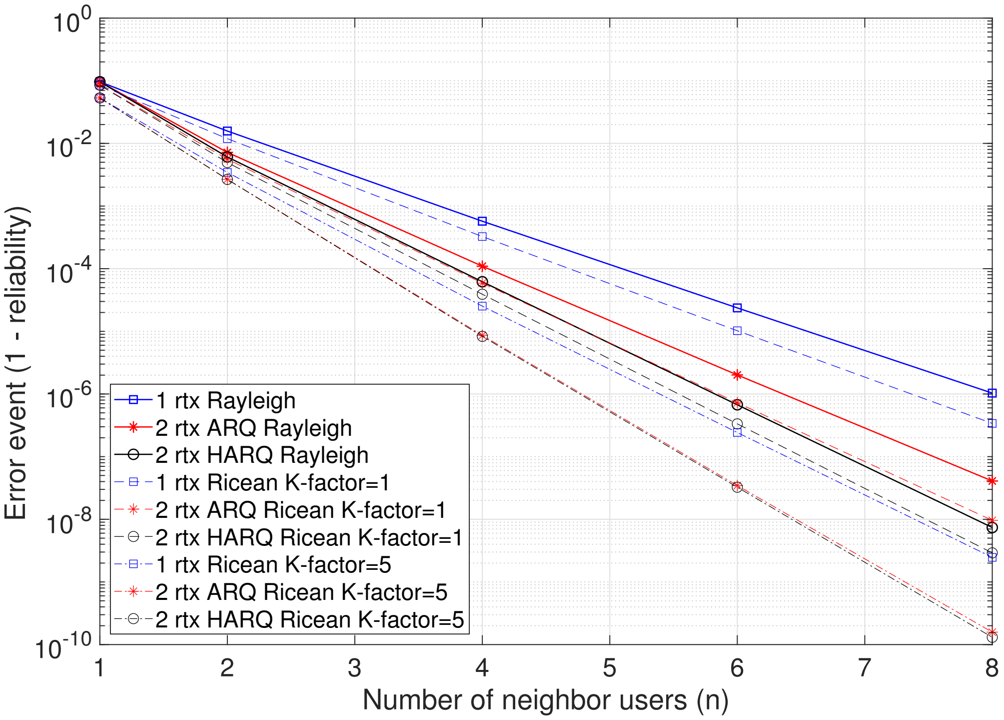

Figure 3.15: Comparison of reliability by cooperative transmission for Rayleigh fading and Ricean Fading with K-factor {1,5} for a fixed operation point of $\rho = -13$ dB

Consequently, for a constant operating point ($\rho = -13$ dB), the attainable reliability performance for Ricean K-factor=5 is maximum, showing gains by two orders of magnitude compared to the Rayleigh fading performance for $k \geq 2$ users. For a large K-factor, the difference in reliability performance between HARQ and ARQ vanishes. The probable reason is that one of the two retransmissions does not provide any useful contribution. This can be interpreted to be the first retransmission, since the selected channel for retransmission may have been so poor that its impact on HARQ is negligible. Fundamentally, ARQ and HARQ schemes mainly differ in their combining process at the receiver. Therefore, it can be derived from the results (2 rtx Ricean fading) that the second retransmission contributes the most, and minimal gains are achieved from the first retransmission due to poor SNR.

Further, we intend to find the best compromise in the trade-off between transmit power usage and the slope of the reliability curve. If the number of cooperating users do not suffice to meet the reliability requirement, a power boost can be applied to improve the performance further. For instance, we re-evaluate the behavior of Ricean fading (K-factor=5) by using a power boost of 3 dB to the actual operation point $\rho = -6$ dB, demonstrated in Figure 3.16. We observe an evidently improved reliability performance for Ricean fading due to the additional gains from the increase in transmit power, as the operation point is now shifted by 3 dB. The reliability target of 10^{-5} can be attained with 6 users cooperating only with a single retransmission. The performance is further improved with two retransmissions using ARQ and HARQ schemes, which need 4 users for cooperation to reach the same reliability. Compared to the single retransmission (1 rtx Ricean), a difference of more than one order of magnitude in reliability is detected when $k \geq 2$ users cooperate. As explained above, the two retransmission schemes, ARQ and HARQ, differ only in the treatment of the second retransmission. Therefore, for K-factor=5, the HARQ scheme does not show any noticeable difference in reliability compared to the ARQ scheme.

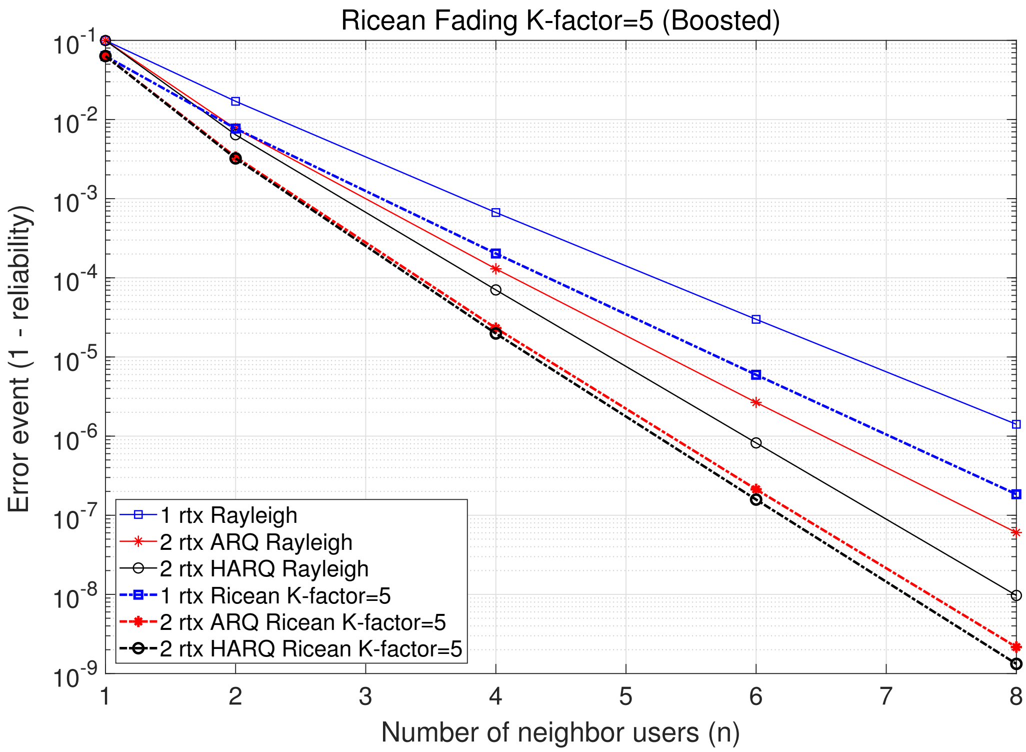

Figure 3.16: Comparison of reliability by cooperative transmission for Rayleigh fading and Ricean Fading with K-factor = 5 with a power boost of 3 dB

To conclude, a trade-off can be derived based on the system requirements and design preferences. A suitable power margin should be selected to achieve the reliability target considering the number of users available for cooperation.

3.2.5 Impact of Power Offsets on Reliability

We now move to a more realistic scenario when the n UEs are located at different distances from the target user, which leads to distinct average power per link. Therefore, it is crucial to evaluate the reliability performance of CoRe, considering the different positions of users.

Relationship between Distance and Power Offsets

Path-loss is the attenuation in power experienced by a signal due to propagation in free space from a transmitter to a receiver. The path-loss measure increases with an increase in the link distance between the transmitter and its respective receiver. The path-loss is a function of the square of the distance between the transmitter and receiver and the frequency of the transmitted signal [50]. The well-known relation between path-loss and distance can be illustrated as follows:

$$PL_{dB} = 10\log_{10}\left(\frac{4\pi d}{\lambda}\right)^2 \tag{3.25}$$

where: PL_{dB} = Path-loss from the transmitter to the receiver [dB]
d = link distance between the transmitter and the receiver [m]
λ = wavelength of the propagated signal [m]

Due to the impact of path-loss, the power of the transmitted signal undergoes degradation, and thus the received power level is attenuated relative to the transmitted power level. The Friis' transmission equation [1] is used to express the factors influencing the received power level and their relationship due to propagation at distance d:

$$P_r = P_t G_t G_r \left(\frac{\lambda}{4\pi d}\right)^2 \tag{3.26}$$

It can be expressed in decibels as follows:

$$P_r = P_t + G_t + G_r + 20\log_{10}\left(\frac{\lambda}{4\pi}\right) - 20\log_{10}(d) \tag{3.27}$$

where: P_r = received signal power [dB]
P_t = transmitted signal power [dB]
G_t = gain of the transmitting antenna [dBi]
G_r = gain of the receiving antenna [dBi]

Thus, the received power is proportional to the square of the link distance between the transmitter and receiver. Therefore, considering this relationship, we model different user link distances using a power offset measure to indicate the power loss per link. A higher power offset value implies a larger link distance relative to the reference power offset of unity (no power loss).

Reliability Analysis for CoRe with Power Offsets

Considering the same scenario for CoRe illustrated earlier in the preceding section, we extend our reliability analysis now by taking into account different link distances reflected by different power offsets for neighbor users. The worst-case scenario of D2D links modeled as Rayleigh fading channels is investigated. The first user is set to be the reference with no power loss, i.e., its power offset is given by $\Theta_1 = 1$. We define the user constellation of k users taken from the total set of user constellations $\mathcal{U}(k)$ that can be drawn from a set of $n \geq k$ distinct users, as follows

$$u = [u_1, \ldots, u_k] \quad \text{such that} \quad u \in \mathcal{U}(k) \quad \text{and} \quad n \geq k \tag{3.28}$$

The users present in the user constellation u are assumed to be ordered according to their distance to the target user (Node-A), which implies increased power scaling for those users.

The power scaling levels for the k users in u are given by

$$\Theta(u) = [\Theta_{u_1}, \ldots, \Theta_{u_k}] \tag{3.29}$$

The pdfs for the individual users in u can be calculated by scaling the Gamma distribution with these power levels

$$g_{u_k}(x) = f(x; 1, \Theta_{u_k}) \tag{3.30}$$

For $i \in [2,\ldots,k]$ simultaneously transmitting users, their joint pdf is calculated by the convolution of their corresponding Gamma distributions

$$\begin{aligned} f_{i=2}(x) &= g_{u_1}(x) * g_{u_2}(x) \\ f_{i+1}(x) &= f_i(x) * g_{u_{i+1}}(x) \end{aligned}$$

The joint pdf $f_k(x)$ obtained in the last step represents the unscaled weighted pdf for the k simultaneously transmitting users of the particular user constellation u, which we denote as $\hat{f}(x;u,1)$. The outage probability can then be computed similarly to Eq. (3.8) to

$$\int_0^{n\rho} \hat{f}(x;u,1)dx =: \hat{q}_u(x \leq n\rho)$$

which we denote by $\hat{q}_u(x \leq n\rho)$ now.

With similar considerations taken for (3.13), the reliability of a single cooperative transmission for n users can be updated to

$$\hat{q}_{1tx}(n) = (\bar{p}_0)^n + \sum_{k=1}^{n} p_0^k (\bar{p}_0)^{n-k} \sum_{u \in \mathcal{U}(k)} \hat{q}_u(x \leq n\rho) \tag{3.31}$$

where:
- n = total number of users
- k = number of users that retransmit
- u, v = user constellations for retransmissions
- p_0 = probability of successful reception of the original packet
- $\bar{p}_0$ = probability of failure in the reception of the original packet
- ρ = target channel gain
- $q_X(x \leq n\rho)$ = channel outage probability for X users
- $\hat{q}_{1tx}$ = error probability with first retransmissions

Note that every $k \in [1,\ldots,n]$ creates $\binom{n}{k}$ unique user constellations $u \in \mathcal{U}(k)$, and hence the binomial coefficient in Eq. (3.13) is replaced by the sum over user constellations u here.

For considering two retransmissions, the n UEs are distributed over two disjoint user subsets U_1 and U_2 of size n_1 and n_2, respectively.

$$\begin{aligned} U_1 &= [u_1,\ldots,u_{n_1}] \quad | \quad n_1 < n \\ U_2 &= [u_{n_1+1},\ldots,u_{n_1+n_2}] \quad | \quad n_2 < n \\ \text{such that,} \quad n &= n_1 + n_2 \end{aligned}$$

Correspondingly, $\mathcal{U}_1(k)$ and $\mathcal{U}_2(k)$ now represent the total set of user constellations for k users selected from each of the two subsets. For simplicity, we maintain the assumption of Rayleigh fading distributions with equal average power per link for the links between users from the two distinct subsets, so the expression in Eq. (3.15) will remain unchanged. As elaborated above, to yield equation (3.31), the reliability for cooperative retransmissions given by the expressions in (3.17), (3.18), and (3.19) can be updated similarly: The term $\binom{n}{k}$ from the previous expressions is replaced by a sum over all $\binom{n}{k}$ possible user constellations u from $\mathcal{U}_1(k)$ and $\mathcal{U}_2(k)$, respectively. Given that v represents the constellation of k UEs having performed the first retransmission, the probability that the packet cannot be decoded after the second retransmission is updated as follows

$$\begin{aligned}
\hat{p}_{arq} &= (\bar{p}_1)^{n_2} + \sum_{r=1}^{n_2} p_1^r (\bar{p}_1)^{n_2-r} \sum_{u \in \mathcal{U}_2(r)} \hat{q}_u \left(x \leq \frac{n}{2}\rho \right) \\
\hat{p}_{harq}(v) &= (\bar{p}_1)^{n_2} \cdot q_v \left(x \leq \frac{n}{2}\rho \right) \\
&+ \sum_{r=1}^{n_2} p_1^r (\bar{p}_1)^{n_2-r} \cdot \sum_{u \in \mathcal{U}_2(r)} \hat{q}_{u \cup v} \left(x \leq \frac{n}{2}\rho \right)
\end{aligned} \tag{3.32}$$

where, $u \cup v$ represents the union of the user constellations v (from first retransmission) and u (from second retransmission).

In case there was no first retransmission at all (i.e., $k = 0$), the probability that the packet cannot be decoded after the second retransmission yields

$$\hat{p}_{k=0} = (\bar{p}_0)^{n_2} + \sum_{r=1}^{n_2} p_0^r (\bar{p}_0)^{n_2-r} \sum_{u \in \mathcal{U}_2(r)} \hat{q}_u \left(x \leq \frac{n}{2}\rho \right) \tag{3.33}$$

where, each $r \in [1, \ldots, n_2]$ creates $\binom{n_2}{r}$ unique sets constituting $\mathcal{U}_2(r)$. The overall error event for cooperative retransmissions can be expressed as

$$\begin{aligned}
\hat{q}_{2tx} &= (\bar{p}_0)^{n_1} \hat{p}_{k=0} + \sum_{k=1}^{n_1} p_0^k (\bar{p}_0)^{n_1-k} \cdot \hat{q}_{tot} \\
\hat{q}_{tot} &= \begin{cases} \sum_{v \in \mathcal{U}_1(k)} \hat{q}_v \left(x \leq \frac{n}{2}\rho \right) \cdot \hat{p}_{arq} & \text{for ARQ} \\ \sum_{v \in \mathcal{U}_1(k)} \hat{p}_{harq}(v) & \text{for HARQ} \end{cases}
\end{aligned} \tag{3.34}$$

where: n = number of total users
n_1 = number of users in first subset
n_2 = number of users in second subset
k = number of users cooperating in first subset $k \in n_1$
r = number of users cooperating in second subset $r \in n_2$
ρ = target channel gain
p_1 = probability of successful reception, after the first re-transmission
$\bar{p}_1$ = probability of failure in reception, after the first re-transmission
$q_X(x \leq \frac{n}{2}\rho)$ = channel outage probability for X users transmitting

Reliability Performance Evaluation Considering Power Offsets

Adopting the same setting from section 3.2 for the evaluation, Figure 3.17 demonstrates the error event for single and two retransmissions with HARQ considering different user power offsets. We assume four distinct power values in multiples of 2, each assigned to a pair of users. Hence, the vector of power offsets for the total set of users U (comprising all n users) is given by

$$\Theta(U) = [1,1,2,2,4,4,6,6] \tag{3.35}$$

Taking into account these power offsets, the performance of single retransmission (1 rtx) exhibits apparent degradation compared to the reference case of equal power per channel, yielding a loss of more than two orders of magnitude for $n = 8$ cooperating users. Further, the cooperative HARQ scheme is evaluated based on the following three types of clustering strategies:

1. **Evenly distributed users:**

   The UEs are evenly distributed among the two subsets according to their power offsets, yielding two user sets with identical power offset vectors, i.e.,

$$\Theta(U_1) = \Theta(U_2) = [1,2,4,6] \tag{3.36}$$

2. **Best users first:**

   Unlike evenly distributed clustering, the UEs are distributed among the two subsets based on their strength. The strength of the users is defined by their power offsets, such that the strong UEs are the ones that have the smallest power offsets. In best users first clustering, the first subset contains the strong users, and the second subset contains the weak users.

$$\Theta(U_1) = [1,1,2,2] \quad \text{and} \quad \Theta(U_2) = [4,4,6,6] \tag{3.37}$$

3. **Best users second:**

   Similar to the best users first clustering, the UEs are distributed among the two subsets based on their strengths. As explained above, the power offset dictates the strength of the users. In this clustering mechanism, the first subset contains the weak users, and the second subset contains the strong users.

$$\Theta(U_1) = [4,4,6,6] \quad \text{and} \quad \Theta(U_2) = [1,1,2,2] \tag{3.38}$$

Firstly, we focus on clustering with even power distribution. We observe from Figure 3.17 that, compared to 1 rtx with power offsets, reliability can be significantly improved, yielding a gain of more than two orders of magnitude for $n = 8$ users. Secondly, the strong users are allocated to one of the two subsets, shown by the solid red and solid green curves in Figure 3.17. Comparing these two cases, we observe a difference of almost one order of magnitude for $n = 8$ cooperating users. The best performance is attained if the strongest users transmit second. This can be attributed to the fact that the users in the second set have received the original packet with a higher probability p_1 from Eq. (3.15). Hence their likelihood of retransmitting it is significantly increased. Since the strongest users have better channels than the users in the other set, the higher probability for transmission results in reliability improvements.

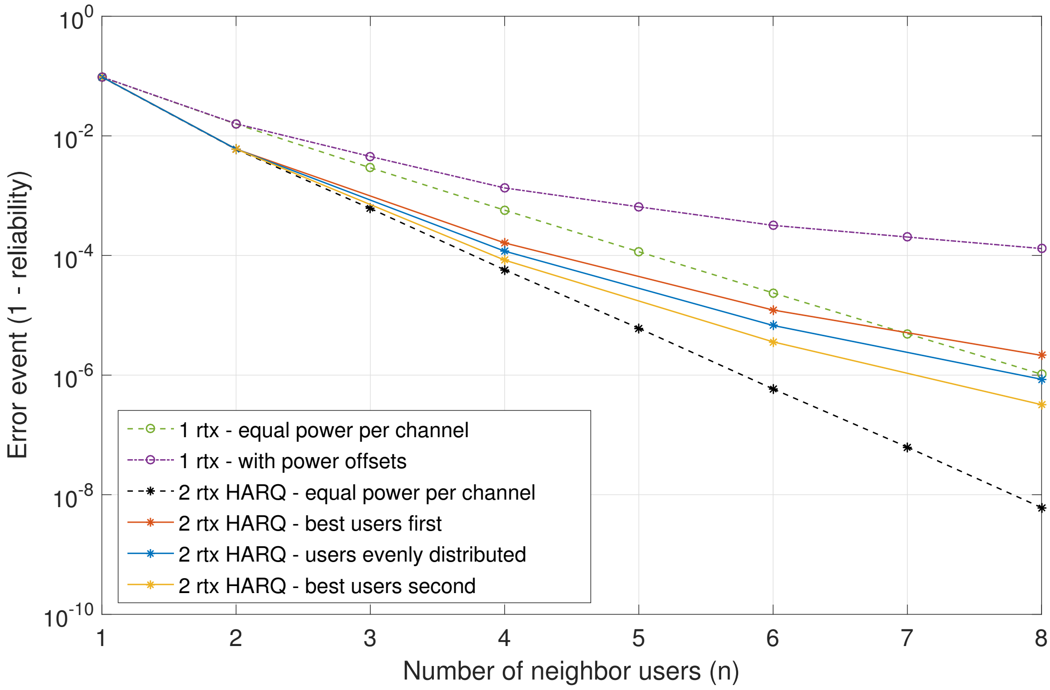

Figure 3.17: Improvement of the reliability by cooperative transmission of neighbor users with power offsets $[1,1,2,2,4,4,6,6]$.

Finally, we note that for 2 rtx HARQ with power offsets and the proper user grouping, the performance degradation compared to the reference case of 2 rtx HARQ with equal power per channel amounts to significantly less than two orders of magnitude for $n = 8$ users, exhibiting a clear advantage over the case of 1 rtx also in this respect.

3.3 Summary

This chapter illustrates the design, implementation, and evaluation of the proposed CoRe scheme targeting the stringent URLLC QoS requirements. The fundamental idea is to exploit the neighbor users available in the vicinity and their diversity, to improve the reliability of successful data reception within the URLLC latency budget in a resource-efficient manner. In scenarios where users are mobile and densely populated, a radio communication link obstruction is highly likely due to shadowing caused by larger devices or other obstacles. Thus, the traditional retransmission technique via the original link is replaced by retransmissions via sidelink in the CoRe scheme. The neighbor users are used for retransmitting lost packets via D2D links to the target user. In order to benefit maximum from the available diversity, we allow different sets of users to cooperatively retransmit the same packet in consecutive retransmissions in the same resource.

Firstly, we evaluate the CoRe scheme analytically to assess the attainable reliability from the different number of neighbor UEs potentially used for cooperatively retransmitting via SL. For the theoretical analysis, channel outage probability is considered as the measure to evaluate reliability. At first, we start with a baseline scenario, in which all D2D users are assumed to have equal link distance to the target user. The two common channel fading distributions: Rayleigh fading and Ricean fading, used to illustrate the statistical time-varying nature of the channel, are investigated and compared for the CoRe scheme. For Rayleigh fading D2D channels, the performance for $k = 1$ to $k = 6$ cooperatively retransmitting UEs; it is observed that the outage probability decreases by one order of magnitude with every additional user added to the cooperation cluster for retransmission. While the channel outage performance considering Ricean fading for D2D channels for the two cases of factor-K (1 and 5), the outage probability shows a further decline per user added to the cooperation cluster. Further, the reliability of the CoRe scheme for ARQ and HARQ retransmission schemes is analyzed with SFN as the reference case. The results indicate a gradual increase in reliability with an increasing number of cooperating users, especially for the HARQ scheme with two retransmissions. In contrast, the traditional SFN scheme shows a saturation in reliability for more than two cooperating users. Comparing the reliability performance of CoRe for Ricean fading D2D channels to Rayleigh fading D2D channels, the results interestingly exhibit a trade-off in transmit power and the number of users cooperating. The outcome for Ricean fading D2D channels highlights benefits in terms of lower power margin. Thus, the right power margin can be chosen depending on the system requirements and the available number of cooperating users. Nevertheless, the assumption of all D2D channels as independently Rayleigh fading can be considered the upper bound (worst-case scenario) and the region of concern for URLLC reliability and latency requirements. Therefore, our further investigation considers Rayleigh fading channels as the reference point to provide a prevailing solution applicable to all potential channel conditions.

Next, we evaluate CoRe analytically for a practical scenario where D2D users are located at different distances from the target user leading to distinct average power per link. Different user clustering of the two user groups for retransmission attempts is compared for attainable reliability. We conclude that the highest reliability is achieved when the strongest users transmit in the second HARQ retransmission attempt, while all neighbors equally distanced from the target user is an ideal scenario for HARQ with two retransmissions.

4

Cooperative Retransmission Scheme (CoRe) for V2X: System-level Evaluation

In this chapter, we extend our investigation on the CoRe model for a realistic scenario focusing on one of the most challenging use cases: V2X communication. To this aim, we perform a system-level evaluation to model all necessary components of the wireless system. Our performance evaluation presents latency and reliability measures attained by CoRe, along with the required number of retransmissions. Finally, we discuss different power control mechanisms and propose an optimal solution for CoRe.

4.1 Vehicle-to-Everything (V2X) Communication

In the course of 5G, V2X has developed from basic vehicular communication to reliable vehicular connectivity enabling advanced functions essential to support autonomous driving. V2X is defined to support Vehicle-to-Infrastructure (V2I), Vehicle-to-Network (V2N), Vehicle-to-Vehicle (V2V), and Vehicle-to-Pedestrian (V2P) communications, as shown in Figure 4.1. V2X has been designed to operate in two modes: first: device-to-network communication, which uses the cellular link for V2N type of communications; second: D2D direct communication is used for V2V, V2P, and V2I services. There has been broad research on V2X since LTE-V2X in Release 14, advancing to 5G V2X in the past years. Key technologies such as adaptive beamforming [78] for efficient and reliable networks, physical layer designs [62], and non-orthogonal multiple access for high-reliable and low-latency broadcast transmission [76], have been studied. 5G-V2X has been expected to provide support for vehicular safety features like forward collision warning, blind spot indication, emergency brake-light warning, accident warning, etc. [117], which demand ultra-high reliability of 99.999% and low latency down to $5-10$ ms. Thus, rendering URLLC communication to become a key service for 5G-V2X.

The availability of link diversity from the numerous vehicles present in the vicinity and the dire need for URLLC to ensure road safety makes our CoRe model the best fit to serve V2X. As stated above in Section 2.3.2 and proved by our analytical study on the CoRe scheme in Section 3.2, the advantages of cooperative relaying help to meet the URLLC QoS demands, which has been additionally studied in the context of V2X communication, such as multi-hop highway communication [65], ALOHA protocol to maximize the throughput [35], two-phase transmission scheme for URLLC [107].

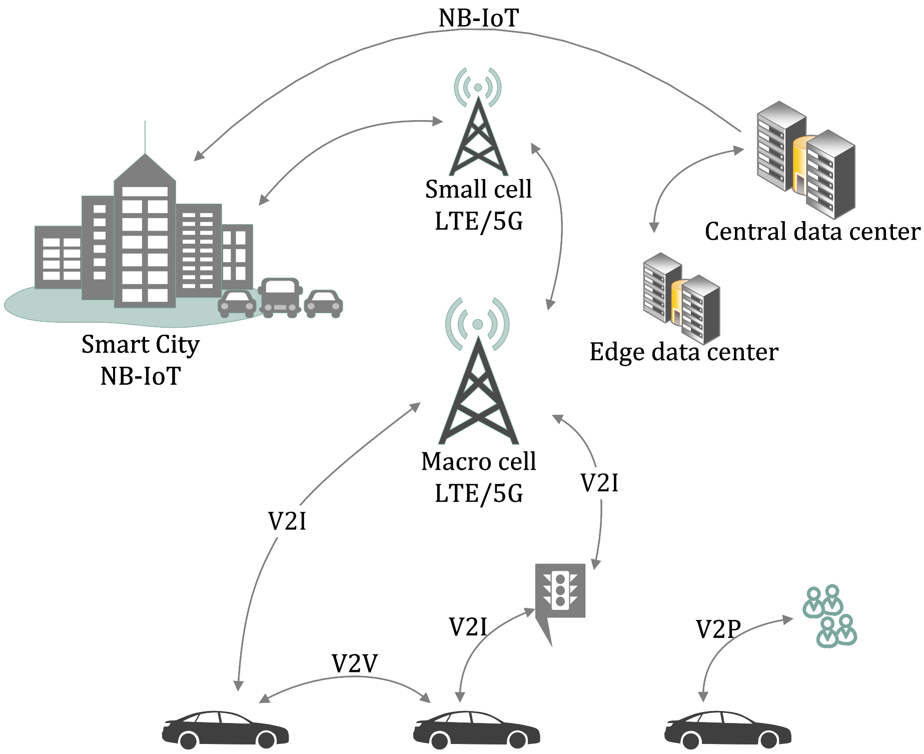

Figure 4.1: Vehicle-to-Everything (V2X) [120]

4.2 System Design and Simulation Setup

First, we discuss the general system setup and the configuration applied for the system-level evaluation of our proposed CoRe scheme. This system and its solutions are designed and developed using the well-known discrete-event-driven network simulator, NS-3 [43] [41] [79]. The LENA module from NS-3 is adapted and extended to enable the functioning of the CoRe scheme. In this evaluation, multiple independent user constellations (user drops) are simulated and averaged to ensure sufficient statistics. Unlike the traditional HARQ retransmissions, which occur via the original link (DL) used for initial transmission, a system compatible for CoRe via SL is developed in the course of this thesis. Here, the DL transmissions are the first transmission attempts for each packet, realized as a multicast transmission to allow the packet reception also by neighbor UEs. A fully loaded task-sensitive network is considered, with all UEs transmitting in UL and DL to all other UEs in the network, thus engaging most of the UEs in cooperative retransmission. Additionally, the SL is assumed to be in-band such that the total bandwidth is shared (time division duplex (TDD) mode), where D2D communication uses the UL resources and experiences interference from UL and D2D transmissions in the neighboring cells. The process of HARQ retransmission via D2D is established for the error-prone DL transmissions. Here, HARQ retransmissions are carried out based on the LTE DL HARQ timings using 8 HARQ processes, which are prioritized over other transmissions. Hence, the HARQ RTT amounts to 2 ms with a TTI size of 250 μs and 8 HARQ processes. Different users are considered for retransmissions, which are selected based on the chosen user-selection scheme elaborated below in detail in Section 4.3, and thus the signals at the receiver are combined using the Maximal Ratio Combining (MRC) type of combining technique (illustrated in Section 3.1.2). The chase combining at the receiver enables aggregating packets received via different D2D retransmissions.

We apply a channel and QoS-aware scheduler (CQA) [51], a DL scheduling method that considers the head-of-line (HOL) delay, the guaranteed bit rate (GBR), and channel quality over different subbands. The scheduler can be split into two phases, time domain (TD) and frequency domain (FD) scheduling, which are jointly applied. In the TD (at each TTI), users are grouped based on HOL delay as a priority in order to enforce that the FD scheduler considers first the flows with the highest delay to reduce the waiting time for transmissions. Furthermore, the FD scheduler schedules the users in a proportional fair manner. Influenced by the link adaptation strategy in [86], we alter the adaptive modulation and coding scheme (AMC) to support 99.999% reliability after three retransmission attempts by adjusting the target block error rate (BLER) for URLLC. The latency of successful receptions is measured at the medium access control (MAC) layer, which inherently includes the queuing and processing delays.

4.2.1 V2X System Model

We consider a multi-cell network topology constituting seven tri-sector sites with an inter-site distance (ISD) of 200 m and each sector is referred to as a cell. The location of sites is fixed as per hexagonal geometry, with the central site being at coordinate (0,0) and the placement of 21 cells, respectively. We assume a bandwidth of 20 MHz, consisting of 100 RBs in the time-frequency domain and 420 active users in our multi-cell scenario. The UEs are dropped uniformly around the 21 cells and are attached to the cell with the strongest signal based on the UE position, yielding 20 users per cell on average. The mobility of the UEs is modeled using the SUMO mobility generator for a V2X highway scenario (shown in Figure 4.2).

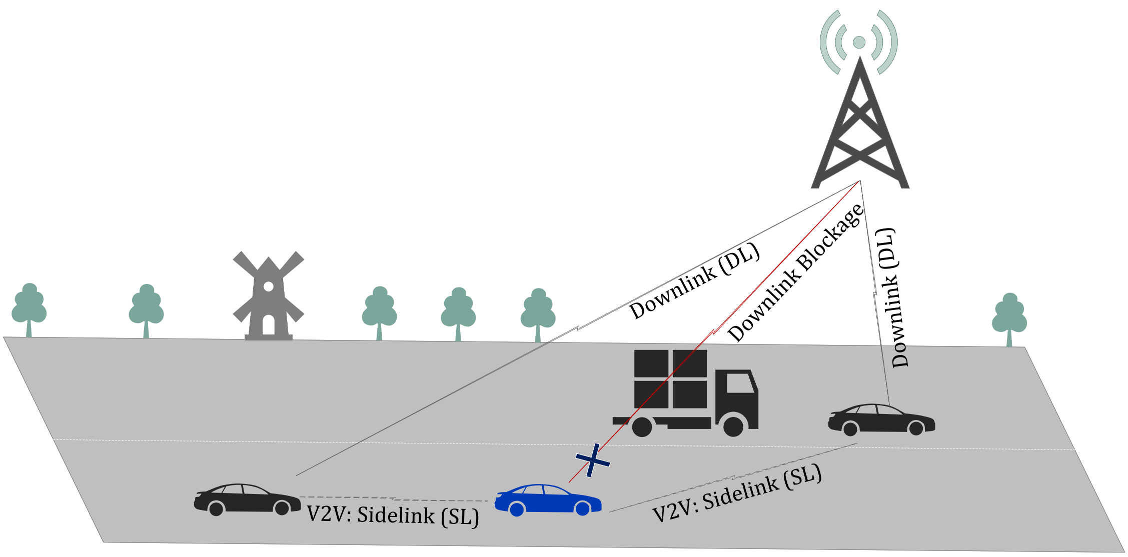

Figure 4.2: V2X scenario

In the scope of this thesis, we focus on scenarios such as a traffic jam where the vehicles are mobile at a slow speed, such as pedestrian speed. At the same time, our CoRe model can be easily adapted for highly mobile use cases. Other simulation parameters are described in Table 4.1.

Table 4.1: V2X - System configuration

Parameters	**Value**
Layout	Hexagonal grid
Bandwidth	20 MHz
Carrier frequency	2.3 GHz
No. of cells	21
No. of UEs	420
Inter-site distance	200 m
TTI size	250 μs
Packet size	200 bytes
Traffic load (per cell)	5 Mbps
gNB transmit power	23 dBm
UE transmit power	10 dBm
UE mobility	3 Kmph
Antenna system	2*2 MIMO
UE distribution	Uniformly
DL channel	Cost-231 Hata channel model
D2D channel	3GPP-Winner II channel model

For DL propagation, the Cost-231 Hata path loss model simulating the urban environment with statistical shadow fading is applied, while SL propagation is modeled by the 3GPP-Winner II suburban channel model [32], which provides accurate and realistic channel properties suitable for evaluating the V2V links [39]. Wireless channels between every D2D pair are assumed to undergo independent frequency selective fading. The WINNER generic channel model is a stochastic model with two levels of randomness, i.e., the large-scale parameters such as delay spread, shadow fading, and angular spreads, and the small-scale fading parameters such as delays, number of clusters, and powers. Different propagation channels have been modeled in WINNER [32][39], considering scenarios like indoor office, typical urban micro-cell, large indoor hall, outdoor to indoor micro-cell, hotspot metropole, rural environment, etc. When considering V2X communication, the channel models of interest are suburban, typical urban macro-cell, bad urban macro-cell, outdoor to indoor macro-cell, and rural macro-cell [39]. In this thesis, we particularly consider the suburban macro-cell channel model to represent one of the typical traffic scenarios of V2X communication. In our selected suburban macro-cell setup, the infrastructure mainly comprises distanced residential complexes or houses within a range of one to two floors. Here, the mobile stations are at street level, and the base stations are located well above the rooftops of the infrastructure to enable wide area coverage [32][39].

The path-loss model developed based on the measurements is presented below

$$PL = A\ \log_{10}(d[m]) + B + C\ \log_{10}\left(\frac{f_c[GHz]}{5.0}\right) + X \tag{4.1}$$

We consider the sub-urban macro-cell channel condition and environment to model the expected behavior of vehicular traffic. The free space path-loss model considering the characteristics defined for the sub-urban macro-cell scenario is formulated as follows. Here, the distribution of shadow fading is log-normal with the standard deviation described by the WINNER model.

$$PL_{free} = 23.8\ \log_{10}(d) + 41.2 + 20\ \log_{10}(\frac{f_c}{5.0}) \tag{4.2}$$

$$PL = \begin{cases} 40.0\ \log_{10}(d) + 11.65 - 16.2\ \log_{10}(h_{BS}) & \\ -16.2\ \log_{10}(h_{MS}) + 3.8\ \log_{10}(f_c) & \sigma = 6 \quad \text{LOS} \\ & \\ (44.9 - 6.55\ \log_{10}(h_{BS}))\log_{10}(d) + 31.46 & \\ +5.83\ \log_{10}(h_{BS}) + 23.0\ \log_{10}(f_c) & \sigma = 8 \quad \text{NLOS} \end{cases} \tag{4.3}$$

where, PL_{LOS} and PL_{NLOS} is the LOS path-loss (dB) and NLOS path-loss (dB) respectively, f_c is the career frequency (MHz) and d is the link distance (m) with $d_{BP} < d < 5$ km for LOS and 50 $m < d < 5$ km for NLOS. The antenna heights for the sub-urban model are $h_{BS} = 25$ m and $h_{MS} = 1.5$ m, and the propagation velocity in free-space given by $c = 3.0 * 10^8$ m/s. The break-point distance d_{BP} is computed using

$$d_{BP} = 4 * h_{BS} * h_{MS} * \frac{f_c}{c} \tag{4.4}$$

The LOS probability for sub-urban propagation channel is approximated as follows

$$P_{LOS} = \exp\left(\frac{-d}{200}\right) \tag{4.5}$$

4.3 User Selection and Grouping Schemes

Recalling our CoRe model, the most obvious question that arises is, "Which users should actually cooperate and retransmit?". Thus, to this aim, we first compare and analyze different user selection and grouping schemes. A set of users is formed based on the D2D distance or link quality defined by the average signal-to-noise ratio (SNR) between the neighbor UEs and the target UE (u_T). A user set may contain all the users in the cell or a subset of users from the cell. Once the user set U for the target UE (u_T) is established, the next step is user selection for retransmission. For every retransmission, the process of user selection is triggered independently. The following three methods are proposed and evaluated for the selection of the user for retransmission.

Let n be the number of neighbor users to target UE u_T, eligible for retransmission (size of the user group), k be the actual number of users cooperatively retransmitting, and $U = \{u_1, u_2, \ldots, u_n\}$ be the set of eligible neighbors (user set). In this evaluation, k users in $\{1, 2, 3\}$ are selected, and n is the total number of users eligible for retransmission.

4.3.1 Method 1: Random-User Selection

We start with an intuitive method of user selection based on a random draw. In this method, we consider an eligible user set (U) consisting of all active users in the cell. In order to perform retransmission via SL, k users are selected randomly from the already created user set. Random-user selection is a simple method taken as a reference whereby each UE in the set has an equal chance of being selected for retransmission. In this scheme, k randomly chosen users from all the users in the cell transmit cooperatively.

4.3.2 Method 2: Best-User Selection

Next, we move to a sophisticated method taking into account the quality of the D2D link. The target UE selects the users with the best average D2D channel quality to itself for retransmission, assuming that each user is aware of the average channel quality to its neighbors. Average SNR is considered a measure to determine the channel quality of these D2D links. Unlike the random user selection scheme, this selection method is more systematic.

Here, the set of users U contains all the n users available in the cell. For every retransmission, the k best users are selected to transmit cooperatively. Hence it is likely that each retransmission is carried out by the same set of users.

4.3.3 Method 3: User-Combination Selection

Finally, we design an advanced user selection method considering the fundamentals of our CoRe model and aiming at maximum diversity gains. In this selection and grouping method, a subset of the best users is created based on their average SNR, from the user set U, which contains all users in the cell. Different combinations are formed from the pre-selected subset of best users, and a unique combination is selected for every retransmission. Due to this distinct user selection for each retransmission, the identical signal is sent via multiple independently fading transmission paths in each retransmission. This scheme allows the use of diversity from the best D2D links first while considering additional diversity sources in successive retransmissions. The grouping by user-combination technique is illustrated as follows:

Let,

- n be the available users in the cell,
- m be the pre-selected subset of best users from n available users in the cell, and
- k be the number of users present in each combination transmitting cooperatively.

According to permutation and combination theory, the total number of possible combinations is given by

$$C(m,k) = \frac{m!}{k!(m-k)!} \tag{4.6}$$

For instance, $m = 3$ and $k = 2$, considering user set $U = \{u_1, u_2, u_3\}$, the following user combinations are created,

$$\begin{aligned} \text{First user pair} &: (u_1, u_2) \\ \text{Second user pair} &: (u_1, u_3) \\ \text{Third user pair} &: (u_2, u_3) \end{aligned}$$

For the first retransmission, the best user pair is selected (u_1, u_2), then using the permutations, a user set containing the best user combined with others from the set is selected, and so on, allowing a unique selection for all three retransmissions.

4.4 Performance Evaluation of Cooperative Retransmission Scheme (CoRe)

The performance of the CoRe scheme for the aforementioned user selection schemes compared to the conventional DL retransmission scheme is evaluated. The simulation configuration and parameters are elaborated above in Section 4.2 and summarized in Table 4.1. A V2X scenario mainly targeting DL multicast transmissions is considered, where HARQ retransmissions are modeled either via DL or D2D. The DL transmissions are the initial transmission attempts for each packet, for which the retransmissions are considered in case of unsuccessful DL reception. The blocking of DL is not modeled explicitly; however, it is reflected by the statistical shadow fading model implemented in the Cost-231 Hata model. Figure 4.3 represents the latency performance with target reliability for the different cooperative user selection methods. The complementary cumulative distribution function (CCDF) in this latency evaluation indicates the probability of the latency exceeding a certain latency value given on the x-axis, i.e., $p(d \geq x)$. The plateaus in the curve are caused as an effect of the HARQ RTT and queuing delay, and highlight the successive (re-)transmission attempts. The leftmost plateau represents the first transmission, followed by other plateaus for consecutive retransmissions. The performance attained with the traditional DL HARQ scheme (black curve), where all retransmissions are performed via DL, is taken as a reference for the analysis.

In this evaluation, a fixed amount of power is allocated for each retransmission to ensure a fair comparison, i.e., the total constant power is always shared equally among all k users transmitting cooperatively. As illustrated in Section 4.3, n and k are chosen based on the grouping scheme. For the first two methods, i.e., method-1 (random-user) and method-2 (best-user selection), the number of users retransmitting (k) is selected from eligible neighbors (n), i.e., all users in the cell, where $n = 20$. In the first case, when applying the random-user selection method with $k = 1$ (dashed red curve), $k = 2$ (dashed green curve), and $k = 3$ (dashed magenta curve), it can be observed that the probability of higher latencies reduces continuously with the increasing number of cooperating users, thanks to the additional diversity gains. Analyzing the random selection method is helpful to highlight the effects of diversity even using such a simple, no-brainer method. At least three cooperating users ($k = 3$) are needed to observe gains better than the traditional DL HARQ scheme. Hence, for this case, we can conclude that there is always (at least) one user who can provide substantially better link quality than the DL. In method-2 (best-user selection), the probability of retransmissions is reduced by one order of magnitude compared to the traditional DL retransmissions. As an effect of the close proximity of D2D UEs, yielding a better link quality results in higher SINR, which translates to a higher probability of successful decoding and hence more reliable transmission compared to the DL HARQ. Increasing the number of cooperative users to $k = 2$ (solid green curve) and $k = 3$ (solid magenta curve) indicates a further improvement in the delay performance (after the first plateau) for the second and third retransmission compared to best-user selection $k = 1$, highlighting the gains from additional diversity.

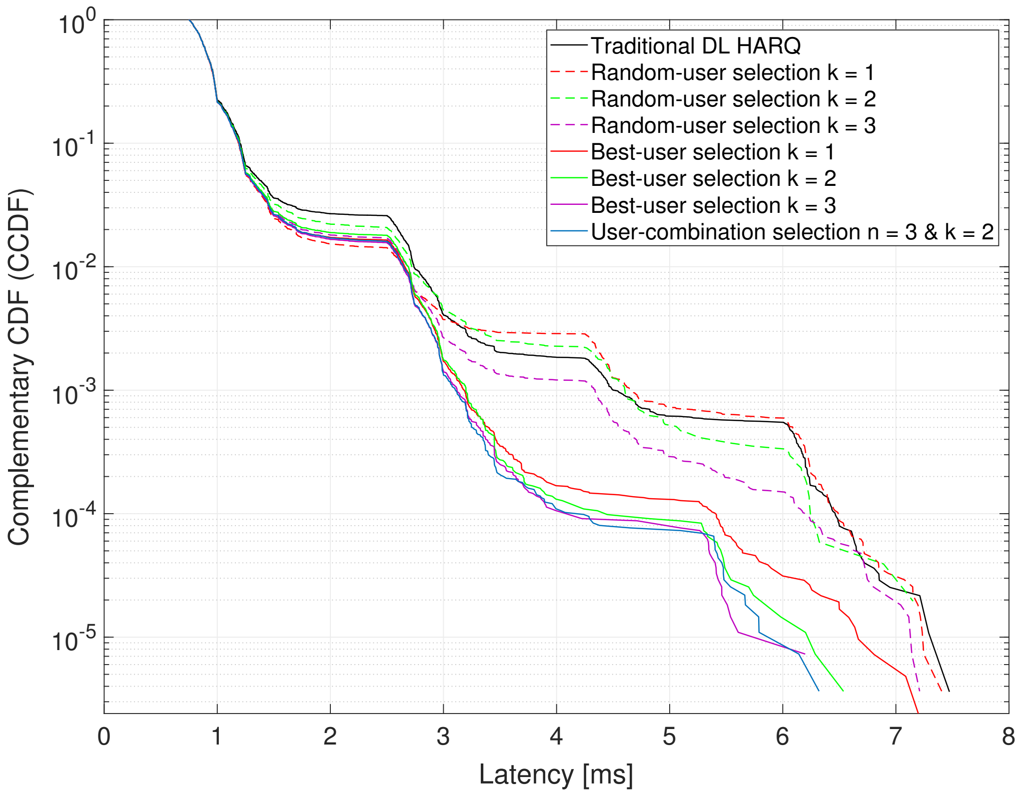

Figure 4.3: Latency performance: Comparing different user-selection methods

As a consequence of replacing retransmissions via DL with retransmissions via SL, a smaller number of DL resources are needed since retransmissions via SL are more reliable and less required due to the better SINR conditions. As depicted in the figure, the level of the first plateau is lower for the cooperative scheme compared to the conventional DL scheme. This implies fewer resources being used on average due to a lower number of retransmissions, in turn causing lower interference compared to DL HARQ and, hence, a lower probability for a failed first transmission. Further, in method-3 (user-combination scheme), different user combinations are considered for retransmissions (blue curve), where a subset of $m = 3$ best users is selected from $n = 20$ available users in the cell. User combinations containing $k = 2$ users are formed as explained in Section 4.3.3: $(u_1, u_2), (u_1, u_3), (u_2, u_3)$, with (u_1, u_2, u_3) being in descending order of average SNR.

This implies that two users always transmit, but in each retransmission attempt, a different pair is picked from the user set of $m = 3$ users to make use of the full diversity provided by the m best users. Interestingly, the user-combination method performs better than the best-user method with $k = 2$, highlighting the gains from additional diversity made available by adding a third user to the set of m best users. Furthermore, method 3 with $k = 2$, in essence, performs equivalent to the best-user selection scheme with $k = 3$ while being less complex. For instance, the complexity due to synchronization between UEs is comparatively reduced with a lower number of users (k) cooperatively transmitting.

To get further insights into the behavior of the different user-selection schemes, we evaluate the SINR conditions for retransmissions (Section 4.3), demonstrated in Figure 4.4. The SINR at the receiving target UE reflects the ratio of useful signal from the cooperatively retransmitting UEs composed by constructive addition of their channel gains and the interference caused by the users in all adjacent cells. The performance for DL HARQ (black curve) attains the lowest median SINR at 10 dB with a steeper slope, where the shape reflects the typical effects observed from fading in DL transmission. Here, the SINR varies in a range of 30 dB, which is attributed to large and small-scale fading. Next, with the random-user scheme, we observe a slightly better median SINR, which improves with k cooperating users. However, the random selection of users leads to a broader slope of the curve since UEs at unfavorable locations in the cell, such as the other end of the cell, can participate in the cooperative transmission. This affects the SINR for certain UEs, which is reflected in the left tail of the curve, showing a worse performance than the DL HARQ scheme. The

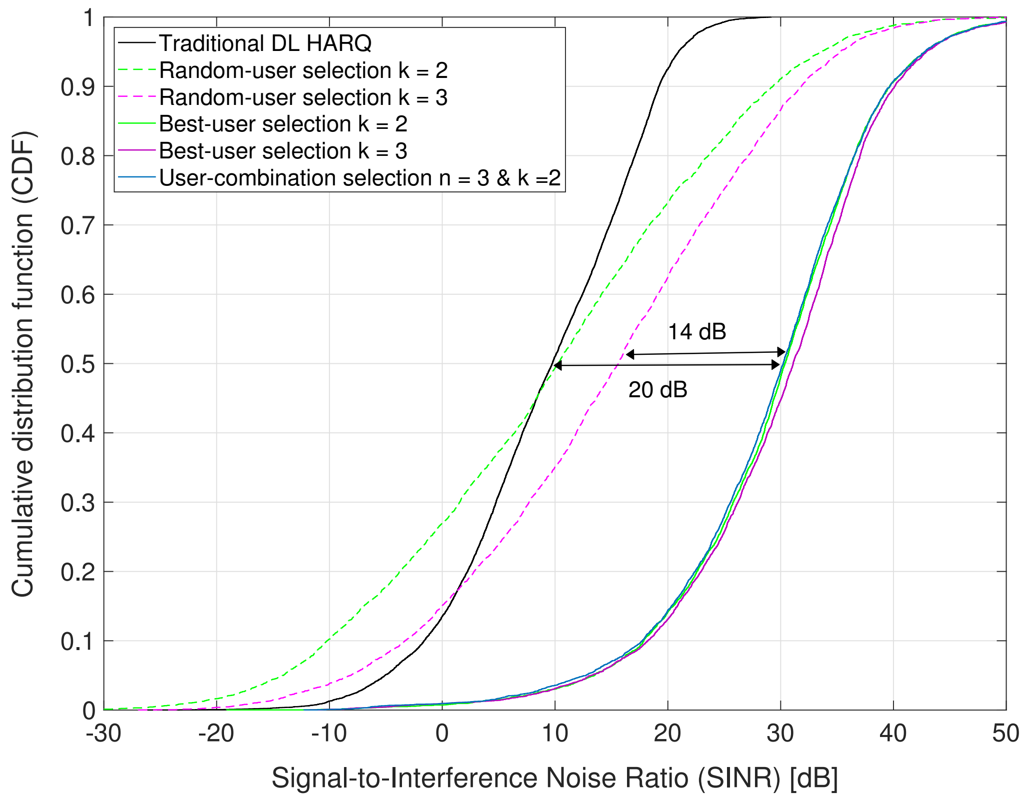

Figure 4.4: SINR performance: Comparison of SINR for retransmissions with different user-selection methods

results display larger gains in terms of SINR for the best-user and user-combination schemes, with an increase in SINR by 20 dB and 14 dB on average, compared to the traditional DL HARQ and cooperative random-user selection, respectively. These two schemes with $k = 2$

users are comparable in their achieved SINR, but the user-combination scheme attains better latency performance (Figure 4.3) by virtue of additional diversity gains. We observe a further minimal increase in SINR with the best-user selection $k = 3$, which, however, does not translate to a substantial performance gain in latency. This indicates that the increased SINR cannot be beneficially utilized since the packet can already be successfully decoded with the SINR attained by $k = 2$ cooperating users.

Further, we analyze the effect of the cooperative scheme on the number of required retransmissions, as demonstrated in Figure 4.5. In this analysis, we consider only the cases where the first transmissions failed, and retransmissions were required, which amounts to 2% of the total transmissions for the user-combination cooperative scheme, as observed by the first plateau settling at $2 * 10^{-2}$ in Figure 4.3. For all retransmissions, here, we evaluate the accumulated success rate of the succeeding 1st, 2nd, and 3rd retransmissions (Retx).

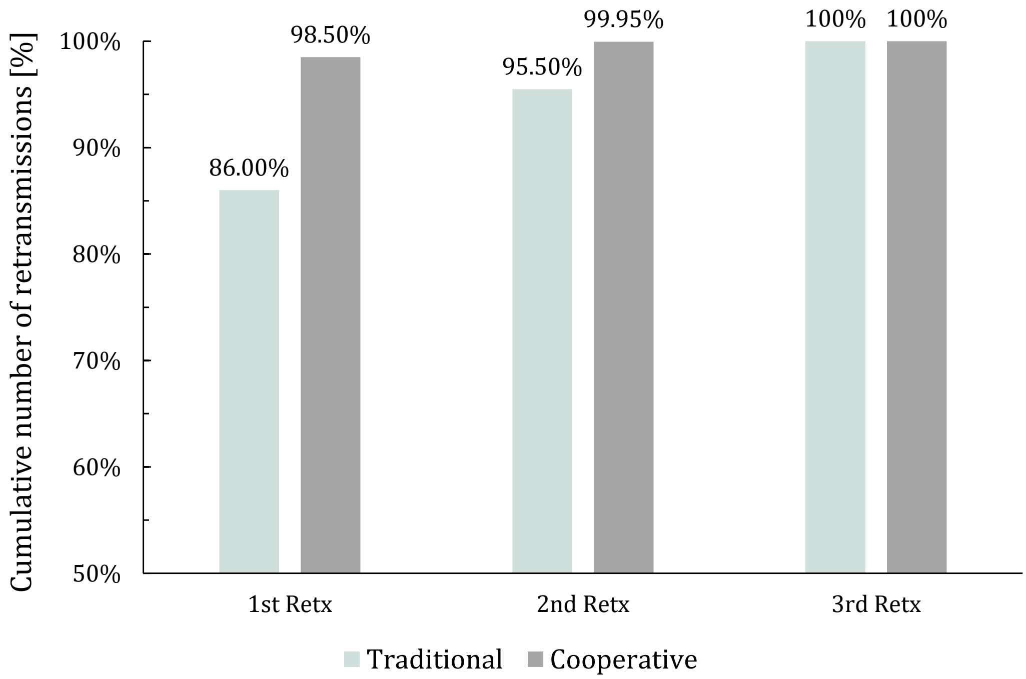

Figure 4.5: Successful retransmissions relative to the total number of retransmissions for each Retx attempt.

With the cooperative scheme, the majority of the retransmissions (98.5%) are successfully received in the first retransmission (1st Retx) attempt. Whereas, with the traditional DL scheme, the success rate of the first retransmission attempt is 86%, being significantly lower. The overall reliability of the second retransmission is computed as follows

$$\text{Success rate} = 1 - \text{error rate}$$

$$\begin{aligned}\text{Probability(Failure of initial transmission)} &= 1 - \text{Probability(Occurrence of 1st retransmission)} \\ &= 1 - 0.98 = 2 * 10^{-2}\end{aligned}$$

$$\begin{aligned}\text{Probability(Failure of 2nd retransmission)} &= 1 - \text{Success rate of 2nd retransmission} \\ &= 1 - 0.9995\end{aligned}$$

Thus, we obtain the probability that 1st transmission plus the two retransmissions are erroneous, which is the negated value of the reliability, is computed as follows

$$\begin{aligned}
\text{Reliability after 2nd retransmission} &= 1-\text{Error event after 2nd retransmission}\\
&= 1-\text{Probability(Occurrence of 1st retransmission)}\\
&* \text{Probability(Failure of 2nd retransmission)}\\
&= 1-(1-0.98)*(1-0.9995)\\
&= 1-0.99999\\
&= 99.999
\end{aligned}$$

Hence, the attainable reliability with a maximum of two retransmissions is 99.999%, representing that two retransmissions are sufficient for a successful reception with a reliability of 99.999%. As it can be read from Figure 4.3 (blue curve), a maximum latency of 6 ms is needed for successful second retransmissions. Whereas, in the traditional DL scheme, three retransmissions are required to attain the reliability of 99.999% with a latency of around 7.5 ms. Thus, the analysis reveals that the cooperative scheme can save one retransmission, which in essence, reduces the latency and, as indicated earlier, shortens the queuing delays, which also yields an improved usage of the available resources.

Subsequent to the huge SINR margin of 20 dB offered by the favorable cooperative schemes (method 2 and method 3), we expect a possibility of further transmit power saving for the cooperating UE while maintaining the delay performance. This suggests the beneficial application of power control, taking into account the SL path-loss based power constraint for the cooperative transmissions, with the aim to minimize the transmit power usage.

4.5 Power Control (PC) for Cooperative Retransmissions

4.5.1 Motivation and State-of-the-art

Power is an essential resource in wireless communication, which must be utilized wisely. Transmit power control (PC) has been shown to be one of the key features beneficial to reduce the interference in the system [30, 33, 94]. When considering densely populated mesh networks and the CoRe solution for URLLC, PC must be applied efficiently to mitigate the interference imposed on the system if multiple D2D UEs are simultaneously transmitting in order to make efficient use of the available power [110]. The UE transmit power should be allocated depending on path-loss to the target UE so as to use only as much power as needed to successfully decode the packet at the target UE. In our CoRe model, the retransmissions are carried out by amplify/equalize and forward, reusing the same modulation and coding scheme (MCS) determined for the first DL transmission. Here, the target UE selects the users for retransmission (assisting UEs). The measure of DL power constraint derived using DL channel condition is normally used as a general measure for PC to mitigate the interference at the BS, and therefore, we use it as the upper bound. PC schemes mainly depend on the path-loss measurements experienced at the assisting UE, given by the DL and SL channels towards the BS and the target UE, respectively. This leads to DL and SL power constraints necessary for PC mechanisms in D2D communication.

A plethora of research has been conducted on PC to improve the battery life of the devices. Authors in [33], present an overview of different PC mechanisms in UL and analyze the performance in terms of cell-edge bitrate and cell capacity. Here, the authors suggest fractional path-loss compensation of the open loop mechanism with the target to improve the cell capacity. Similarly, in [30], the authors tune the standard open loop PC, which results in a gain of 20% on the average cell throughput. Inspired by the advantages of PC in the uplink, PC in SL has attracted a lot of research in recent times, triggering various investigations. PC methods for D2D, such as a reinforcement learning algorithm proposed in [102] for adaptive PC, targets to increase the system throughput, and a distance-based PC for D2D in [72] shows an improvement in terms of spectral efficiency. For D2D PC in underlay mode, the authors in [94] propose two algorithms to solve the optimization problem of maximizing the achievable sum-rate of the D2D link while fulfilling the minimum rate requirement of the cellular link. However, this solution is limited to a system design where a single D2D link is considered that shares a resource with only one cellular link. The authors in [100] propose an optimal PC algorithm considering point-to-point transmissions, in which the power is incremented gradually with consecutive HARQ retransmissions for lower outage probabilities. We extend this PC algorithm for the dual-user cooperative retransmissions via SL by allowing a power boost with every retransmission attempt.

We consider the existing PC mechanism and design an optimal power allocation scheme tailored for CoRe with dual-user SL-assisted retransmissions. The following methods of PC are investigated for determining the UE transmit power for the CoRe scheme.

4.5.2 Static-SNR Scheme: DL-Based Power Control (PC)

The open loop power scheme [33] is the most commonly applied PC algorithm in UL. It is based on wideband average SNR and path-loss measurements at the transmitting UE. The general scheme, including open loop and closed loop operation, is based on a fixed targeted received SNR level SNR_{target}, where the UE/cell-specific nominal power P_0, can be calculated as given by

$$P_0 = SNR_{target} + P_n \tag{4.7}$$

where: SNR_{target} = targeted received SNR level
P_n = noise power level
P_0 = nominal power

The UE power constraint is derived based on the following PC equation [33]

$$P = \quad 10 \cdot \log_{10}(M_{RBs}) + P_0 + \alpha \cdot PL + \delta + f_c \tag{4.8}$$

where: M_{RBs} = number of physical resource blocks
P_0 = cell-specific nominal powers
α = path-loss compensation factor
PL = path-loss estimate at the UE
δ = a value depending on the chosen modulation and coding scheme
f_c = function for closed loop correction value

For open loop operation, which will be considered in the scope of this thesis, α is set to unity, while δ and f_c are set to zero. The UE transmit power is limited by its maximum transmit power P_{max}, which is expressed by

$$P_i = \min\{P_{max}, P\} \tag{4.9}$$

where: P_i = transmit power for the UE
P_{max} = maximum transmit power
P = power constraint for the UE

In case of more than one neighbor users cooperatively retransmitting in the same retransmission time instance, the maximum transmit power is equally shared among the cooperating users, yielding a discounted P_{max}. The above power constraint can be applied for two variants considering the path-loss values for SL and DL, i.e., PL_{dl} and PL_{sl}, detailed in the following. Here, we take the DL-based scheme as a generic reference, in which the DL path-loss measurement at the transmitting/assisting UE is considered. This scheme mainly targets to mitigate the interference at the BS during UL transmission since D2D and UL are considered to be in-band. Hence, the nominal power P_0, according to Eq. (4.7), refers to the targeted SINR level at the BS, and; hence, we denote it as P_0^{BS}.

$$P_0^{BS} = SNR_{target}^{BS} + P_n \tag{4.10}$$

The downlink power constraint P_{dl} is correspondingly given as

$$P_{dl} = 10 \cdot \log_{10}(M_{RBs}) + P_0^{BS} + PL_{dl} \tag{4.11}$$

yielding the transmit power

$$P_i = \min\{P_{max}, P_{dl}\} \tag{4.12}$$

where: P_{dl} = power constraint based on DL path-loss
P_0^{BS} = nominal power for targeted SINR level at the BS
PL_{dl} = DL path-loss measure

4.5.3 Dynamic-SNR Scheme: SL-MCS Based Power Control (PC)

For the SL-based scheme, the path-loss measurement from the D2D communication link between assisting UE and target UE is considered. The nominal power P_0, according to Eq. (4.7), now refers to the targeted SINR level at the target UE, and hence we denote it as P_0^{tUE}.

$$P_0^{tUE} = SNR_{target}^{tUE} + P_n \tag{4.13}$$

The SL power constraint is then given as

$$P_{sl} = 10 \cdot \log_{10}(M_{RBs}) + P_0^{tUE} + PL_{sl} \tag{4.14}$$

where: P_{sl} = power constraint based on SL path-loss
P_0^{tUE} = nominal power for targeted SINR level at the target UE
PL_{Sl} = SL path-loss measure

The generic static-SNR SL-based PC is further tailored specifically to our cooperative retransmission scenario of CoRe, where the target SINR can be computed dynamically based on the selected MCS for a particular packet transmission. Since an identical packet with a fixed MCS is retransmitted via SL, the power is now also controlled according to the MCS chosen for the packet to be retransmitted by the assisting UEs. Hence, in contrast to the static-SNR PC scheme, the P_0^{tUE} in Eq. (4.14) is updated dynamically depending on the MCS of each packet to be retransmitted. The target SNR in Eq. (4.7) may be set higher since now we do not intend to keep the interference at the receiver below a certain level as in the DL path-loss based PC scheme, but instead, we target to attain the desired SNR level at the receiving UE, ensuring successful reception of the transmitted packet.

It is important to note that the DL power constraint P_{dl} obtained above still remains valid since the interference at the BS always needs to be kept below a certain level. Therefore, it may overrule the SL power constraint P_{sl}, yielding the overall transmit power, P_i, as follows

$$P_i = \min\{P_{max}, P_{dl}, P_{sl}\} \tag{4.15}$$

4.5.4 Optimal Power Allocation Algorithm

Finally, we investigate an advanced power allocation mechanism focusing on our URLLC specific QoS requirements. Since for URLLC, the target outage probability (ϵ) is to be attained after a total of M retransmissions, it is reasonable to allow for an increased power boost in every single retransmission to gradually approach this target. This enables a power-efficient URLLC communication, as in most cases a moderate amount of transmit power will be sufficient to achieve the SINR required at the receiver to successfully decode the data packet, while only in a few cases a large transmit power is needed to compensate for poor channel conditions due to small-scale fading effects. The problem of optimum power allocation for URLLC using HARQ-based retransmission has recently been solved by the authors in [100]. They consider a point-to-point transmission where retransmissions over independently fading Rayleigh channels are assumed. These conditions correspond to our scenario where a single user retransmits the packet at a time while fully compensating for the path-loss effect. Hence, we reuse this power allocation algorithm for this reference case. However, since the key aspect of our CoRe scheme is the cooperative retransmission by at least two users, we extend the analysis from [100] to find the optimum power allocation for this case of dual-user retransmission in CoRe. We assume the channels to be Rayleigh fading (i.e., NLOS), because it has been noted to be the worst-case scenario in our evaluation (refer to Section 3.2.1 and 3.2.2). We use this assumption for a generous estimate of the transmit power, which ensures that URLLC requirement is reliably met (since the exact K-factor of Ricean channel is assumed to be unknown, and the direct link may be subject to blocking in any D2D link). Hence, we adopt a conservative approach for power allocation by assuming that the single D2D links are independently Rayleigh fading.

At first, we briefly recap the algorithm for single-user retransmission from [100]. The optimum power allocation ρ_m for each retransmission $m \in \{1, \ldots, M\}$ is the outcome of the following optimization problem

$$\min_{\rho_m} \sum_{m=1}^{M} \rho_m E_{m-1}$$
$$\text{s.t.}\, 0 \leq \rho_m,\, E_M \leq \epsilon \tag{4.16}$$

where: M = maximum number of retransmissions
E_m = outage probability up to the m^{th} retransmission
E_0 = 1
ϵ = outage probability

For ARQ-based retransmissions,

$$E_m = \prod_{i=1}^{m} \epsilon_i \tag{4.17}$$

where: ϵ_i is the outage probability of the i^{th} transmission.

For calculating ϵ_i based on the power ρ_i used, the asymptotic approximation for Rayleigh fading channels is used, given by

$$\epsilon_i = \phi / \rho_i \tag{4.18}$$

The SNR obtained from Shannon capacity for the rate R used in the packet transmission is represented by ϕ as

$$\phi = 2^R - 1 \tag{4.19}$$

Considering our CoRe model, the HARQ-based retransmissions are processed using chase combining (CC) as the same original packet is retransmitted in every attempt. Compared to the ARQ case, this outage probability contains an additional factor, $M!$, yielding

$$E_M^{CC-HARQ} = \frac{\phi^M}{M! \prod_{m=1}^{M} \rho_m} \tag{4.20}$$

Using the Lagrangian λ to capture the second condition in Eq. (4.16), solving the optimization problem yields the optimum power allocations

$$\rho_M = \sqrt{\phi\lambda} \tag{4.21}$$

$$\rho_m = \sqrt{2\phi\rho_{m+1}} \tag{4.22}$$

The Lagrangian λ can be found by substituting the power allocations in Eq. (4.20), setting it equal to the overall outage probability ϵ and, solving for λ. For $M = 3$ retransmissions, which corresponds to the figure used in our later evaluations, we obtain

$$\lambda = \phi \cdot \left((3!\,\epsilon)^{8/7} \cdot 2^{4/7}\right)^{-1} \tag{4.23}$$

To address the solution for dual-user retransmissions in CoRe, the asymptotic approximation for the outage probability needs to be adapted, and we need to redo the optimization based on this new approximation. For the dual-user retransmission using transmit diversity schemes, a constructive addition of the channel powers from the users' independently Rayleigh-fading channels is achieved, realizing two-fold diversity gain [15]. This two-fold diversity gain will double the asymptotic slope of the outage probability vs. SNR (in the logarithmic domain).

Following the analysis in [15], we can derive the asymptotic approximation for the outage probability of the dual-user case to yield

$$\epsilon_i = \frac{10\phi}{\rho_i^2} \tag{4.24}$$

Given this updated approximation and following the steps from the preceding analysis, the outage probability for HARQ-CC will be updated for the dual-user case to

$$E_M^{CC-HARQ} = \frac{(10\phi)^M}{M!\prod_{m=1}^{M}\rho_m^2} \tag{4.25}$$

After redoing the optimization based on this altered function for the outage probability, we obtain the following optimum power allocation terms

$$\rho_M = \sqrt[3]{\frac{2\cdot 10\phi\lambda}{M}} \tag{4.26}$$

$$\rho_m = \sqrt[3]{\frac{3\cdot 10\phi\rho_{m+1}}{m}} \tag{4.27}$$

As mentioned above, the Lagrangian λ is found by substituting these power allocations in Eq. (4.25), setting it equal to ϵ and solving for λ. For $M = 3$, we obtain for the dual-user case

$$\lambda = \sqrt{10\phi} \cdot \left((3!\,\epsilon)^{27/26} \cdot 2^{1/13} \cdot 3^{8/13}\right)^{-1} \tag{4.28}$$

The power allocations ρ_m for single-user and dual-user retransmissions are delineated versus the rate R in Figure 4.6. We assume a target outage probability for URLLC of 10^{-5} to be attained after the 3^{rd} retransmission, while the probability of success for the initial (in our scenario: downlink) transmission is assumed to be 10^{-2}. The figure shows that the dual-user case requires significantly less transmit power than the single-user case, thanks to the additional degree of diversity used. Moreover, we observe that the successive power boost from one retransmission to the next is significantly smaller for the dual-user case.

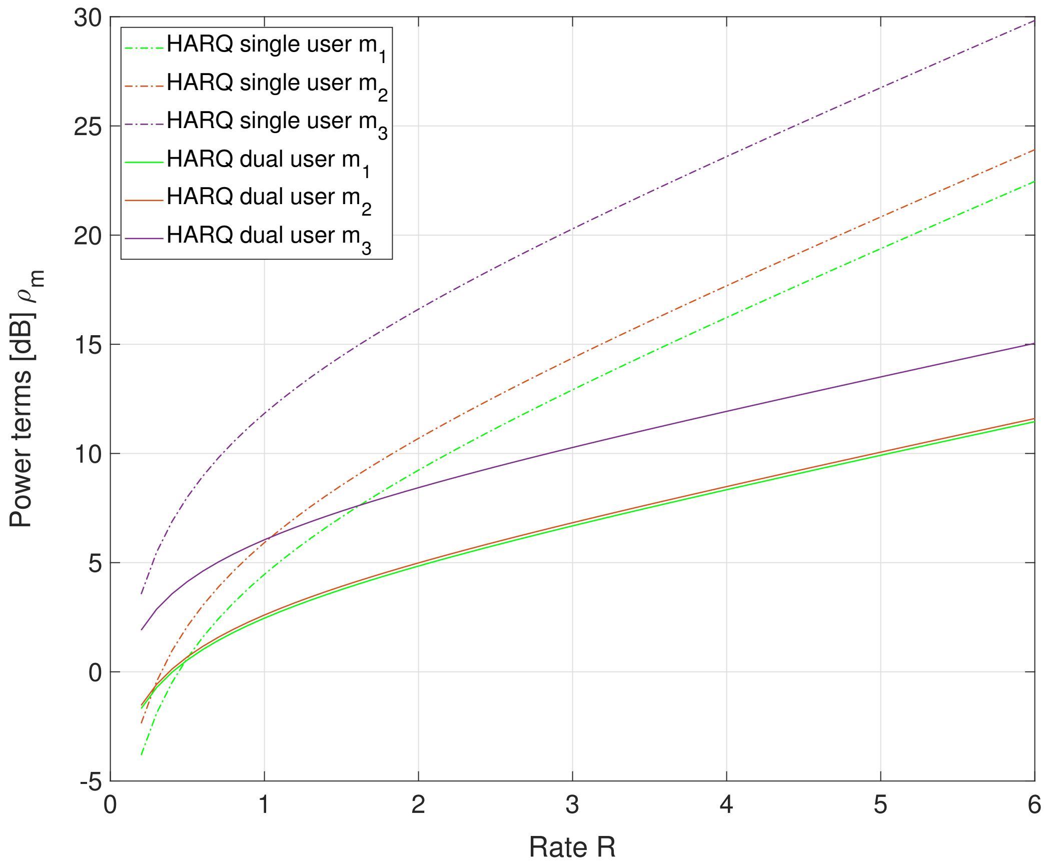

Figure 4.6: Power terms based on Optimal PC algorithm

Each power allocation ρ_m is applied to our reference SL-based PC scheme, given by Eq. (4.14) and Eq. (4.15) by setting it equal to the targeted SINR (at the target UE) in Eq. (4.7), which yields the corresponding P_0^{tUE}. Note that due to the dependency of ρ_m on the rate R through $\phi = 2^R - 1$, the power is now also controlled according to the MCS chosen for the packet to be retransmitted by the assisting UEs.

4.6 Performance Evaluation with Power Control (PC)

We evaluate the performance of the optimal PC algorithm for single-user CoRe and dual-user CoRe elaborated above compared to the conventional static-SNR DL-based and SL-based PC schemes. The system design and simulation configurations described above in Section 4.2 and Table 4.1 are applied for this PC analysis as well. The latency of successful receptions is measured at the medium access control (MAC) layer, which inherently includes the queuing and processing delays.

Considering the V2X system model illustrated in Section 4.2.1, we evaluate the power savings from the optimal power allocation compared to the DL-based PC scheme while proving that the latency performance is not compromised. In this investigation, a maximum transmit power of 10 dBm is considered for D2D transmissions via SL.

Figure 4.7 shows the cumulative distribution function (CDF) of the transmit power used by the retransmitting users, aggregated over all $M = 3$ retransmissions, for applying the different PC schemes. The reference case of DL-based PC is represented by the black curves, dashed and solid curves for single and dual-user cases, respectively. As limited by the

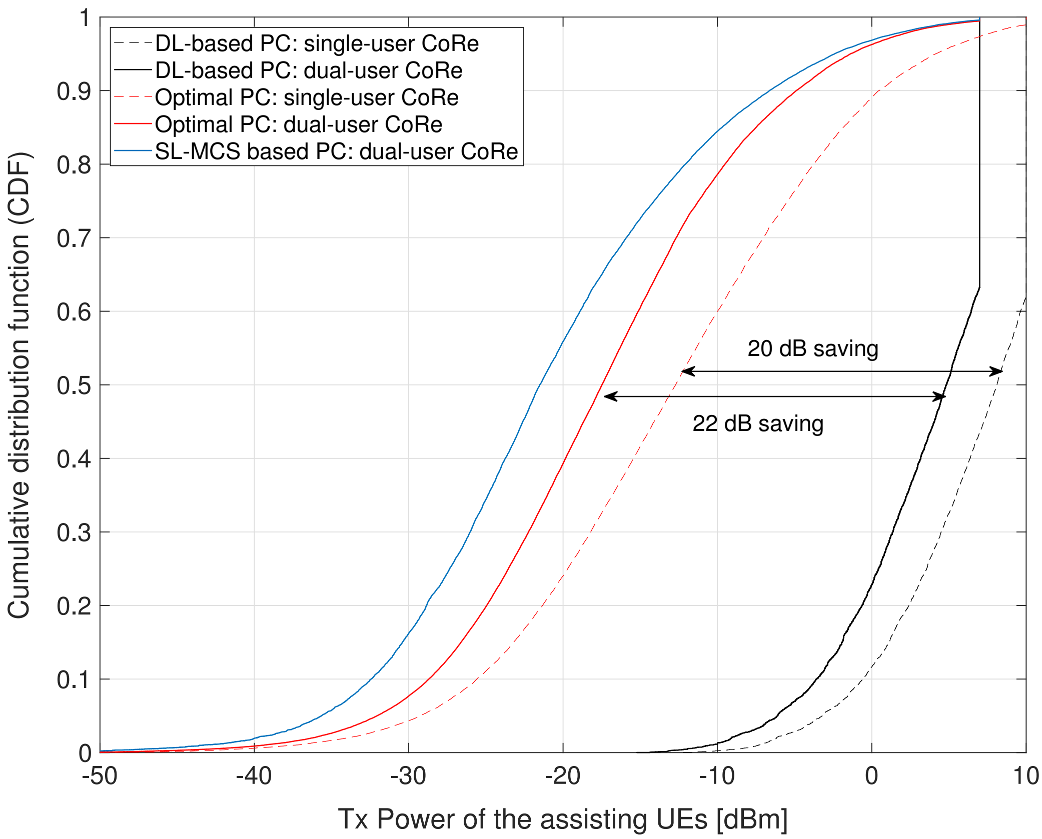

Figure 4.7: Power saving from Optimal PC compared to the conventional DL-based PC

DL-based power constraint only to protect the BS and using P_{max} otherwise, this scheme consumes the maximum transmit power among all schemes. For the dual-user case, the actual transmit power is always 3 dB lower than in the single-user case, which represents the discount factor considered to account for the total power being contributed by two users. The solid blue curve shows the UE transmit power when the SL-MCS based power constraint using the SL path-loss is applied, serving as the power level where the power boost sets off. The red curves in between those curves represent the optimal power allocation with the target reliability of $\epsilon = 10^{-5}$. Comparing these to the DL-based scheme, we observe a significant power saving, which amounts to 20 dB for the single-user case (measured for the median) and increases to 22 dB for the dual-user case, highlighting a gain of an additional 2 dB when going from single-user retransmission to cooperatively retransmitting users. Moreover, the slope of the two red curves reveals that the variance in the transmit power is significantly reduced for the dual-user case compared to the single-user case, making visible the gain from the additional channel diversity, thus stabilizing the signal conditions.

When looking at the corresponding latency performance of the schemes with optimal PC and other reference PC in Figure 4.8, we observe that the latency performance required for URLLC type of service can be readily attained by all the schemes except the SL-MCS based PC scheme. As the SL-based power constraint P_{sl} aims at achieving a constant average SNR at the receiver (target UE), applying this constraint results in performance degradation due to channel fading. Therefore, we take our SL-MCS based PC as the reference level where the power boosting for the retransmissions sets off. In fact, power boosting is used to overcome the deviation of the channel due to the small-scale fading effects. The optimal PC scheme and the reference DL-based PC attain reliability, $\epsilon = 10^{-5}$, after the 3rd retransmission (represented by the 4th and rightmost plateau of the delay performance curves). Hence, the results confirm that the power savings highlighted in Figure 4.7 indeed do not compromise the URLLC performance, as postulated by the corresponding requirement considered in the optimization process.

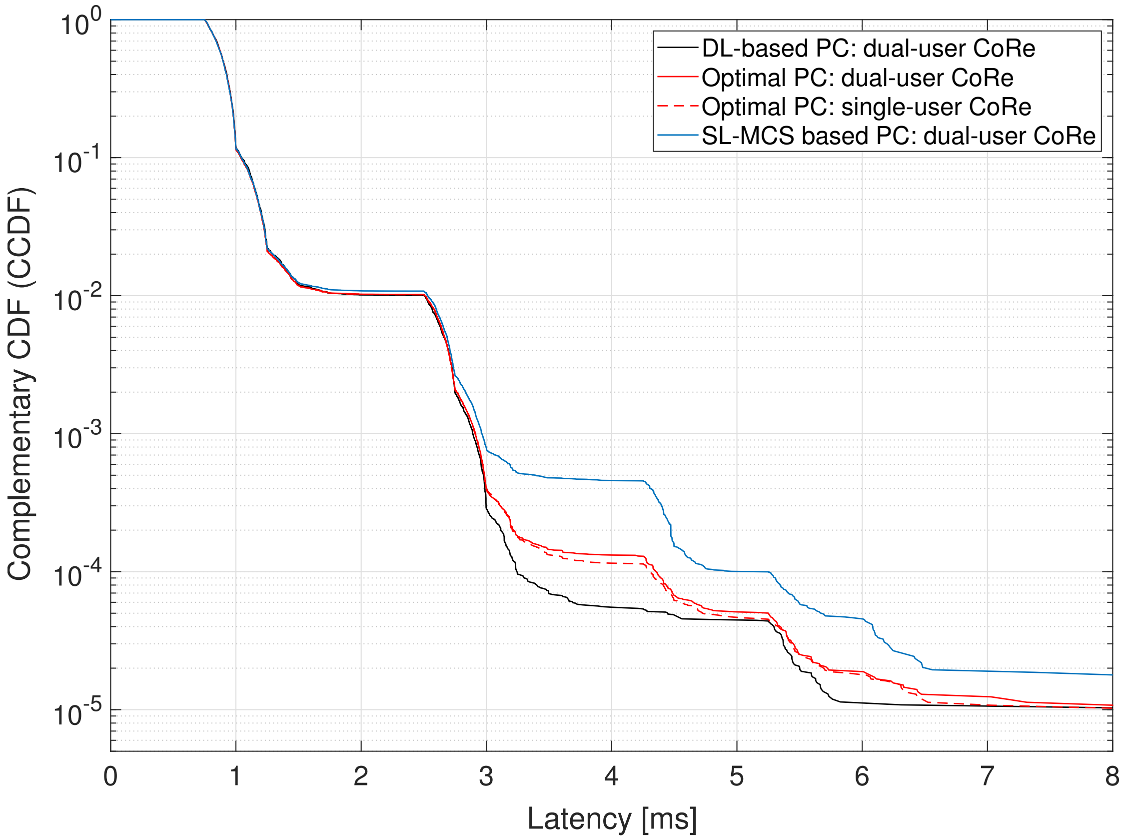

Figure 4.8: Latency Performance with Optimal PC scheme compared to conventional PC

Finally, we depict the SINR conditions measured at the receiving target UE in the form of a CDF in Figure 4.9. The results show that maximum received SINR is attained with the DL-based PC scheme and minimum received SINR is attained with the SL-MCS based PC scheme. The received SINR attained with the optimal PC schemes lies in between, with a difference of roughly 20 dB to the DL-based reference curve, which aligns with the observations made from Figure 4.7. We observe further that the SINR curve for dual-user is much steeper than for single-user, again highlighting the effect of diversity stabilizing the channel and thus reducing its variance. Moreover, we observe that the received SINR is lower for the dual-user case in the median and above, compared to the single-user, while it is equal in the left tail of the CDF. This indicates that the optimal PC strongly focuses on the poor channels (represented mainly in the left tail of the CDF). Thanks to the reduced channel variations due to additional diversity, less excessive power is spent for boosting, resulting in a smaller median SINR while still being sufficient to fulfill the reliability target, though (Figure 4.8).

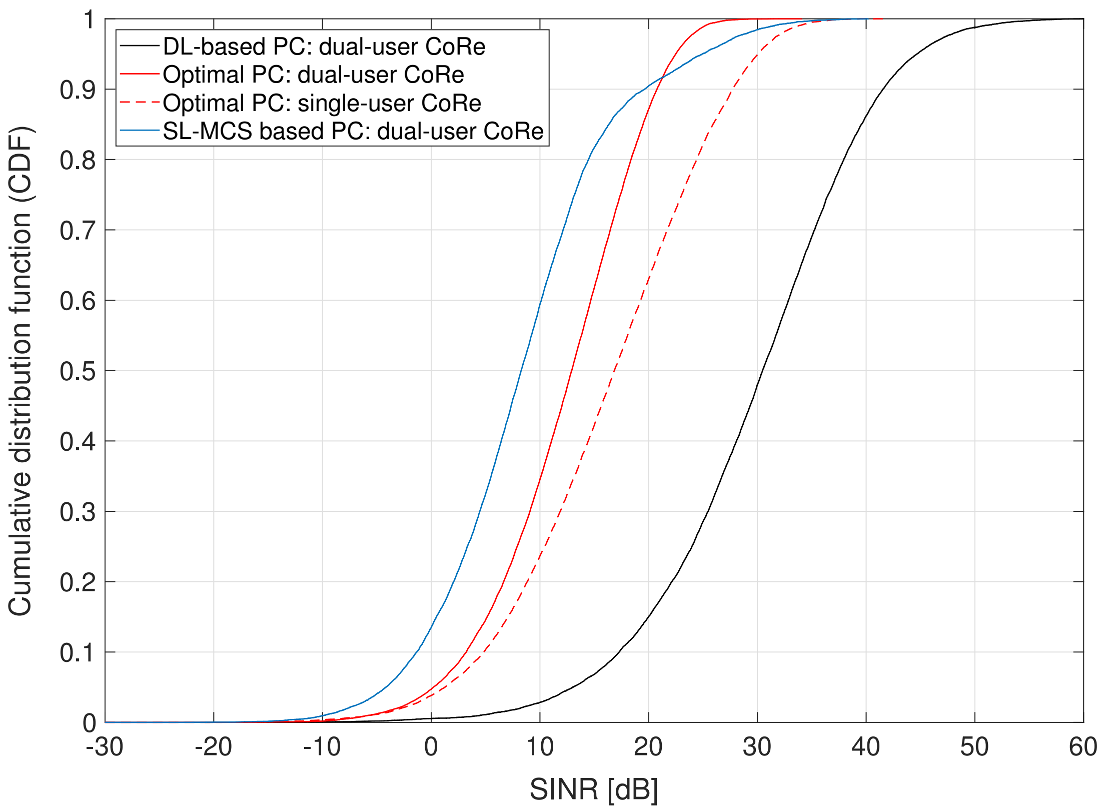

Figure 4.9: SINR performance for different PC schemes

Hence, from this investigation, we conclude that to reduce interference while maintaining the delay performance, both DL-based and SL-based path-loss measures should be considered together with further enhancements in terms of appropriate power boosting as realized by the optimal PC algorithm. In particular, the retransmission-specific PC strategy investigated in this thesis provides an optimum trade-off with regard to system performance and power saving.

4.7 Summary

In this chapter, we move the focus to more practical evaluation scenarios, which are infeasible to emulate using analytical models. A system-level evaluation of the *CoRe* scheme is presented considering the V2X scenario. The system design, simulation configurations, and the V2X system model are illustrated in detail. The evaluation in this chapter is intended to gauge the performance of the CoRe scheme for realistic scenarios using a system-level network simulator, NS3, as the platform.

Initially, three different user selection and grouping schemes for CoRe are investigated: (1) random-user selection: users are selected and grouped randomly; (2) best-user selection: the best users are selected, and grouped sequentially for every retransmission; and (3) user-combination selection: best users are selected and a unique combination of users is formed for every consecutive retransmission. The latency performance for a URLLC target reliability of 10^{-5} is examined for the three user selection methods. The simulation performance for CoRe shows lower latencies compared to the traditional DL retransmissions. Thus, fewer resources are required on average because of the reduced number of retransmissions. Comparing the three user selection schemes, it can be inferred that the user-combination method is the most efficient. It can attain the reliability target of 10^{-5} by using only two users for every retransmission, unlike the best-user selection with $k = 3$ users. Using the CoRe scheme, 98% of the retransmissions are already successful in the first retransmission attempt, whereas only 86% of the first retransmissions are successful when traditional DL retransmissions are applied. Hence, a reliability of 99.999% can be attained already after two retransmission attempts by implementing CoRe instead of original DL retransmissions which need at least three retransmissions to fulfill URLLC target reliability.

Further, we extend the research on CoRe by employing an optimal power control (PC) mechanism for the SL-assisted retransmissions, mainly to mitigate the interference to BS and other D2D users, probable due to a large number of D2D UEs transmitting. The transmit power allocation is mainly based on the path-loss from each user cooperating to the target user. Three different PC methods are investigated for CoRe: (1) Static-SNR DL-based PC scheme: power allocation is dependent on the DL power constraint, and it mainly targets to mitigate the interference at the BS; (2) Dynamic-SNR SL-MCS based PC scheme: power allocation is dependent on the SL power constraint and the MCS of the packet, with the aim to attain the desired SNR level at the receiver; and (3) Optimal PC scheme: allows gradual increments in power boost with every retransmission and extends the dynamic-SNR SL-MCS based PC scheme. The CoRe scheme with these PC methods is examined by taking the DL-based PC as the reference case for single-user (one user retransmits in every retransmission) and dual-user (two users retransmit in every retransmission). Consequently, the optimal PC scheme shows a significant reduction in power consumption for single-user and dual-user retransmissions. While consuming considerably less transmit power, the outcome of CoRe with the optimal PC scheme underlines that the URLLC performance is not compromised and the reliability target of $\epsilon = 10^{-5}$ can be successfully achieved.

5

Cooperative Retransmission Scheme (CoRe) for IIoT with Further Extensions

In this chapter, we extend our investigation on the CoRe model to a realistic scenario focusing on the next challenging use case: Industrial IoT (IIoT) communication. We present a system-level performance analysis of CoRe and propose a new radio resource management algorithm for better utilization of resources.

5.1 Industrial IoT (IIoT) Communication

Internet-of-things (IoT) is defined as the network of smart devices that enables data gathering and control in real-time using sensors and actuators. Henceforth, Industrial IoT (IIoT) refers to the application of IoT using these smart devices to ease, strengthen, and automate the production and manufacturing processes in the industrial context. The core pillars of Industry 4.0 are presented in Figure 5.1, such as IoT for device interaction, big data for extracting and analyzing information, cloud computing for easy access and data storage using remote servers, augmented reality for virtual tasks and training, autonomous robots to perform designated tasks without human interaction, and automated additive manufacturing.

Components such as sensors, robots, automated guided vehicles (AGVs), wearables, and unmanned aerial vehicles (UAVs) can be interconnected wirelessly to facilitate industrial use cases (Figure 5.1).

Unlike traditional production systems, future production lines supporting customized products are expected to be more dynamic. Customization of products requires the special assembly of the production lines tailored to the product. Thus, frequent reconfiguration and rearrangement of the production line setup is deemed necessary. Under this vision of smart factories, connectivity among devices availing wireless links will provide high flexibility and avoid mechanical breaks of cables while moving. Thus, future factories will constitute a massive number of devices capable of interacting with each other via a wireless connection, supported by massive machine-type communication (mMTC), allowing the transmission of short packets with low data rates. However, typical applications in IIoT demand high reliability of 99.999% within a strict latency budget of $1-5$ ms to enable a steady production system, calling for ultra-reliable low-latency communication (URLLC) service. The abundant devices in the neighborhood allowing a direct device-to-device (D2D) connection in such

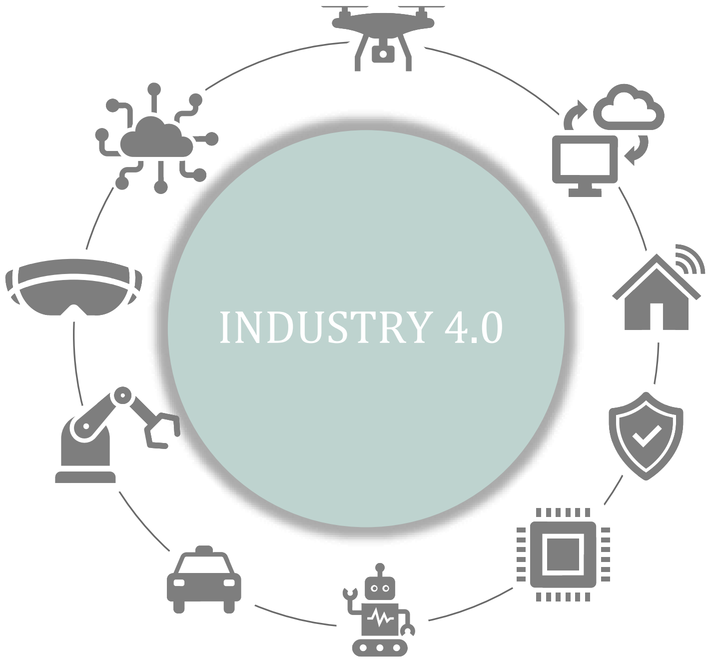

Figure 5.1: Industrial IoT (IIoT) Use cases [93]

an industrial factory scenario can form a mesh network similar to the vehicle-to-everything (V2X) application scenario (refer to Section 4.1) investigated in the preceding chapter. However, the probability of link blockage is higher in a factory hall containing small ultra-dense cells due to the dense machine deployments and many continuously mobile AGVs in close proximity to the machines. Thus, this makes IIoT another promising application for the *CoRe* scheme. Therefore, we further extend our research on CoRe by considering an industrial factory setup as detailed in the next Section.

5.2 System Design

5.2.1 Industrial Factory System Model

We consider an Industry 4.0 factory scenario, as shown in Figure 5.2, assuming multiple AGVs moving around in the factory, representing mobile communication nodes. The network deployment scenario follows the 3GPP modeling guidelines for industrial factory networks [99]: an indoor factory with dense clutter and low base station height (InF-DL) with a network topology, as given in Figure 5.3, is considered. NS-3, the discrete-event-driven network simulator [43], along with QuaDRiga [119], a channel generator for the industrial factory channel propagation model [99], is used for performance analysis. The general system design configuration presented in Section 4.2 is applied. Unlike the traditional hexagonal topology used in cellular networks, as per the 3GPP specification [99], a typical industrial factory topology is designed for a rectangular room layout representing the factory hall. Transmit and receive points (TRPs)/BSs were deployed according to a regular squared grid with a constant distance between the TRPs in any direction. For the sake of consistency and simplicity, we consider a BS to function similarly to a TRP of an indoor factory hall.

A factory hall deployment of $120 * 60$ m, as illustrated in Figure 5.3, with 18 BSs/TRPs mounted on the ceiling with an inter-site distance of 20 m is considered. We assume a bandwidth of 20 MHz, consisting of 100 resource blocks (RBs) in the time-frequency domain, and 180 active users. The user equipment (UEs) are dropped uniformly in the factory area and are attached to the strongest BS/TRP based on average received power, yielding ten users per TRP on average.

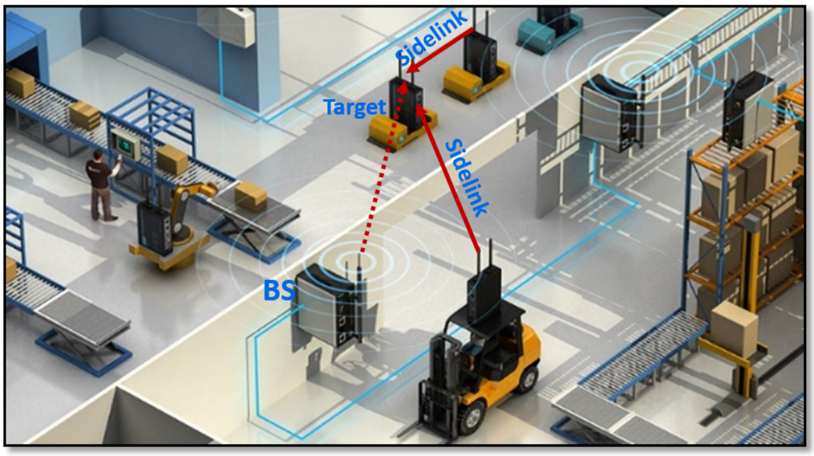

Figure 5.2: Factory automation scenario [118] [110]

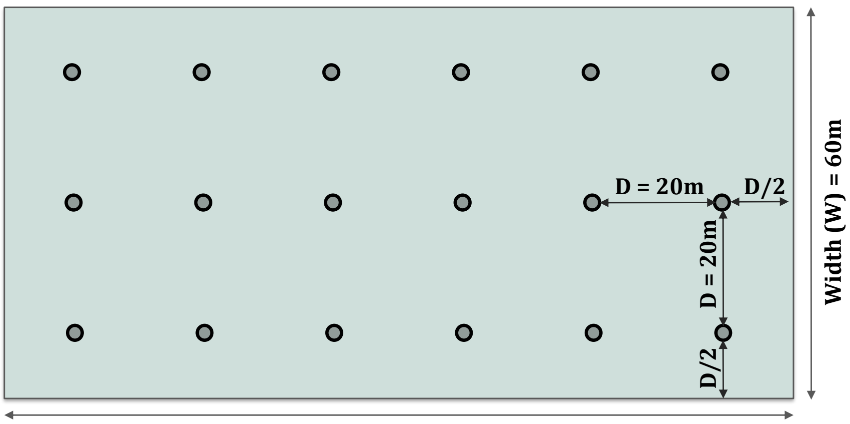

Figure 5.3: Network Topology - Factory automation: 18 TRPs mounted on the ceiling

The abundant AGVs in a factory fall can establish radio links to other AGVs, thus forming direct connections via SL between AGVs. Assuming a factory environment with rich scattering, which is a common observation from measurements in typical factory halls due to the infrastructure and setup of a large number of machinery and mobile AGVs distributed all over the factory floor. Therefore, the AGVs will experience independently fading channels to other AGVs if they are spaced more than half a wavelength apart. The assumption of independent fading also holds for Ricean channels with a strong LOS component, as long as the K-factor does not become very large. Note that measurements in factories have shown that the K-factor of Ricean channels typically lies significantly below 10. As per the 3GPP specification on channel modeling, K-factor for indoor factory channels is suggested to be 5 to 7 dB [99].

All the UEs are assumed to be always in an active state, ready to assist with retransmissions if needed. User mobility of pedestrian speed is modeled considering the slow-moving AGVs in a factory. Similarly, in this evaluation, multiple independent user constellations (user drops) are simulated and averaged to ensure sufficient statistics. Further simulation parameters are described in Table 5.1.

Table 5.1: Industrial Factory - System configuration

Parameters	**Value**
Layout	Factory room 120*60m
Bandwidth	20 MHz
Carrier frequency	2.3 GHz
No. of cells	18
No. of UEs	180
Inter-site distance	20 m
TTI size	250 μs
Packet size	48 bytes
Traffic load (per cell)	5 Mbps
BS/TRP transmit power	23 dBm
UE transmit power	10 dBm
Antenna system	2*2 MIMO
UE mobility	3 Kmph
UE distribution	Uniformly
Channel model	InF DL model

We use the Indoor factory-dense-low clutter (InF-DL) channel model with dense clutter and low base station height (both transmitter and receiver are below the average height of the clutter), as defined by 3GPP [99]. Clutter in the industrial context consists of shelves, machinery, assembly line, metallic objects, or other stationary equipment in a factory hall.

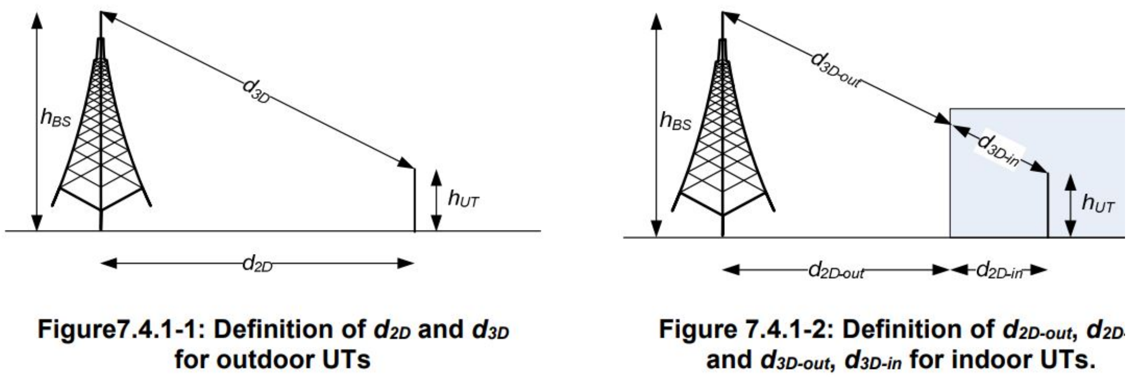

Figure 5.4: Definition of distances in factories [99]

The definition of distances in factories in this 3GPP channel model [99] illustrated in Figure 5.4, is given by

$$d_{3D-out} + d_{3D-in} = \sqrt{(d_{2D-out} + d_{2D-in})^2 + (h_{BS} - h_{UT})^2} \tag{5.1}$$

where: d_{2D} = 2D distance
d_{3D} = 3D distance
h_{BS} = height of the base station (BS)
h_{UT} = height of the user terminal (UT)

The probability of line of sight (LOS) P_{LOS} is defined as a function of distance d_{2D}:

$$P_{LOS} = \exp\left(\frac{-(d_{2D})}{k_{subsce}}\right) \tag{5.2}$$

where,

$$k_{subsce} = \exp\left(\frac{-(d_{clutter})}{\ln(1 - C_{density})}\right) \tag{5.3}$$

Here, $d_{clutter}$ = 2m defines the typical clutter size and $C_{density}$ = 60% is the clutter density i.e., the percentage of surface area occupied by clutter.

The path-loss models for LOS and non-LOS (NLOS) components defined by InF-DL channel model are stated below:

$$PL = \begin{cases} 31.84 + 21.5 \lg(d_{3D}) + 19.0 \lg(f_c) & \text{LOS} \\ 18.60 + 35.7 \lg(d_{3D}) + 20.0 \lg(f_c) & \text{NLOS} \end{cases} \tag{5.4}$$

where, PL_{LOS} and PL_{NLOS} is the LOS path-loss (dB) and NLOS path-loss (dB) respectively, f_c is the career frequency (MHz) and d_{3D} is the 3D link distance (m).

where: d_{2D} = 2D distance
d_{3D} = 3D distance
P_{LOS} = probability of LOS path-loss
P_{NLOS} = probability of NLOS path-loss
$d_{clutter}$ = size of the clutter [m]
f_c = carrier frequency
$C_{density}$ = the percentage of surface area occupied by the clutter

We apply the industrial channel model [99] illustrated above in our system-level evaluation, as the dense clutter channel model represents a commonly observed stringent factory hall scenario in industrial IoT use cases. The clustering-based inter-cell interference coordination (ICIC) mechanism elaborated below in Section 5.2.2 is applied to mitigate interference induced by the closest neighboring BSs/TRPs.

5.2.2 Interference Management and Power Control (PC)

In the given industrial network topology, the interference introduced in a factory hall scenario can be large due to the numerous closely located sites in a small cell network. Especially, inter-cell interference (ICI) can be inevitable, causing a higher impact in such densely populated small-cell factory networks [109, 45]. To solve the problem of inter-cell interference (ICI), several interference coordination techniques such as frequency partitions, coordinated multi-point (CoMP) [58, 36], and enhanced inter-cell interference coordination (eICIC) [42] where the dominant interfering cell is muted [46], have been studied. Authors in [80] conclude that eICIC using muting, where the serving cell schedules its UE on the resources which are muted for the interfering cell, helps in improving the reliability and latency for URLLC. Convinced by the benefits and its simple realization, we adopt this well-known principle of muting [42] and implement a user-centric clustering-based ICIC scheme to mitigate interference from the nearest neighbor BSs.

We apply the UE-centric clustering on a per-user basis, where a cluster of the four closest BSs to the UE is formed. The members of the cluster are selected depending on their distance to the UE, which the user can determine based on the path-loss measured for the downlink signals. We assume each user to be served only by a single BS, while the other three closest BSs (members of the cluster) are muted in the resources which are used by the serving BS for that user. This measure translates to a frequency reuse factor of four within the cluster of four BSs to eliminate the major source of ICI. Such coordinated resource management requires synchronization among the BSs, which allows the member BSs of the cluster to be aware of their nearest BSs and their respective radio resource management. This can be easily facilitated by fully coordinated centralized architectures [106], which are likely to be used in future factory networks.

We consider the set of all BSs to be Q with size Q_s, which contains the surrounding BSs including the BS to which the target device (AGV) is connected.

$$\begin{aligned} Q &= \{BS_1, BS_2, BS_3 \dots BS_{Q_s}\} \\ |Q| &= Q_s \end{aligned} \tag{5.5}$$

Without any clustering of BSs for interference mitigation, the SINR at the target device (AGV) is given by (5.6). The term on the numerator depicts the useful signal from the serving BS, and the first term on the denominator computes the interference from all other BS present in the neighborhood.

$$\hat{\eta}_{AGV} = \frac{P_{BS_i}\zeta_{BS_i,AGV}}{\sum_{j\neq i, j=1}^{j=Q_s} P_j \zeta_{BS_j,AGV} \; + \; N_0} \tag{5.6}$$

Let us consider the cluster of closest BSs to be C, given as

$$\begin{aligned} C &= \{BS_1, BS_2, \dots BS_{C_s}\} \quad \text{such that} \quad C \in Q \\ |C| &= C_s \end{aligned} \tag{5.7}$$

The original set of all BSs Q (5.5) can be split into two sets C and R. Given the cluster of BSs C in (5.7), the remaining BSs are given by set R as

$$\begin{aligned} R &= Q \setminus C = \{BS_1, BS_2, \dots BS_{R_s}\} \quad \text{such that} \quad R \in Q, C \in Q \\ |R| &= R_s = Q_s - C_s \end{aligned} \tag{5.8}$$

The SINR at the target AGV computed in (5.6) can be re-formulated for the case without muting as

$$\hat{\eta}_{AGV} = \frac{P_{BS_i} \zeta_{BS_i,AGV}}{\sum_{l \neq i, l=1}^{l=R_s} P_l \zeta_{BS_l,AGV} + \sum_{k \neq i, k=1}^{k=C_s} P_k \zeta_{BS_k,AGV} + N_0} \tag{5.9}$$

In the above equation, the second term in the denominator indicates the interference power by the nearest base stations in cluster C. At the same time, the first term is the interference power from the remaining BSs, excluding the ones in the cluster set C.

where: i = index of the serving BS to which the target device (AGV) is attached to
j = index of BSs in set Q
k = index of BSs in set C
l = index of BSs in set R
Q = set of all BSs
C = set of the closest BSs to the serving BS
R = set of remaining BSs excluding BSs in C
Q_s = total number of elements in set Q of BSs
C_s = total number of elements in set C of BSs
R_s = total number of elements in set R of BSs
P_X = transmit power of device X
$\zeta_{X,Y}$ = channel gain between device X and device Y
N_0 = noise power

We illustrate the UE-centric clustering in Figure 5.5 for a snapshot of our industrial factory scenario [116]. Here, AGV1 is served by the strongest BS, i.e., BS1. A cluster of four BSs is formed for AGV1, constituting the serving BS and the three closest BSs (BS2, BS3, and BS4) to itself. For the resources allocated to AGV1, the members of its cluster (BS2, BS3, and BS4) other than the serving BS are muted. Thus, the strongest ICI that could be caused by the neighboring BSs shown by dashed arrows is eliminated for AGV1. The attainable SINR at the AGVs can be computed using (5.10) correspondingly. Similarly, AGV2 and AGV3, being served by BS2 and BS3, respectively, form clusters of their own and eliminate the interference from their cluster members, i.e., the three nearest neighbor BSs. This resource-based UE-centric clustering is applied dynamically to all the active UEs in the network.

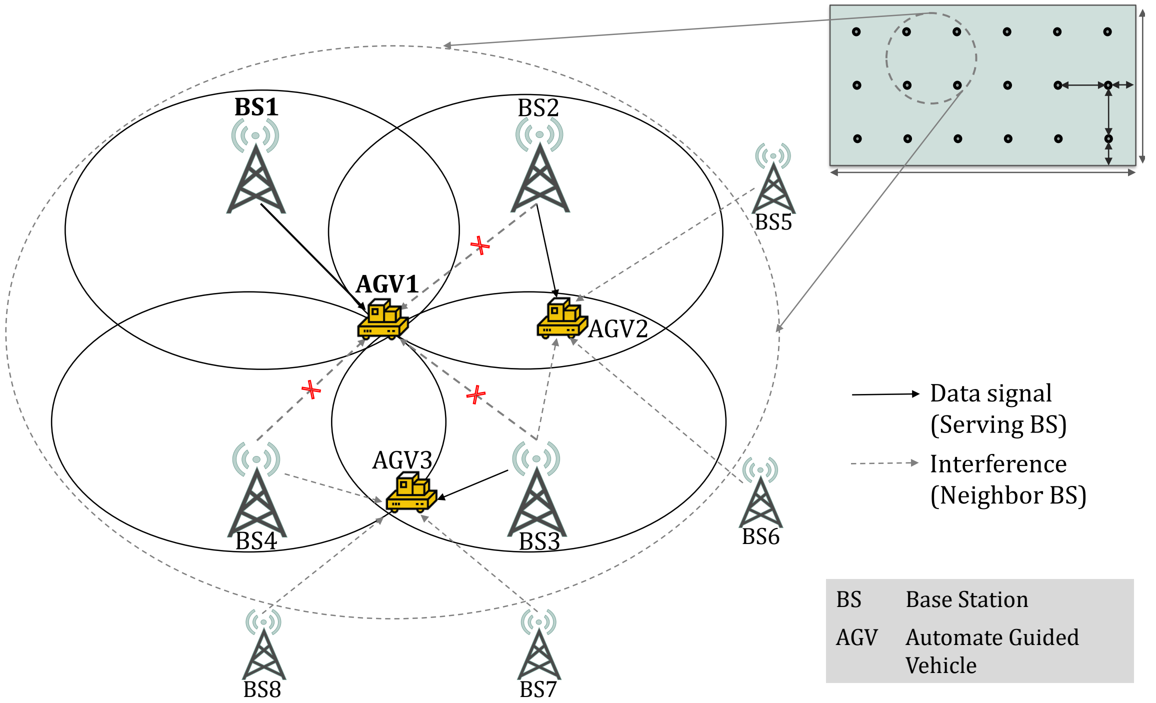

Figure 5.5: UE-centric Clustering-based Inter-Cell Interference Coordination (ICIC)

Applying the UE-centric clustering with cell muting, the interference imposed by the cluster of nearest BSs is eliminated. Thus, the SINR at the target AGV is now only affected by the interference from the remaining BSs in set R. Henceforth, referring to Eq. (5.9), the SINR after user-centric clustering-based interference mitigation can be written as

$$\eta_{AGV} = \frac{P_{BS_i}\zeta_{BS_i,AGV}}{\sum_{l\neq i,l=1}^{l=R_s} P_l\zeta_{BS_l,AGV} \; + \; N_0} \tag{5.10}$$

The interference from the cluster of closest BSs C containing C_s number of BSs is nullified; thus, the second term in Eq. (5.10) becomes

$$\sum_{k\neq i,k=1}^{k=C_s} P_k\zeta_{BS_k,AGV} = 0 \tag{5.11}$$

Further, when considering SL-assisted cooperative retransmission in CoRe, management of transmit power allocation has been shown to be one of the key aspects beneficial to reduce the interference further that may be imposed on the system if multiple D2D UEs are simultaneously transmitting [110]. As highlighted in Section 4.5, the need for PC is inevitable for power efficient as well as resource-efficient cooperative transmissions. Thus, the UE transmit power is allocated depending on the path-loss of the assisting UE to the target UE to allow for a balanced user contribution when multiple users are cooperating by applying the PC schemes stated above (Section 4.5).

5.3 Performance Evaluation with Power Control

The performance of the CoRe scheme with user-centric clustering-based ICIC and PC for single-user and dual-user retransmissions, elaborated in Section 4.5, is evaluated compared to the conventional DL retransmissions. Applying the generic system design stated in Section 4.2, including the configurations of the factory setup illustrated above in Section 5.2.1, we analyze two cases: single-user and dual-user cooperative retransmissions (CoRe) [116]. In single-user CoRe, only one distinct user retransmits per transmission attempt, whereas in dual-user CoRe, two distinct users cooperatively retransmit in every retransmission.

Figure 5.6 represents the latency performance of the CoRe scheme in comparison to the traditional DL retransmissions. The reference case of conventional DL retransmissions is shown in the solid black curve, where the probability of retransmission is much higher compared to all cases of cooperative retransmission. The plateaus in the curve highlight the successive (re-)transmission attempts from left to right, which are caused as an effect of the HARQ RTT and queuing delay. The performance with cooperative retransmissions highlights an evident reduction in the overall probability of retransmission up to one order of magnitude at the plateaus. A reliability target of $\epsilon = 10^{-5}$ is already attained after two retransmission attempts with the CoRe scheme. For the cases of CoRe, we observe a lower probability of retransmission when dual-user is considered, thus, highlighting additional gains from diversity.

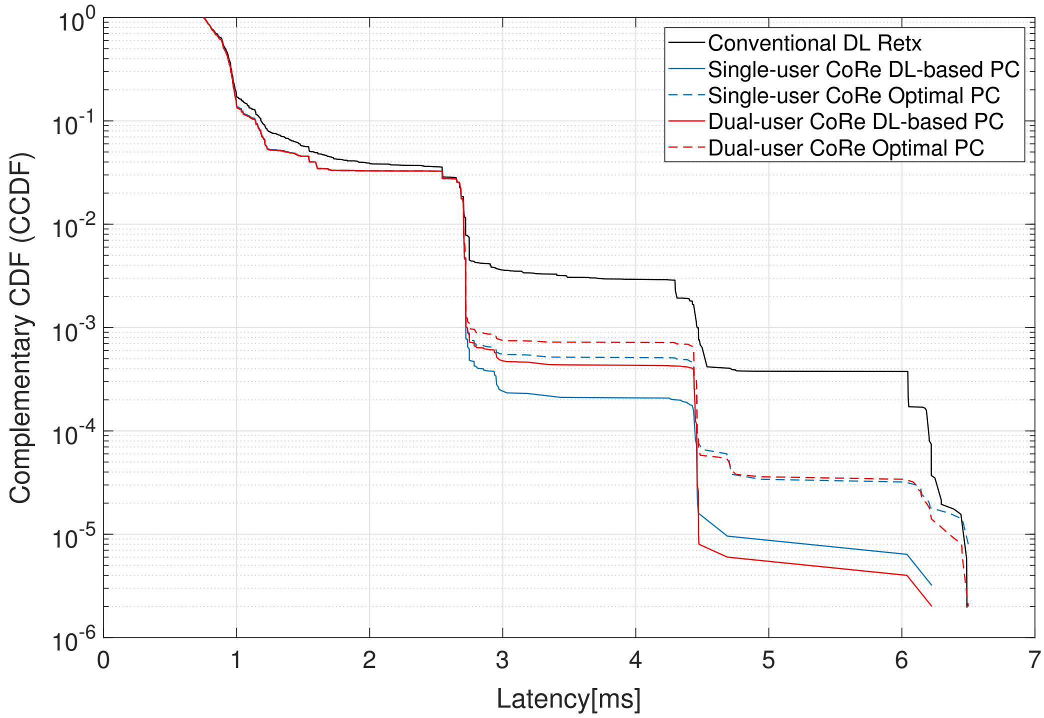

Figure 5.6: Latency Performance with Optimal PC scheme compared to conventional PC

Further, the optimal power allocation (Section 4.5.4) scheme for single-user and dual-user CoRe, allows for saving transmit power for the retransmissions. Here, the end latency performance can be maintained or even improved using the optimal PC, which also attains the reliability target of $\epsilon = 10^{-5}$ after two retransmissions while providing huge power savings compared to the DL-based PC scheme, shown in Figure 5.7, explained below.

The optimal power allocation scheme with respect to its transmit power consumption is investigated compared to the DL-based PC scheme. A maximum transmit power of $P_{max} =$ 10 dBm is considered for SL transmissions. Figure 5.7 shows the cumulative distribution function (CDF) of the transmit power used by the retransmitting users, aggregated over all $M = 3$ retransmissions. The reference case of DL-based PC is represented by solid curves with blue and red curves for single and dual-user CoRe, respectively. As limited by the DL-based power constraint only to protect the BS and using P_{max} otherwise, this scheme consumes transmit power with a median of roughly −5 dBm when single-user is considered. However,

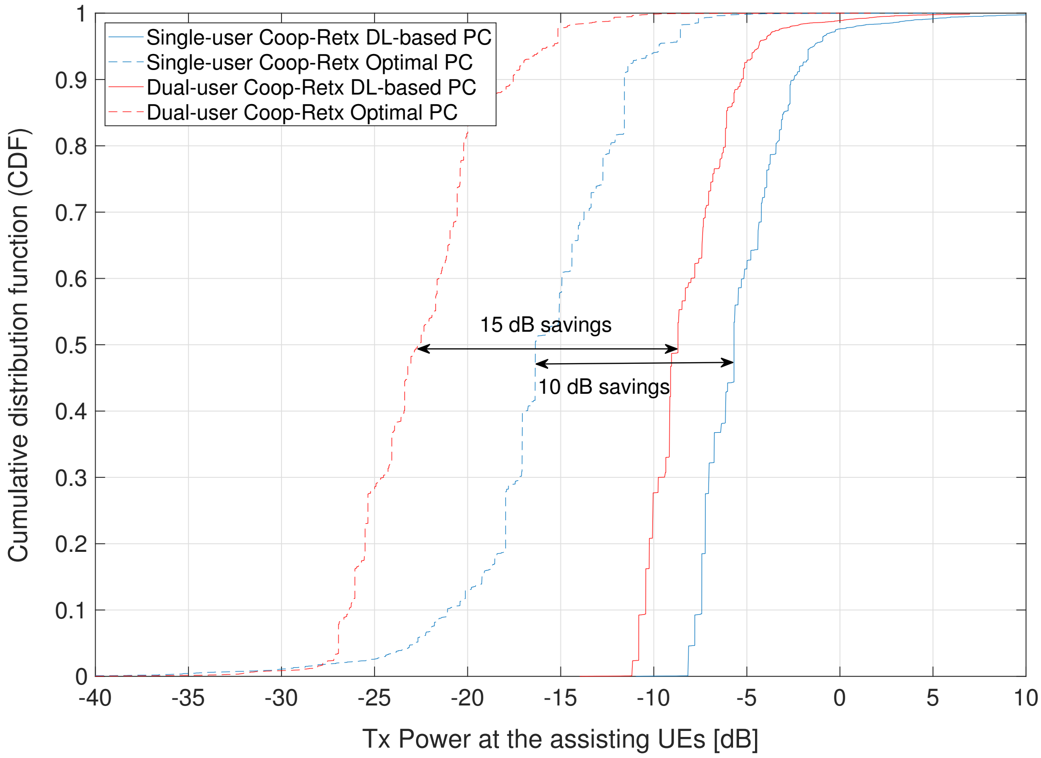

Figure 5.7: Power saving of retransmitting UEs by applying optimal PC

here P_{max} is never applied since the DL-power constraint always discounts it due to the short link distance between the BS and its associated UEs in a factory hall. For the DL-based PC, the curve for dual-user is shifted to the left by a discounted factor of 3 dB, as the power is divided among the two cooperating users. The dashed curves represent the optimal power allocation with a target reliability of $\epsilon = 10^{-5}$. Comparing these to the DL-based PC scheme, we observe a significant power saving, which amounts to 15 dB and 10 dB for the dual-user and single-user cases, respectively (measured for the median). Relatively less transmit power is needed for dual-user CoRe, which justifies the lower power boost for dual-user HARQ retransmissions derived from optimal PC mechanism compared to single-user HARQ, as depicted above in Figure 4.6. Moreover, the steeper slope of the dashed red curve reveals that the variance in actual transmit power is evidently reduced for the dual-user case compared to the single-user case, making visible the gains from the additional channel diversity, thus, stabilizing the signal conditions.

Additionally, we depict the SINR conditions measured at the receiving target UE in the form of a CDF in Figure 5.8. Here the SINR statistics are for all transmissions, including the first DL transmissions (whereas only retransmissions are considered in Figure 5.7). The results show an overall SINR attained with the SL-assisted CoRe (dual-user CoRe with optimal PC) that is always better than the conventional DL retransmissions. A larger difference can be seen in the two curves for the very low received SINRs below 20 dB (left tail of the CDF) when the packet is likely to fail, and thus, PC attains significant improvement for such severe cases. This indicates that the retransmission via a different link (SL) helps to improve the SINR for such instances in particular. The result clearly shows an improved SINR with cooperative retransmission; however, a significant difference is not seen in these overall SINR performance curves since the retransmissions amount only to roughly one percent of the total transmissions (as seen in Figure 5.6).

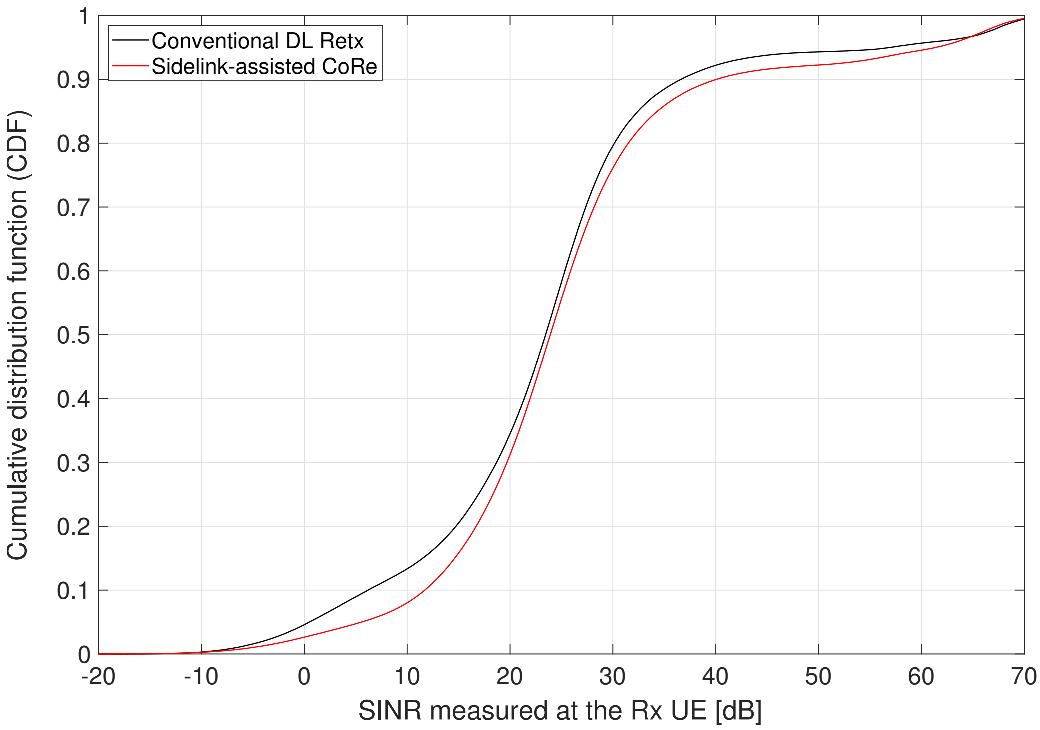

Figure 5.8: SINR performance comparison of Cooperative retransmission scheme to conventional DL retransmissions

PC for SL-assisted cooperative retransmissions has proven to quantify huge power savings compared to the traditional DL-based PC (Figure 5.7) while maintaining the reliability performance for URLLC, as shown above by simulation outcomes 5.6. The stringent requirements of URLLC service bring us to the next important aspect of resource management. Radio resources are scarce, and services like URLLC demand a large number of resources to fulfill the stringent reliability and latency requirements, which is especially critical for the large number of URLLC links indispensable in industrial factory applications. The observed substantial power savings by virtue of our D2D optimal PC scheme [110] lead to small D2D transmit powers, resulting in an interference level at the BS close to the noise floor. This indicates a possibility to further improve resource consumption in a network assisted by SL retransmissions, likely allowing the reuse of resources allocated to the D2D users by UL users.

5.4 Underlay Radio Resource Management (RRM)

5.4.1 Motivation and State-of-the-art

The substantial reduction in power consumption attained by our optimal power allocation for SL offers the possibility of resource reuse for other UL transmissions in the cell, which relates to the concept known as underlay communication. Traditionally, underlay communication [37] [101] is defined as the reuse of resources allocated to cellular users by the D2D users. In our work, the D2D transmit power determines the received signal power for the D2D communication link and the potential interference that may be induced on the receiving BS (since D2D and UL are in-band). There have been several studies on power allocation techniques to mitigate interference and improve the system throughput in underlay communication. Authors in [63] have proposed a QoS-driven power allocation scheme for a co-channel mode underlaying network (cellular and D2D users share the same radio resources) and an orthogonal-channel mode network (radio resources are divided for cellular and D2D users). Their evaluation shows that improved effective capacity is achieved when the D2D average SINR is larger than the average SINR for the link between the D2D user and the BS and that the co-channel mode has higher gains compared to the orthogonal-channel mode. In [38], a coexistence of D2D with cellular communication is studied by applying a simple transmit power reduction for D2D to reduce the interference on cellular users by limiting the SINR degradation of cellular users to 3 dB at a five percentile outage probability. As a result, the authors schedule DL/UL resources to D2D users based on the location of the D2D user pair, suggesting UL resource sharing for a D2D user pair located far away from the BS, whereas DL resource sharing for a D2D user pair that is close to the BS. A particle swarm optimization-based power allocation has been proposed in [75], ensuring the minimum rate of each user. They show the efficiency of D2D communication in single-cell underlay cellular networks, as the PC avoids interference and, thus, improves overall system throughput. Research by experts has highlighted the importance of transmit power control and its connection to efficient resource allocation, eventually allowing benefits for underlay type of communication.

In the last decade, D2D underlay communication has gained attention, leading to ample proposals on pairing D2D and cellular users, resource allocation, and interference management to improve the system performance using the underlay mechanism. Authors in [105] recommend a pairing scheme of D2D and cellular users by finding a set of D2D links for each cellular user and further optimizing the pairing by inverse popularity algorithm in underlay, with the goal of enhancing the total throughput. These results show that throughput increases marginally when D2D users are paired with cellular communication to user underlay. An elaborate study [37] on D2D communication as an underlay in LTE-advanced concludes that the performance of D2D links reusing cellular resources (underlay) may increase the overall throughput by up to 65% compared to D2D traffic relayed via the network. A fast resource allocation algorithm assigning higher priority to unpopular D2D users, defined by the number of channels that can be reused, is suggested in [101], although considering a single-cell scenario affected by intra-cell interference only. Researchers in [40] propose an alternative greedy heuristic algorithm to reduce the D2D interference on cellular users, showing improved network throughput when D2D users share cellular user resources. Along with transmit power, the distance between the D2D transmitter and the cellular user and the D2D distance is also considered an important criterion for resource allocation. Here, the maximum distance threshold is fixed to 25 m as suggested by [37], translating to lower transmit power, thus, accepting only those D2D users for resource sharing whose distance is less than 25 m. Interference coordination and transmit power control are prerequisites for underlay types of communications. Transmit power control and underlay resource allocation go hand-in-hand, targeting to improve spectral efficiency.

5.4.2 Flipped-Underlay Radio Resource Management (RRM)

Motivated by the resource demand arising from URLLC QoS requirements and inspired by the benefits in power consumption due to the low transmit power for retransmissions via SL, which in turn reduces the in-band UL interference, we extend our research to investigate whether and how the radio resources can be reused. Our results indicate a potential for resource sharing among the D2D and UL users, which we realize using underlay communication. We propose a novel efficient resource management technique using underlay communication, named *Flipped-Underlay*, which is presented below with details [116].

Our proposed novel flipped-underlay is an inverted mechanism where D2D and UL users function in underlay, and a higher priority is assigned to D2D transmissions. It is specially designed for the CoRe model, where D2D retransmissions assist unsuccessful DL transmissions. Therefore, the cellular UL users are allocated resources second, followed by D2D users, which can be reused with D2D users. Traditionally, with respect to D2D underlay communication, most of the research has always been focused on D2D users underlaying cellular networks with a higher priority to cellular users [63] [38] [105] [101]. On the contrary, in our scheme, the roles of UL users and D2D users are reversed now in comparison to the conventional underlay schemes; hence, we named it *Flipped-Underlay*. Thus, the resources allocated to D2D users with priority are further considered for reuse by UL users.

In the scope of this work, we consider UL and D2D users to be in-band, as mentioned before. In a non-underlay mode (on the left in Figure 5.9), UL users are allocated resources in an orthogonal manner to resources already allocated to the D2D users, meaning that there is no overlapped resource sharing among the D2D and UL users. Whereas the proposed underlay mode (on the right in Figure 5.9) allows resource sharing among D2D and UL users, in which the UL users can be assigned resources already allocated to D2D users for retransmission. The core idea of the flipped-underlay scheme is to first identify which resources can be reused by UL transmission as the received power level at the BS is low enough and second, to find the UL UE that does not impose additional interference on D2D target UE.

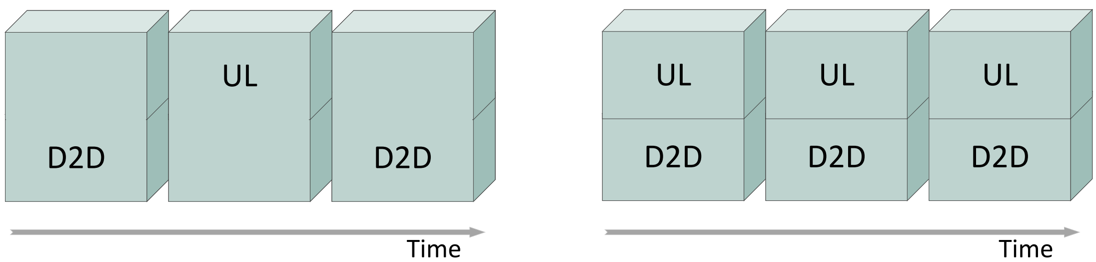

Figure 5.9: Non-underlay and Underlay mode

A snapshot of a single cell BS of the network is illustrated in Figure 5.10, showing different communication links and interference imposed on the D2D users, $d1$ and $d2$, and the UL user u. The solid links highlight the useful communication link, while the dashed links represent the interference from different users. The link between users $d1$ and $d2$ highlights the D2D link called sidelink (SL). The intra-cell interference imposed by the UL user u on the target D2D UE (receiving user) $d2$ is shown in the dashed violet link. The figure also indicates different ICI links to the target D2D UE $d2$ caused by other AGVs like AGV x and AGV y, which are served by the neighbor cell BS'.

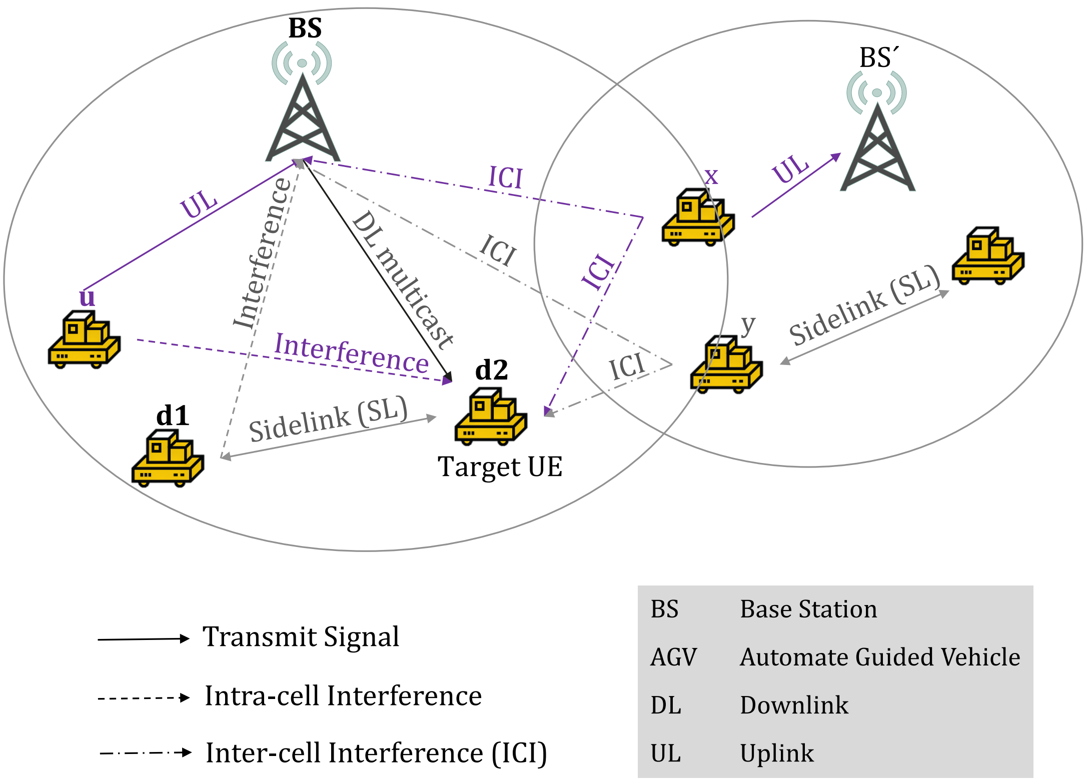

Figure 5.10: Underlay Single-cell Structure

Considering the example scenario illustrated above, we analyze the SINR and attainable rate for non-underlay and underlay modes in the following.

Non-underlay resource allocation mode

In the non-underlay mode (NU-mode), the resources are allocated orthogonally to UL users and D2D users.

The SINR of the target UE ($d2$) on resources r in non-underlay mode (NU-mode) can be given as

$$SINR_{d2,r}^{NU-mode} = \frac{P_{d1,r}\zeta_{d1,d2,r}}{ICI_{d2,r} + N_0} \tag{5.12}$$

Thus, the attainable rate (C) of the target UE ($d2$) in orthogonal mode on resources r with bandwidth B_r can be expressed as

$$\begin{aligned} C_{d2,r}^{NU-mode} &= B_r \log_{10}\left(1 + SINR_{d2,r}^{NU-mode}\right) \\ &= B_r \log_{10}\left(1 + \frac{P_{d1,r}\zeta_{d1,d2,r}}{ICI_{d2,r} + N_0}\right) \end{aligned} \tag{5.13}$$

Similarly, the SINR and the achievable UL rate of the BS on resources r' in non-underlay mode (NU-mode) is given by

$$SINR_{BS,r'}^{NU-mode} = \frac{P_{u,r'}\zeta_{u,BS,r'}}{ICI_{BS,r'} + N_0} \tag{5.14}$$

$$\begin{aligned} C_{BS,r'}^{NU-mode} &= B_{r'} \log_{10}\left(1 + SINR_{BS,r'}^{NU-mode}\right) \\ &= B_{r'} \log_{10}\left(1 + \frac{P_{u,r'}\zeta_{u,BS,r'}}{ICI_{BS,r'} + N_0}\right) \end{aligned} \tag{5.15}$$

Underlay resource allocation mode

In the underlay mode (U-mode), as described above, the resources are reused among UL users and D2D users. The SINR and, thus, the attainable rate in underlay mode are also dependent on binary variable α, which determines if resources r are allocated to an UL user (u) in underlay mode.

$$\alpha_{r,d2} = \begin{cases} 1 & \text{if resources r allocated to user d2 are reused} \\ 0 & \text{otherwise} \end{cases} \tag{5.16}$$

Consequently, the Eq. (5.12)-(5.13) for underlay mode can be expressed as

$$SINR_{d2,r}^{U-mode} = \frac{P_{d1,r}\zeta_{d1,d2,r}}{\alpha_{r,d2}P_{u,r}\zeta_{u,d2,r} + ICI_{d2,r} + N_0} \tag{5.17}$$

Thus, the rate of the target UE ($d2$) in underlay mode on resources r with bandwidth B_r is updated as

$$\begin{aligned} C_{d2,r}^{U-mode} &= B_r \log_{10}\left(1 + SINR_{d2,r}^{U-mode}\right) \\ &= B_r \log_{10}\left(1 + \frac{P_{d1,r}\zeta_{d1,d2,r}}{\alpha_{r,d2}P_{u,r}\zeta_{u,d2,r} + ICI_{d2,r} + N_0}\right) \end{aligned} \tag{5.18}$$

The additional term in the denominator indicates the interference power from the UL user u. If the resource reuse binary variable is toggled on, $\alpha_{r,d2} = 1$, only then the UL user u is allocated the same resources as D2D user $d1$. The value of $\alpha_{r,d2}$ is dependent on different thresholds to keep the interference power below the noise floor, illustrated later in detail. Further, the SINR and the rate of the BS on resources r' in underlay mode (U-mode) are given by

$$SINR_{BS,r'}^{U-mode} = \frac{P_{u,r'}\zeta_{u,BS,r'}}{\alpha_{r,d2}P_{d1,r}\zeta_{d1,BS,r} + ICI_{BS,r'} + N_0} \tag{5.19}$$

$$\begin{aligned} C_{BS,r'}^{U-mode} &= B_{r'}\log_{10}\left(1 + SINR_{BS,r'}^{U-mode}\right) \\ &= B_{r'}\log_{10}\left(1 + \frac{P_{u,r'}\zeta_{u,BS,r'}}{\alpha_{r,d2}P_{d1,r}\zeta_{d1,BS,r} + ICI_{BS,r'} + N_0}\right) \end{aligned} \tag{5.20}$$

5.4.3 Flipped-Underlay Resource Allocation (FURA) Algorithm

We propose the *Flipped-Underlay Resource Allocation (FURA)* algorithm as the primary decision maker for the selection between non-underlay and underlay resource allocation modes for UL users. The list of D2D users D scheduled in a scheduling interval and the list of UL users U awaiting resources for UL transmissions in the same scheduling interval are created.

$$\begin{aligned} D &= \{d_1, d_2, d_3, \ldots, d_n\} \\ U &= \{u_1, u_2, u_3, \ldots, u_m\} \end{aligned}$$

These user lists D and U are provided as input to the FURA algorithm. The output of the algorithm is the resource allocation of all UL users: underlay resource allocation is applied if the defined eligibility criteria are met; otherwise, the UL users are allocated resources in the conventional orthogonal manner (non-underlay mode). At first, the list of all D2D users retransmitting in the current scheduling interval is sorted in ascending order of the imposed interference power from the assisting UE to the BS: $P_{d_i}\zeta_{d1,BS}$, which is a product of the D2D transmit power and its path-loss to the BS.

$$P_{d_i}\zeta_{d_i,BS} \leq P_{d_{i+1}}\zeta_{d_{i+1},BS} \leq P_{d_{i+2}}\zeta_{d_{i+3},BS} \leq \ldots \leq P_{d_n}\zeta_{d_n,BS} \quad \forall d_i \in D \tag{5.21}$$

The least imposed interference power by the D2D assisting UE in the UL implies a higher likelihood of the power being below the noise floor. This interference-based ordering allows the selection of the user with the most suitable D2D channel conditions to evaluate a possible underlay resource allocation with a potential UL user. The algorithm is structured into two stages:

- Identify which resources can be reused if the received power level at the BS falls below a predefined threshold derived from the noise and interference floor, and
- Check if an UL UE for underlay can be found which creates interference that stays below the threshold for the D2D target UE.

These two stages of the FURA algorithm (shown in Figure 5.11) are performed while iterating through the user list U of cellular UL UEs to be scheduled.

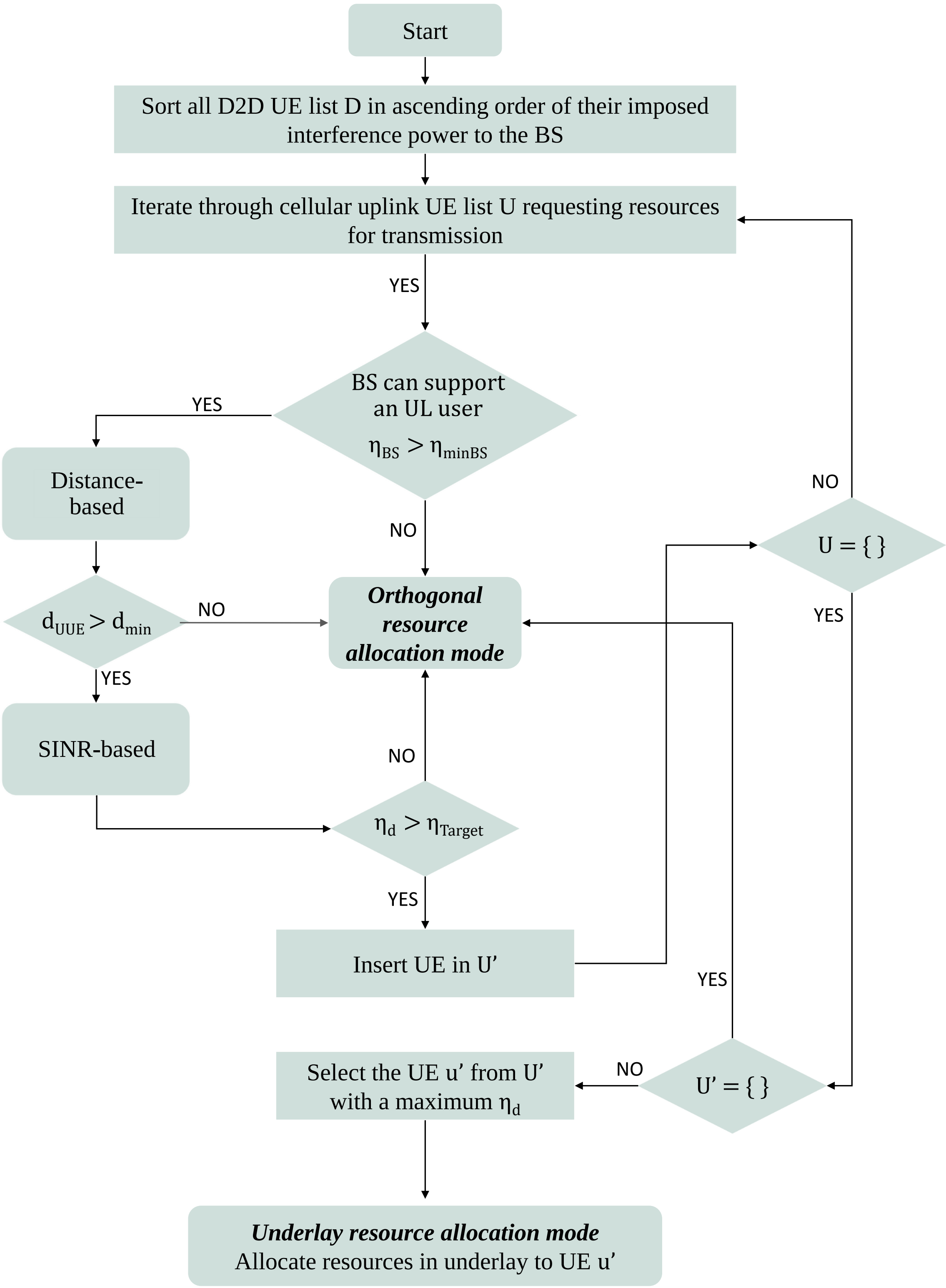

Figure 5.11: Flipped-Underlay Resource Allocation (FURA) Algorithm

In the first stage of the algorithm (Figure 5.11), it is checked whether the BS can afford an additional UL user based on the minimum SINR threshold at the BS, denoted by η_{minBS}, in order to guarantee a minimum rate for the UL user in the same resources assigned to the D2D user. The SINR at the BS η_{BS} stated in Eq. 5.22, is computed considering the impact of the intra-cell interference imposed by the D2D user in the same cell along with the inter-cell interference (ICI) induced by the UEs in the neighbor cells. It is constituted of the UL transmit power P_u and UL channel gain $\zeta_{u,BS}$, impacted by the intra-cell interference caused by the D2D UE d1 with transmit power P_{d1} and channel gain $\zeta_{d1,BS}$, and the ICI caused by the UL users from the neighbor cells, $\sum_{y=1}^{N} P_y \zeta_{y,BS}$.

$$\eta_{BS} = \frac{P_u \zeta_{u,BS}}{P_{d1}\zeta_{d1,BS} + \sum_{x=1}^{M} P_u \zeta_{x,BS} + \sum_{y=1}^{N} P_y \zeta_{y,BS} + N_0} \tag{5.22}$$

The information signaled from the assisting UE to the BS (retransmission ID, D2D transmit power P_{d1}, and the distance/path-loss measure between the assisting UE and the target UE) is necessary for the BS to calculate the intra-cell interference caused by the D2D UE $P_{d1}\zeta_{d1,BS}$. If the SINR criterion ($\eta_{BS} > \eta_{minBS}$) is fulfilled, the algorithm proceeds to the next stage, otherwise orthogonal resource allocation mode is selected for the current UL user, as the BS cannot support the respective UL user in underlay mode. Note that due to the ordering of the D2D users in list D based on the imposed interference power to the BS, all other D2D users will yield a worse SINR η_{BS} with respect to the current UL user.

In the second stage, the eligibility of the UL user for underlay is validated by the D2D target UE perspective, where we check if D2D UE can tolerate the interference induced by a potential UL UE. For this purpose, as an initial criterion, a minimum dynamic distance threshold denoted by d_{min} (Eq. 5.23) is introduced,

$$d_{min} = \left[\frac{\eta_{min} P_u}{P_{d2}\zeta_{d1,d2} - \eta_{min}\sum_{x=1}^{M} P_x \zeta_{x,d2} - \eta_{min}\sum_{y=1}^{N} P_y \zeta_{y,d2} - N_0} \right]^{1/\alpha} \tag{5.23}$$

It mainly depends on the UL transmit power and ensures a minimum distance between the UL UE and the D2D target UE. This minimum distance threshold, given in Eq. 5.23, is computed by taking into account,

- the UL transmit power P_u,
- the D2D target SINR ($\eta_{min} = \eta_{Target}$) mapped from the MCS,
- channel gain of the D2D link $\zeta_{d1,d2}$ using the D2D path-loss between $d1$ and $d2$, and the D2D transmit power P_{d1d2},
- noise power N_0,
- the ICI from M number of cellular UL users and N number of D2D users represented by the terms $\sum_{x=1}^{M} P_x \zeta_{x,d2}$ and $\sum_{y=1}^{N} P_y \zeta_{y,d2}$, respectively, and
- the path-loss exponent α valid for the specific propagation environment (e.g., taken from the indoor factory channel model [99] for industry 4.0 scenarios).

If the distance between the UL user and the target UE meets the initial minimum distance criterion ($\eta_d > \eta_{min}$), a final SINR-based validation is performed to confirm the eligibility of the UL user for underlay mode. To this aim, the D2D target SINR (derived from the predefined MCS of the original DL transmission) is used as an SINR threshold (η_{Target}) for the D2D user. The D2D SINR η_d given in Eq. 5.24 is computed by including the intra-cell interference from a potential UL user ($P_u \zeta_{u,d2}$). Additionally, the ICI caused by the UL users and D2D users in the neighbor is captured by the terms $\sum_{x=1}^{M} P_x \zeta_{x,d2}$ and $\sum_{y=1,y \neq d1}^{N} P_y \zeta_{y,d2}$, respectively.

$$\eta_d = \frac{P_{d2}\zeta_{d1,d2}}{P_u \zeta_{u,d2} + \sum_{x=1}^{M} P_x \zeta_{x,d2} + \sum_{y=1,y \neq u}^{N} P_y \zeta_{y,d2} + N_0} \quad (5.24)$$

If the D2D SINR is larger than the D2D target SINR, the UL user is inserted into the user list U' of eligible UEs, which contains all the UL users eligible for underlay mode. Once an UL user is processed, it is removed from the user list U. Thus, after iterating through all the elements of user list U, i.e., if user list U is empty ($U = \{\}$), the final step is to select the most suitable user for underlay mode from the created user list U' of eligible users. A useful criterion is to select the user u' from the list U yielding the maximum D2D SINR at the target UE for underlay mode in the current resources, i.e., the one causing the least UL intra-cell interference on the D2D target UE. In case none of the UEs from list U can fulfill the distance and D2D target SINR criterion, no underlay can be supported, in turn leaving the user list U to be empty ($U' = \{\}$), and hence the D2D user is exclusively assigned the resources in orthogonal mode.

Once a useful UL user has been found and the UL underlay selection is complete for the first D2D user, the next D2D UE from the user list D is processed to check if a suitable UL user can be found for resource sharing. Similarly, the respective D2D user and UL user matching, followed by the resource allocation procedure for all the D2D users in the user list D, is performed. For the smooth functioning of the FURA algorithm for CoRe, we suggest additional control information signaling described in detail below.

5.4.4 Flipped-Underlay Control Signaling for FURA

The essential control signaling for the functioning of the FURA algorithm is introduced as the *SL Retransmission Information (SLRI)* feedback report (see Figure 5.12 and 5.13). The control

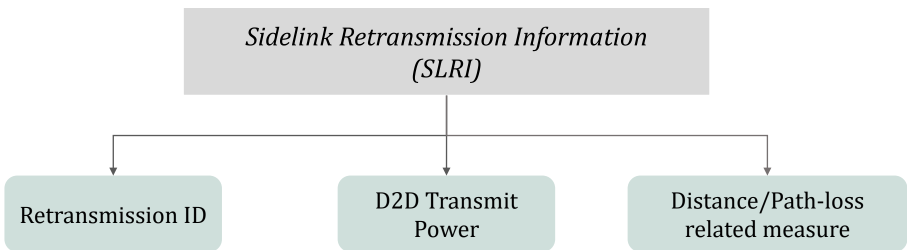

Figure 5.12: Sidelink Retransmission Information (SLRI)

information to be signaled between the target UE, the assisting UE, the UL UE, and the BS is combined together in SLRI feedback. The SLRI report, necessary for the execution of the FURA algorithm at the BS, is composed mainly of three elements: (1) the retransmission ID,

(2) the transmit power required for the retransmission, and (3) a distance/path-loss related measure for the link between the assisting UE to the target UE (Figure 5.12).

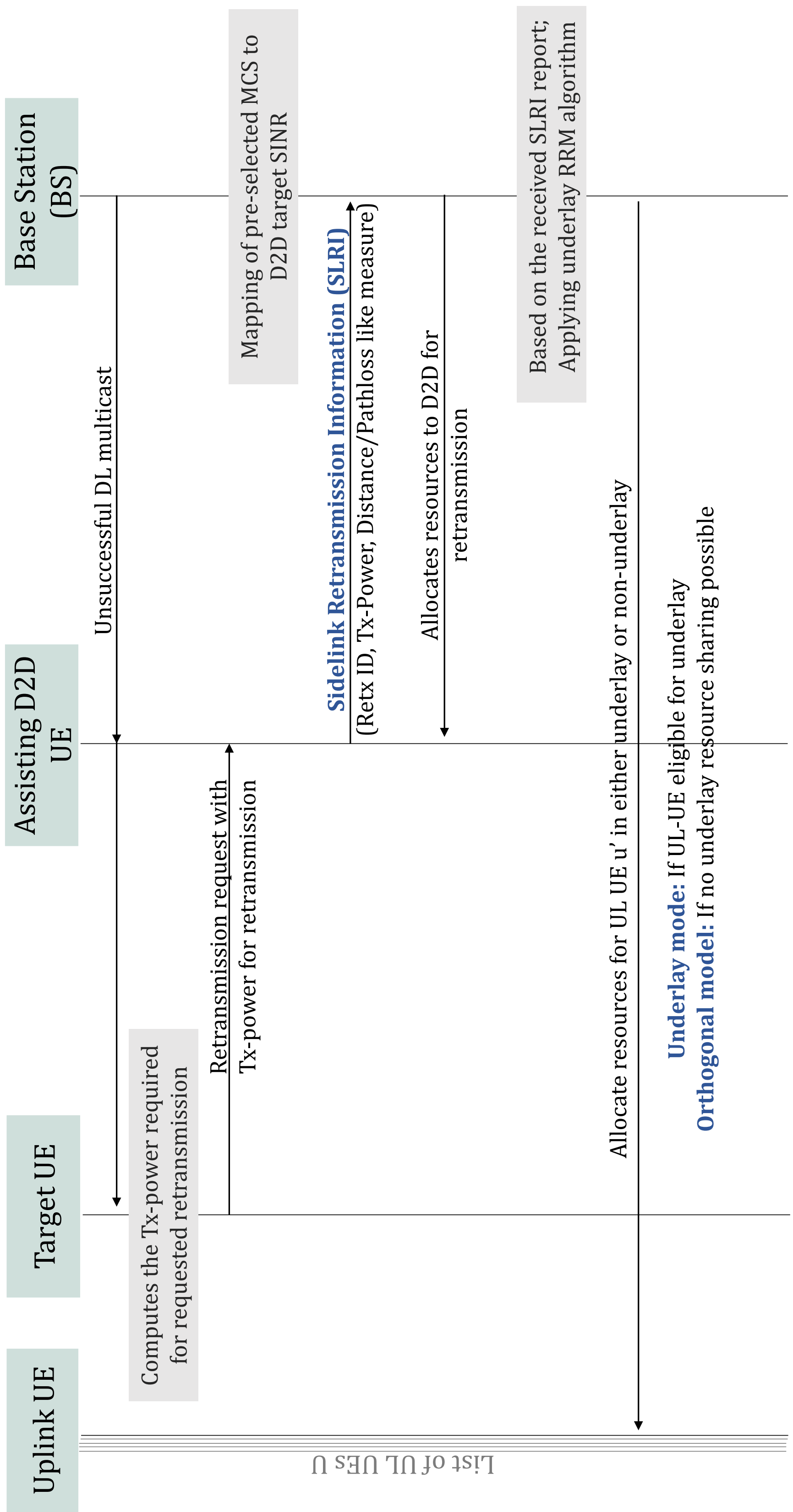

Figure 5.13: Signaling for Underlay RRM

In the CoRe scheme, explained in Section 3.1, followed by an unsuccessful reception of a DL multicast transmission and the selection of assisting D2D UEs, the D2D target UE computes the transmit power required for the retransmission based on the optimal PC scheme (Section 4.5.4). Next, the D2D target UE sends a retransmission request, including the computed transmit power for retransmission to the assisting D2D UE/UEs.

After receiving the retransmission request, the assisting D2D UE sends the SLRI report to the BS (shown in bold). The BS is the central controller for resource allocation and performs the flipped-underlay RRM algorithm presented above. Thus, the BS allocates resources to D2D for retransmission based on the selected scheduling algorithm, i.e., the QoS-aware scheduling algorithm (Section 4.4), which prioritizes the retransmissions via D2D and considers head-of-line (HOL) delay as a criterion to schedule users. As the MCS for the retransmissions remains the same as the original DL transmission, the BS computes the target D2D SINR by mapping the predefined MCS value. The mapped target D2D SINR is further used to evaluate the bearable interference at the D2D target UE. Following the reception of the SLRI report, the FURA RRM algorithm, controlled by the BS, is executed. Consequently, it decides whether any UL UE is eligible for sharing the resources in underlay with the current D2D user. Thus, the outcome decides on the selection of the resource allocation mode among orthogonal and underlay modes.

5.5 Performance Evaluation with Flipped-Underlay RRM

We analyze the performance of the proposed flipped-underlay FURA algorithm (underlay mode) in comparison to the conventional orthogonal (non-underlay mode) resource allocation. The evaluation focuses on SL-assisted CoRe for the same factory automation scenario and the general system model, illustrated in Sections 5.2.1 and 4.2, respectively.

At first, we compare the D2D SINR performance, i.e., SINR for retransmissions only (Figure 5.14), when underlay resource allocation mode is applied using the FURA algorithm to the case when no resource reuse in underlay occurs (orthogonal mode).

The SINR performance at the target D2D UE is of major concern when considering retransmissions via D2D links, which hold the highest priority. Therefore, the scope of this work is mainly focused on the performance evaluation of the DL and D2D. Hence we consider a DL traffic dominated scenario with the assumption that the desired UL SINR is also maintained in underlay mode. Figure 5.14 shows that the D2D SINR attained with underlay mode does not suffer extremely compared to non-underlay mode. The SINR performance for underlay mode is indeed lower than the classical case when no resource reuse happens; however, there is only a negligible difference at the median. This brings us to the question - how would this SINR performance degradation reflect the QoS measures of latency and reliability when underlay is applied?

Recalling the optimal power control methodology from Section 4.5.4, with the aim to allocate controlled transmit power to retransmissions via sidelink. We obtain the power terms shown again in Figure 5.15 used as power boosts for consecutive retransmission attempts. From the reference case of Rayleigh fading channels, revisiting the channel outage performance presented earlier in Figure 3.8, the average channel gain is observed at the 0 dB mark.

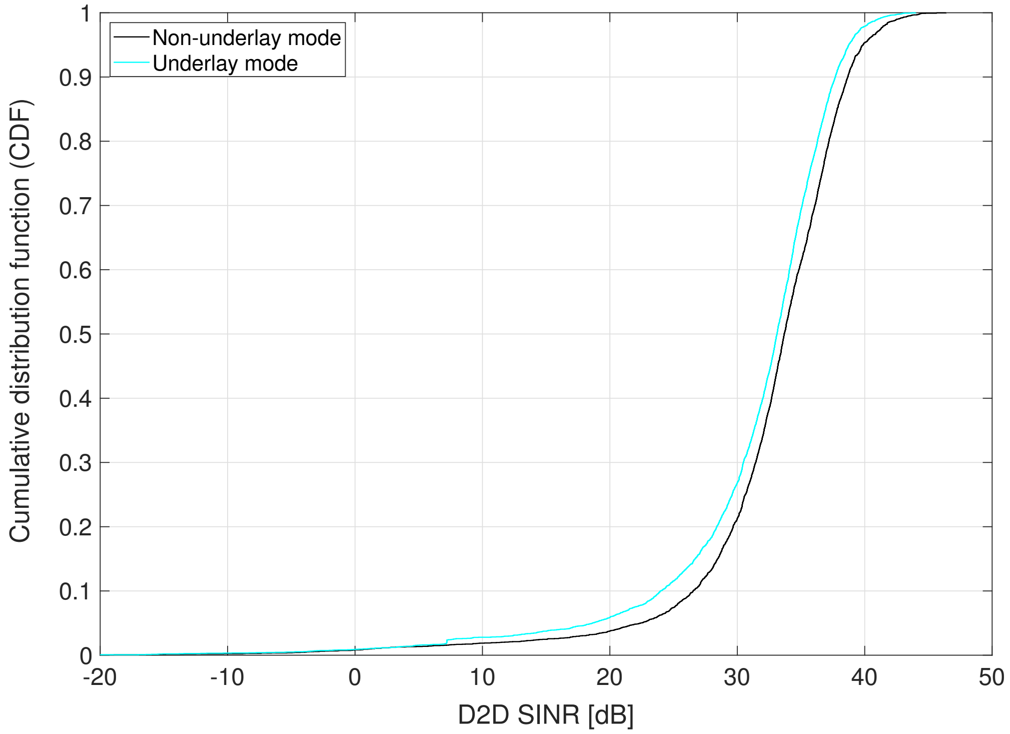

Figure 5.14: SINR performance comparison of underlay to non-underlay mode

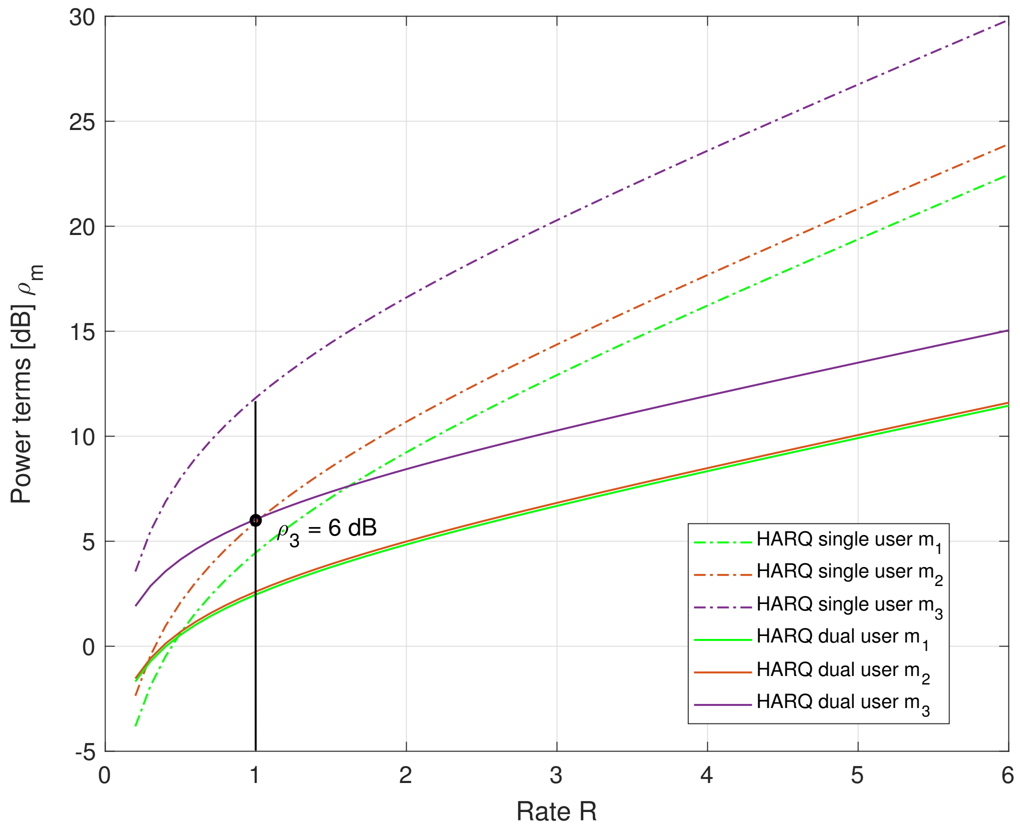

Figure 5.15: Power terms based on Optimal PC algorithm

The power boost using the optimal scheme for m^{th} retransmission depends on the Rate (R) through

$$\phi = 2^R - 1 \tag{5.25}$$

Substituting for the reference average channel gain of 0 dB in the scalar domain as $\phi = 1$ in the above equation, we get

$$2^R - 1 = 1 \tag{5.26}$$

Thus, the attainable rate (R) for the average channel gain of 1 is

$$R = 1 \tag{5.27}$$

When two users are retransmitting (HARQ dual user), reading from Figure 5.15, for $m = 3$ retransmissions, the power term ρ_m is

$$\rho_3\,(R = 1) = 6 \text{ dB} \tag{5.28}$$

Thus, the average reference power of 0 dB is boosted by 6 dB. Recalling the channel outage performance from Figure 3.8, the reference channel gain is now shifted by 6 dB and we obtain the reference operation point of −6 dB

$$\rho = -6 \text{ dB} \tag{5.29}$$

Now, let us re-evaluate the channel outage performance for Rayleigh fading and Ricean fading D2D channels for operation point $\rho = -6$ dB, presented in Figure 5.16.

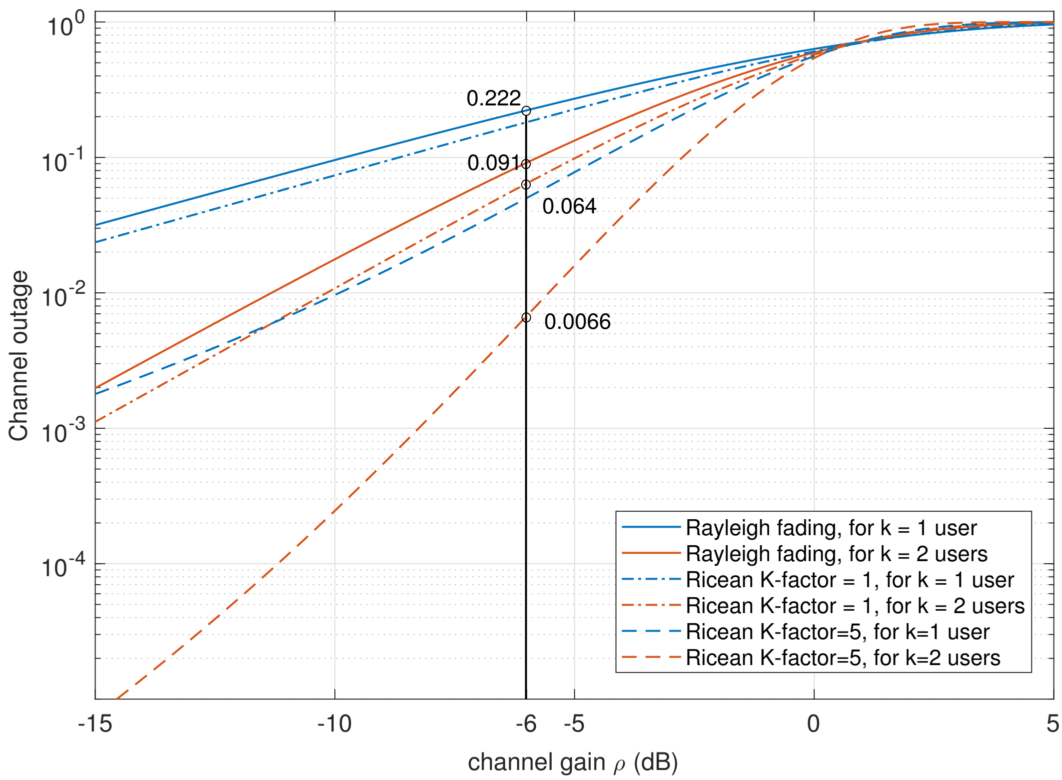

Figure 5.16: Comparison of channel outage for D2D channels modeled as Rayleigh fading and Ricean fading

$$
\begin{aligned}
\text{Channel outage} &:= q(x \leq k_\rho) \\
\text{For Rayleigh fading} &:= q_{Ray_{k=1}}(x \leq -6\,\text{dB}) = 0.222 \\
&:= q_{Ray_{k=2}}(x \leq -6\,\text{dB}) = 0.091 \\
\text{For Ricean fading (K-factor(KF)=1)} &:= q_{Rice_{k=1,KF=1}}(x \leq -6\,\text{dB}) = 0.181 \\
&:= q_{Rice_{k=2,KF=1}}(x \leq -6\,\text{dB}) = 0.064 \\
\text{For Ricean fading (K-factor(KF)=5)} &:= q_{Rice_{k=1,KF=5}}(x \leq -6\,\text{dB}) = 0.049 \\
&:= q_{Rice_{k=2,KF=5}}(x \leq -6\,\text{dB}) = 0.0066
\end{aligned}
\tag{5.30}
$$

Consequently, for the reference operation point of $\rho = -6$ dB, a channel outage probability of 9% is marked for the Rayleigh fading channels with $k = 2$ users. At the same time, a 0.66% channel outage probability is expected when the Ricean fading channel with K-factor=5 is applied for $k = 2$ users. Thus, a lower bound and an upper bound can be derived from the analysis.

The SINR performance can be studied better by evaluating the difference in the actual D2D SINR to the target D2D SINR for the D2D transmissions. Figure 5.17 presents the curves for the instantaneous SINR difference to the target SINR that changes dynamically based on the predefined MCS for the initial DL transmission. The main region of concern is the

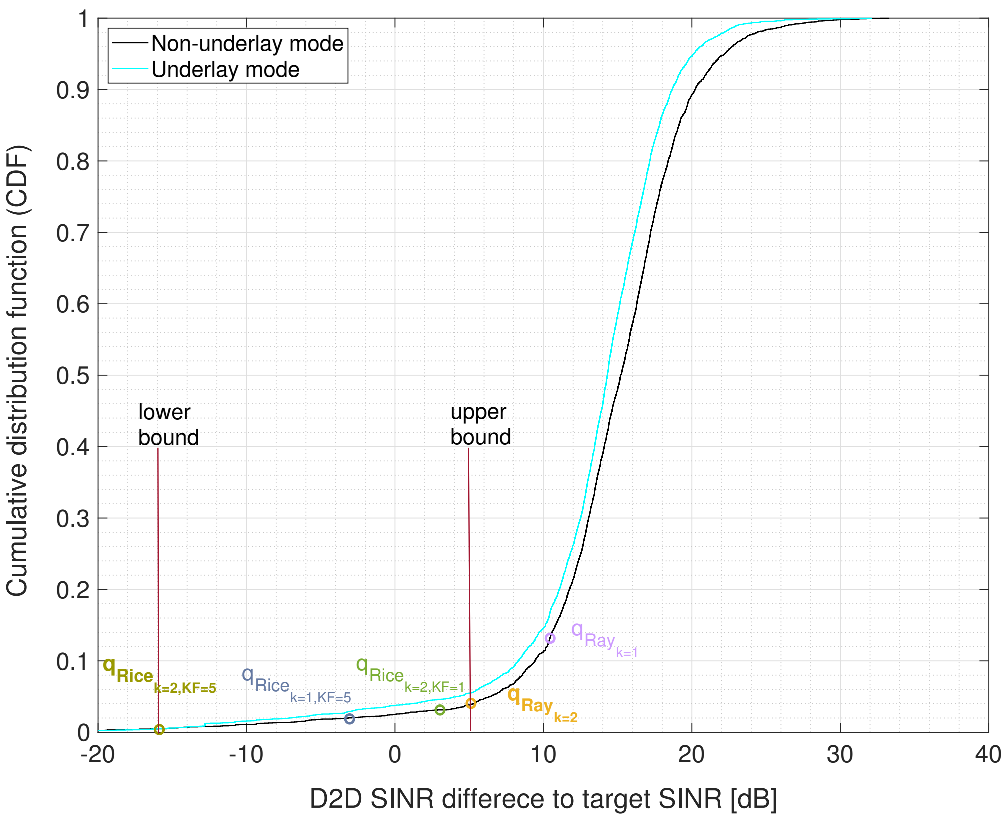

Figure 5.17: Difference in actual SINR performance to target SINR

left tail of the curve, which shows the cases when the actual SINR could not fulfill the D2D target SINR requirement, leading the difference to be below 0 dB. As we can observe for non-underlay mode, roughly 2.4% of the cases cannot fulfill the target SINR whereas around 3.2% of the cases fail to satisfy the target SINR in underlay mode. As a consequence of resource reuse by UL users, there are a few more instances accounting for 0.8% compared to non-underlay mode. This is likely to happen due to the estimated interference (gauged from the path-loss) that can be caused by the UL users reusing the resources allocated to D2D transmissions. Although the overall SINR difference to the target SINR degrades minimally when underlay is applied, it is important to note that the QoS is not affected as the SINR target is fulfilled in all the instances above $0dB$ region, which accounts for approximately 97% of the cases.

Finally, the important measure of resource savings with our underlay FURA algorithm (Section 5.4.3) is evaluated, while it allows a resource allocation decision in underlay mode depending on the distance and SINR criteria. We present the resource usage for underlay and non-underlay modes over a period of 1000 ms in Figure 5.18, where the number of resources allocated to all the users per cell is averaged over every super-frame of 10 ms. We make sure that the overall interference and system setup are consistent for both cases by selecting the same random seed value for a fair comparison. The resource block usage with non-underlay mode (black curve) shows an average of 78 RBs, whereas the number of RBs used when underlay mode (turquoise curve) is applied reduces to around 55 RBs on average. We can observe that a resource saving of 21 RBs on average translates to 27% saving if the resources are reused by the UL users. Thus, the outcome clearly indicates that an efficient spectrum usage and improved system capacity accommodating a larger number of users can be attained by applying the proposed flipped-underlay RRM with the FURA algorithm illustrated in Section 5.4.2 and 5.4.3.

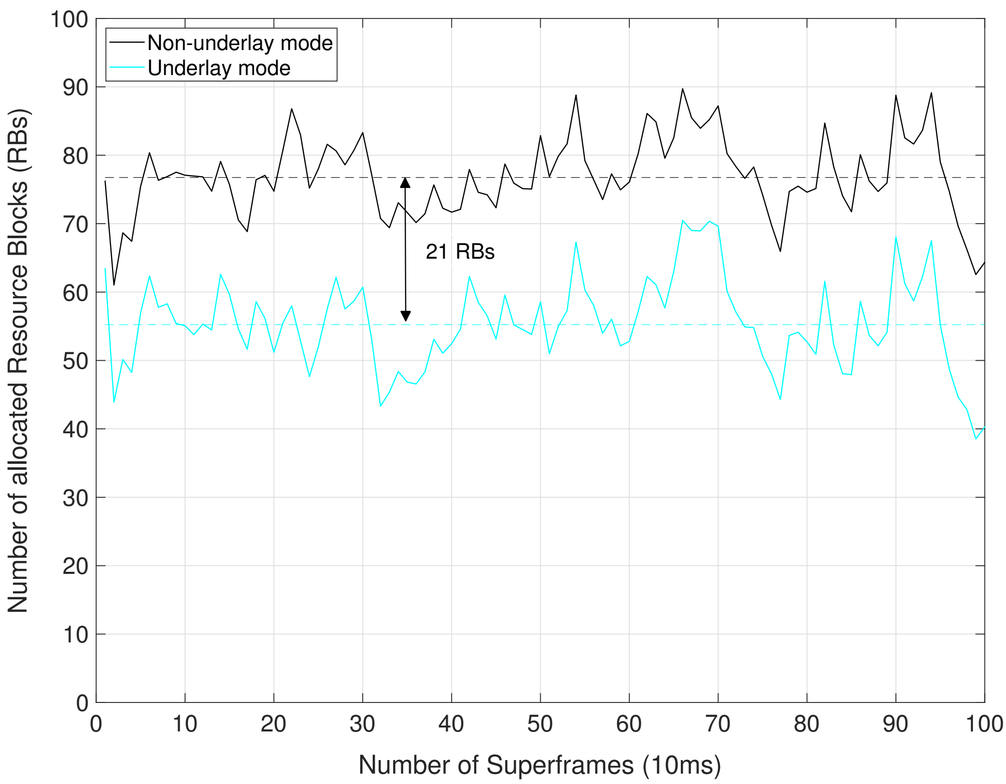

Figure 5.18: Resource savings with underlay mode compared to non-underlay mode

Lastly, we analyze the utmost essential question of how the QoS measures of reliability and latency are affected by these observed resource savings (Figure 5.18) derived from resource reuse. Figure 5.19 represents the latency performance for a reliability target of 99.999% by the complementary CDF for all the transmissions, with the retransmissions marked by the consecutive plateaus in the plot. The first plateau of the curve comes from the initial DL transmissions, which is exactly the same for both underlay and non-underlay modes, as the effect of underlay resource allocation is only triggered from 1st retransmission onward when the resource reuse sets in. The overall latency performance remains in sync with the non-underlay mode with a minor difference. For the 1st retransmission (2nd plateau), it can be seen that underlay mode performance decreases slightly. This can be explained as an effect of resource reuse occurring mostly during the 1st retransmission. Recalling our optimal power control scheme 4.5.4, an incremental power boost is applied for consecutive retransmissions. As a result, the 1st retransmissions are always allocated the lowest transmit power compared to their successive retransmissions. Thus, 1st retransmissions are more prone to UL interference, reflected in the 1st plateau in Figure 5.19. Furthermore, our user selection scheme for cooperative retransmission selects a

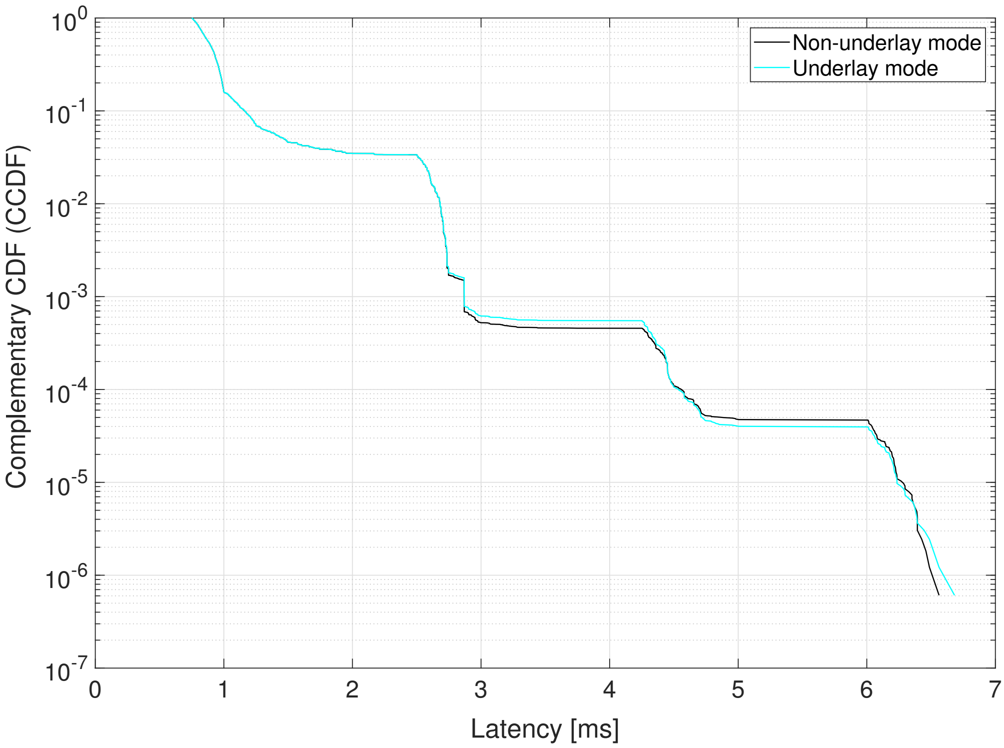

Figure 5.19: Latency performance comparison of underlay to non-underlay mode

distinct user for every successive retransmission, starting with the best-user first. This, in turn, causes the users assigned to 2nd and 3rd retransmissions to use higher initial transmit power, which is further boosted as per the optimal PC scheme. All in all, second and third retransmission certainly transmit with higher transmit power compared to the 1st retransmission, making it less susceptible to be chosen for an underlay resource reuse mode. At the same time, the transmissions needing more than one retransmission presumably experience deteriorating D2D channel conditions. Therefore, it is logical to conclude that the probability of 1st retransmissions is much higher than 2nd and 3rd retransmissions, and hence also more occurrences of underlay mode during 1st retransmissions. Consequently, the simulation result shows the latency performance after the 3rd retransmission to be the same as that of non-underlay mode while fulfilling the reliability target of 99.999%.

5.6 Summary

This chapter presents extensions to the *CoRe* scheme considering a realistic IIoT scenario. Similar to the V2X scenario, IIoT is another most relevant use-case where a large number of users are available, and URLLC is an essential service demanded for the smooth functioning of the industrial automation system. Firstly, the system design constituting the industrial factory system model and system configuration is described. A $120 * 60$ m rectangular factory hall deployment with 18 BSs/TRPs located at a 20 m inter-site distance is considered. Unlike V2X, the BSs are located closely in a compact network setup, and inter-cell interference among the BSs can be unavoidable. Therefore, a UE-centric clustering-based ICIC is applied by forming a cluster of three nearest neighbor BS including the serving BS, in which the three member BSs of the cluster are muted in the resources used by the serving BS. This ICIC mechanism diminishes the major source of ICI to the serving BS.

The CoRe scheme is henceforth evaluated using user-centering clustering-based ICIC and PC for the industrial factory scenario. Similar to the findings in the V2X scenario, the results delineate a lower probability of retransmissions for the CoRe scheme compared to the traditional DL retransmissions, and the reliability performance of 10^{-5} with the CoRe scheme can be accomplished after two retransmission attempts. While fulfilling the URLLC QoS performance, the optimal PC scheme highlights power savings of 10 dB and 15 dB with single-user and dual-user, respectively. It can be clearly observed that lower transmit power is required for dual-user optimal PC even for IIoT use-case, where the users are closely located in a small-cell setup.

URLLC service dictates a demand to fulfill its QoS requirements in a resource-efficient manner, which brings us to the next challenge of resource usage. From the simulation outcome, resource saving can be expected for CoRe compared to traditional DL transmissions. Thanks to the benefits of transmitting consecutive HARQ retransmissions in the same resource and the overall reduced probability of retransmissions, lower consumption of resources can be realized.

Our findings indicate a potential resource sharing opportunity for D2D and UL users, triggering an extension for CoRe with respect to resource reuse actualized by underlay communication. We propose and design the *Flipped-Underlay*, an efficient resource management technique that facilitates resource reuse among D2D and UL users by prioritizing D2D users, unlike the traditional underlay scheme. The key idea of flipped-underlay is to first identify the resources that can be reused by UL users and, second, to find the UL UE that does not impose any interference on the D2D UE. A *FURA* algorithm is proposed and implemented for the selection between underlay and non-underlay (orthogonal) resource allocation modes for the UL users, depending on the distance-based and SINR-based eligibility criteria. Additionally, as a prerequisite to computing the eligibility criteria in the FURA algorithm, we introduce a feedback report named *SLRI* between the target UE, assisting UE, UL UE, and the BS. The SLRI report consists of the retransmission ID, the transmit power, and a path-loss related measure for the target D2D UE and the UL UE.

The simulation results of the proposed flipped-underlay scheme with the FURA algorithm for the factory automation scenario are presented and discussed. The flipped-underlay FURA scheme shows a resource saving of 27% when the already allocated D2D resources are allowed to be reused by the UL users, compared to the non-underlay mode when resources are allocated orthogonally to D2D users and UL users. Although a minor difference in SINR performance is encountered due to resource sharing in underlay, it does not impact the desired QoS. While significant resource savings are observed, it is of prime importance to analyze the QoS performance required for URLLC with flipped-underlay mode. The results show an overall consistent latency performance while attaining reliability of 99.999% with the underlay scheme compared to the non-underlay mode.

The convincing performance and resource savings by the flipped-underlay resource management scheme allow it to serve more URLLC users while fulfilling the QoS demands in a resource-efficient manner. This enables, in essence, to increase the network capacity of the system, which is crucial for factory automation use cases. Although the results of flipped-underlay focus on an industrial factory scenario, they can easily be transformed for V2X communication as well, in which the requirement of a large number of devices persists, which translates to diversity gains. Thus, industrial factory applications, as well as V2X applications, can benefit largely by adapting the proposed power savings and resource reuse by the flipped-underlay FURA scheme.

6 Conclusion

In this chapter, we summarize our main contributions, highlight prospective practical applications, and outline future research directions in cooperative retransmissions.

6.1 Summary

The prime objective of this thesis was to facilitate resource-efficient ultra-reliable low-latency communication (URLLC) type of service in densely populated mesh networks. URLLC is a critical requirement to the digital evolution in sectors such as the automotive and manufacturing industries. In these industry sectors, information exchange among the vehicles/devices must occur with ultra-high reliability within a time frame of a few milliseconds to ensure uninterrupted system operation. For real-world scenarios, such as cars in traffic and machines in a factory, the key challenge lies in supporting a large number of wireless connections in a resource-efficient manner while fulfilling the stringent URLLC service requirements.

To this aim, we designed a user cooperation scheme termed *CoRe* - Cooperative Retransmission scheme, derived from the renowned relay-based transmission techniques, for a downlink (DL) transmission scenario. The fundamental idea of CoRe is to allow simultaneous retransmissions of the same data packet via multiple neighbor devices using cooperative spatial diversity schemes. If a DL transmission failure occurs, the target user requests retransmission from its neighbors, who may have received the original DL transmission successfully, provided that the original transmission was multi-cast. For CoRe, we chose a simple approach for retransmission, where the neighbor device-to-device (D2D) users retransmit the same packet to the target user without decoding the data to respect the delay budget, using a distributed transmit diversity scheme. Combining is applied at the receiver for the constructive addition of identical signals received via different D2D propagation paths. In our fundamental scheme, the transmit power is shared equally among the cooperating users. URLLC service demands a reliability target of 10^{-5} within a latency budget of $1-10$ ms. Therefore, such retransmissions via D2D users can be favorable to achieve these targets in a resource-efficient manner by exploiting the link diversity in the retransmissions.

Firstly, we addressed the challenge of high reliability and the consequent demand for radio resources. We demonstrated the benefits of CoRe with an analytical investigation focusing on channel outage as the reliability measure compared to the traditional single-frequency network (SFN), where multiple nodes transmit the same packet without applying any spatial diversity schemes. Our theoretical analysis showed a gradual improvement in reliability with an increase in the degree of diversity by increasing the number of cooperating users. Numerous users present in the surroundings are exploited to realize a higher degree of diversity in our CoRe scheme, which are used to assist the erroneous DL transmissions. The employment of the distributed transmit diversity scheme mitigates the issue of high resource demand, as the resources are used optimally by all the users retransmitting simultaneously. The applied STBC type of transmit diversity scheme spreads symbols across time and users using the same time-frequency resources. The common densely populated mesh network scenarios are likely to experience a mix of line-of-sight (LOS) and non-LOS (NLOS) communication links, therefore, we initiated evaluation of CoRe with D2D channels modeled as Rayleigh fading as well as Ricean fading channels. Based on our findings, the assumption of all D2D channels being Rayleigh fading is adopted as a lower bound baseline (worst-case scenario). Thus, the CoRe performance is expected to improve under Ricean fading conditions, which are more representative of the practical scenarios considered.

The statistical models are inadequate to reflect all the signal conditions in a multi-cell network. In particular, the components that constitute latency, such as queuing delay, segmentation delay, and processing delay, cannot be modeled analytically without considerable effort. Therefore, motivated by the benefits of CoRe in terms of reliability, we investigated its latency performance under the target reliability requirements using realistic system-level evaluation. Our focus is on the application scenarios where URLLC service is crucial, and where the high density of mobile devices increases the likelihood of obstructing ongoing transmissions. Therefore, we selected two prime scenarios for evaluation, namely, vehicle-to-everything (V2X) communication and industrial internet-of-things (IIoT). We consider the traditional DL retransmissions as the baseline. Our simulation results present the end-to-end latency performance with respect to attainable reliability. The outcome showed that CoRe can attain a reliability target of 99.999% already after two retransmissions, outperforming the state-of-the-art DL retransmission scheme, which needs three retransmissions to achieve the same reliability target. As a result, the total retransmissions are reduced yielding a reduction of the maximum retransmissions to two, which improves latency and shortens the queuing delays, resulting in substantially improved use of available resources. While the presented results demonstrate a latency performance of $6-7$ ms with the hybrid automatic repeat request (HARQ) timings in a long-term evolution (LTE) scenario, this can be further reduced to $1-2$ ms using 5G-NR HARQ timing due to the flexible transmit time interval (TTI) size of $2-3$ OFDM symbols.

Furthermore, as it is essential to choose the users discretely for cooperation, we investigated and evaluated different user selection and grouping methods for CoRe. Our system-level simulation revealed that the most efficient approach is a user-combination scheme, in which two users cooperate during each retransmission (dual-user), with a distinct user pair selected for every consecutive retransmission attempt. In this proposed scheme, we enable the selection of a unique pair of users per retransmission, which allows us to exploit additional diversity gains in every retransmission attempt. Thus, our dual-user CoRe allows using Alamouti code for precoding, which is the only space-time block code (STBC) capable of achieving the full rate. Although an additional degree of diversity can boost reliability when more than two users retransmit simultaneously, the associated rate loss can outweigh the gains. As a result, we highlight that our dual-user CoRe with user-combination scheme is a favorable choice realizing maximum gains to achieve the desired URLLC performance.

To sum up the first phase of our research, we developed a model to enable URLLC service in densely populated mesh networks, which outperforms the common state-of-the-art solutions. It is an important foundation for applications in relevant sectors like IIoT and V2X. In addition to fulfilling URLLC requirements, it is essential to minimize overall system interference in real-world wireless application to ensure uninterrupted operation without compromising transmission quality. This motivation led to the next phase of our investigation, focusing on interference management and power control for the CoRe model.

Considering retransmissions in CoRe via different neighbors raises further an important question regarding the optimal distribution of transmit power among the cooperating users. Therefore, we replace the simplified equal power sharing mechanism used in our initial investigation with a more advanced approach, in which the transmit power is allocated using power control (PC) schemes based on path-loss. At first, we adapted the conventional open-loop PC scheme for CoRe using the DL path-loss measure that mainly targets to mitigate interference at the base station (BS). This lead to a fairly large power consumption with around 40% of the cases consuming the maximum allowed transmit power. Next, we applied the state-of-the-art sidelink (SL) PC scheme suggested for D2D communication, which is mainly based on the SL path-loss measure. In CoRe, the modulation and coding scheme (MCS) selected for retransmissions remains the same as in the original DL transmission. Thus, leveraging from this property, we adapted the baseline SL PC scheme and transformed it to a SL-MCS based PC, in which the power constraint is derived using the SL path-loss measure and the MCS. The application of the proposed SL-MCS based PC showed a significant reduction in power consumption; however, it does not fully satisfy the targeted reliability requirements. Therefore, taking the SL-MCS based PC as a reference, we further optimized the PC for a target reliability of 10^{-5}. To this aim, we extended the optimum power allocation scheme from [100] for CoRe with dual-user retransmissions, where a gradual boost with every retransmission is enabled. The objective of this scheme is to use a minimum power required to attain the URLLC target reliability $\epsilon = 10^{-5}$ after the 3^{rd} retransmission. Consequently, our optimal PC yields reduced transmit power consumption compared to the conventional DL PC for SL, thus, allowing significant power savings while achieving the URLLC target performance.

Consequently, in the second phase of this thesis, we attempted to resolve the issue of high interference in mesh networks, crucial to the real-time V2X and IIoT types of applications. Advancements in transmit power usage are of utmost importance to tackle the system interference in future wireless systems. Such low-power retransmissions in CoRe resulted in negligible interference at the BS. This interesting outcome observed in terms of reduced power consumption can support resource management indicating a possibility of underlay communication among the D2D and uplink (UL) users, and thus inspired the further steps of our research.

We used the well-known underlay communication mechanism as the baseline, which enables resource reuse among UL and D2D users. Thus, keeping in mind the key principles of CoRe, we transformed this conventional underlay technique for CoRe by prioritizing the D2D retransmissions in resource allocation. We proposed a novel radio resource management scheme for CoRe, which we named as *Flipped-Underlay*, in which the D2D retransmissions are allocated resources with priority, followed by the selection of an appropriate UL user for resource reuse. Our *Flipped-Underlay Resource Allocation (FURA) algorithm* enables resource allocation to UL users shared with D2D users in an underlay manner, using the distance-based and SINR-based allocation criteria. Prioritizing D2D transmissions over UL transmissions to serve URLLC users efficiently makes our flipped-underlay mechanism distinct from the existing solutions of underlay communication. In the system-level evaluation, we observed substantial resource savings in the industrial IoT scenario, thanks to the resource reuse enabled by our flipped-underlay scheme.

In this thesis, we targeted the application scenarios where URLLC will play a vital role in the digital evolution of connected-cars (V2X) and connected-factory (IIoT). Thus, our solution can be pronounced as cost-efficient, in which no additional infrastructure setup is required; rather, the existing devices in the environment, such as vehicles in V2X and automated guided vehicles (AGVs) in a factory, can be utilized to support flawless communications. The key value of our CoRe scheme is derived from the numerous available devices that elevate the degree of link diversity. The probability of finding suitable neighbor users who can assist the DL transmission is significantly high in these mesh networks. We conclude that our CoRe scheme is a prime mechanism for attaining ultra-high reliability at minimum latency constraints while improving resource-efficiency. Additionally, the flipped-underlay scheme should be applied to enable resource reuse for efficient management of resources and to increase the resource-efficiency even further, thus benefiting the overall network capacity.

Consequently, our CoRe scheme attains the following four-fold benefits for densely populated mesh networks:

1. Resource-efficient solution for URLLC fulfilling the target reliability of 99.999% within the latency budget of $1-10$ ms.
2. Reduced number of required retransmissions by virtue of D2D link diversity gains while maintaining the reliability and latency requirements for URLLC.
3. Benefits in terms of decreased transmit power consumption as a result of the optimal PC, in turn, allowing resource sharing among D2D and UL users.
4. Importantly, efficient resource usage enables considerable additional resource savings, thanks to the novel flipped-underlay scheme and FURA algorithm.

6.2 Future Work

The contributions of this thesis have focused mainly on developing a resource-efficient versatile solution for URLLC service aiming at evolutionary growth using wireless communication. In the following section, we present the future directions to extend this research. Our solution has shown to benefit from the link diversity gains offered by a large number of nodes in the vicinity, rendering independently fading D2D links. Our innovation on user cooperation via SL has gained increasing attention in the research community, and thus, we have paved the way towards 3GPP standardization for Release 18 and beyond. It can serve as a trigger for digitization and wireless connectivity in various sectors of industry.

Radio resource efficiency being the key objective, this thesis targeted densely populated mesh network scenarios where URLLC service is of prime importance, however extremely challenging. Our proposed *CoRe* scheme is a practical solution applicable to wide range of real world applications where a large number of devices can form a mesh network to create additional paths to any node in the network. A thorough investigation of CoRe has been performed, focusing on two prominent areas of applications: V2X and IIoT. The next leap of wireless communication is headed toward a connected intelligent system as the next generation - 6G is emerging. This new era is envisioned to bring further economic growth with special attention to societal sustainability for enhanced services and use cases well beyond what is supported by current systems. The demand for URLLC is escalating as we move to the next-generation use cases with its potential to revolutionize various industries. To name a few, real-time control, collaborative robots, extended reality, hologram telepresence, unmanned aerial vehicles (UAVs) in disaster response and rescue, telemedicine, public safety, and smart grid. We believe CoRe can be beneficially applied in most of these futuristic scenarios and a further use-case specific tailoring of CoRe for the above-mentioned use cases would enhance the utility for diverse industries. In particular, applications such as UAV-to-UAV for emergency drone fleets, delivery drones, and cooperative surveillance; satellite to device communication for enabling non-terrestrial networks (NTN) and mission critical applications; and extended reality (Augmented reality/virtual reality) for immersive learning, heathcare support and gaming.

In this thesis, we focus on the common low-mobility mesh network scenario keeping in mind the infamous use cases of V2X and industrial automation. Taking into account, in particular, the high-mobility use cases in V2X, this research can be further extended to manage the challenges due to the Doppler effect and fast channel aging. Nevertheless, the proposed CoRe solution can be well suited for high-mobility scenarios, provided that the cluster of neighboring users does not change too rapidly. However, advancements in the CoRe scheme can be deemed essential for certain high-mobility use cases causing frequent updates in the user clusters. As a future research direction, a practical performance evaluation of CoRe for a volatile high-mobility use case can be studied.

We target the issue of link blockage from the original DL transmission; therefore, the retransmissions from neighbors offering alternative paths to reach the target user are of utmost relevance. In the worst-case scenario, when none of the neighboring users can assist the unsuccessful DL transmission, traditional retransmissions via DL can still be employed as a fallback solution. Additionally, in scenarios where shadowing due to obstacles is minimal and the probability of link blockage is lower than densely cluttered environments, retransmissions via sidelink can complement the original DL HARQ retransmissions. Thus, a combined scheme enabling an optimal switching mechanism between DL HARQ retransmissions and HARQ retransmissions via D2D can be an effective approach for specific deployment scenarios.

Another research direction worth addressing for the advancement of CoRe is predictive modeling of the environment. One way to employ prediction models for CoRe is be to predict the constellation of users and potential obstacles that might block the communication link and interrupt URLLC traffic. The machine learning algorithms can be trained for diverse scenarios to make them robust for different use cases. This approach may ease the functioning of CoRe even in scenarios that experience frequent changes in the user constellations. Additionally, artificial intelligence (AI) can be extended across all edge devices and functions of CoRe enforcing built-in learning loops at different stages and uniformly throughout the CoRe system. Features such as obstacle detection, environment prediction, power allocation, user selection, group formation for cooperation and resource allocation, can lead to autonomously adaptive wireless system. With the growth in the field of AI, we can envision an autonomous CoRe framework by application of AI agents in the fundamental pillars of CoRe, end user devices, and the network entity. The benefits realized in this thesis, in terms of spectral efficiency and power savings, can serve as a motivation for future research on developing AI agents for CoRe.

From a practical and industrial standpoint, CoRe is applicable to diverse set of end devices such as mobile phones, AR/VR glasses, AGV, autonomous cars, UAVs, etc., and diverse applications. CoRe can be easily integrated with other advancing technologies such as sensor fusion using environmental sensors, LiDAR sensors, and cameras; forming a flexible autonomous system. Commercially, the spectral efficiency benefits provided by CoRe will be attractive to the wireless network operators while the power saving enhancements at the end devices will be essential to the device vendors. Although, establishing connected systems across various industries with integration of CoRe will require substantial capital investment, once deployed, these systems will be adaptive and flexible for future transitions and emerging technologies such as AI-native advancements. Wireless connectivity via CoRe solution calls for a long-term collaboration among different industry verticals to facilitate a fully functional end-to-end system. Along with the promising benefits of CoRe, its framework and central components can be adjusted and designed to accommodate varying levels of complexity tolerance, depending on the use cases and respective industries. Our findings presented in this thesis lay the foundation for future research on inter-vendor collaborations and corresponding performance anaylsis based on real-time measurements.

6G is expected to cross the boundaries and become an AI-native system that will provide enhanced user experience and sprectral efficiency. The configurable and adaptive properties of CoRe with low network dependencies in dense deployments makes it a prime candidate for future wireless technologies. We believe our CoRe model will serve as a baseline for future cooperative solutions and can be further enhanced with the growth of an AI-oriented approach.

List of Figures

List of Tables

Bibliography

[1] H. Friis. “A Note on a Simple Transmission Formula”. In: *Proceedings of the IRE* 34.5 (1946), pp. 254–256. DOI: 10.1109/JRPROC.1946.234568.

[2] E. C. van der Meulen. “THREE-TERMINAL COMMUNICATION CHANNELS”. In: *Advances in Applied Probability* 3 (1971), pp. 120–154.

[3] H. Burton and D. Sullivan. “Errors and error control”. In: *Proceedings of the IEEE* 60.11 (1972), pp. 1293–1301. DOI: 10.1109/PROC.1972.8897.

[4] T. Cover and A. Gamal. “Capacity theorems for the relay channel”. In: *IEEE Transactions on Information Theory* 25.5 (1979), pp. 572–584. DOI: 10.1109/TIT.1979.1056084.

[5] J. Winters. “On the Capacity of Radio Communication Systems with Diversity in a Rayleigh Fading Environment”. In: *IEEE Journal on Selected Areas in Communications* 5.5 (1987), pp. 871–878. DOI: 10.1109/JSAC.1987.1146600.

[6] G. J. Foschini. “Layered space-time architecture for wireless communication in a fading environment when using multi-element antennas”. In: *Bell Labs Technical Journal* 1.2 (1996), pp. 41–59. DOI: 10.1002/bltj.2015.

[7] S. Alamouti. “A simple transmit diversity technique for wireless communications”. In: *IEEE Journal on Selected Areas in Communications* 16.8 (1998), pp. 1451–1458. DOI: 10.1109/49.730453.

[8] M. Pätzold et al. “On the Statistical Properties of Deterministic Simulation Models for Mobile Fading Channels”. In: *Vehicular Technology, IEEE Transactions on* 47 (Mar. 1998), pp. 254–269. DOI: 10.1109/25.661052.

[9] B. Schein and R. Gallager. “The Gaussian parallel relay network”. In: *2000 IEEE International Symposium on Information Theory (Cat. No.00CH37060)*. 2000, pp. 22–. DOI: 10.1109/ISIT.2000.866312.

[10] A. Dammann and S. Kaiser. “Performance of low complex antenna diversity techniques for mobile OFDM systems”. In: *3rd Int. Workshop on Multi-Carrier Spread-Spectrum and Related Topics*. Sept. 2001.

[11] J. Laneman, G. Wornell, and D. Tse. “An efficient protocol for realizing cooperative diversity in wireless networks”. In: *Proceedings. 2001 IEEE International Symposium on Information Theory (IEEE Cat. No.01CH37252)*. 2001, pp. 294–. DOI: 10.1109/ISIT.2001.936157.

[12] A. Molisch, M. Win, and J. Winters. “Space-time-frequency (STF) coding for MIMO-OFDM systems”. In: *IEEE Communications Letters* 6.9 (2002), pp. 370–372. DOI: 10.1109/LCOMM.2002.802047.

[13] P. Gupta and P. Kumar. "Towards an information theory of large networks: an achievable rate region". In: *IEEE Transactions on Information Theory* 49.8 (2003), pp. 1877–1894. DOI: 10.1109/TIT.2003.814480.

[14] M. Hasna and M.-S. Alouini. "End-to-end performance of transmission systems with relays over Rayleigh-fading channels". In: *IEEE Transactions on Wireless Communications* 2.6 (2003), pp. 1126–1131. DOI: 10.1109/TWC.2003.819030.

[15] J. N. Laneman and G. W. Wornell. "Distributed space-time-coded protocols for exploiting cooperative diversity in wireless networks". In: *IEEE Transactions on Information Theory* 49.10 (Oct. 2003), pp. 2415–2425. ISSN: 0018-9448. DOI: 10.1109/TIT.2003.817829.

[16] J. Laneman, D. Tse, and G. Wornell. "Cooperative diversity in wireless networks: Efficient protocols and outage behavior". In: *IEEE Transactions on Information Theory* 50.12 (2004), pp. 3062–3080. DOI: 10.1109/TIT.2004.838089.

[17] A. PAULRAJ et al. "An overview of MIMO communications - a key to gigabit wireless". In: *Proceedings of the IEEE* 92.2 (2004), pp. 198–218. DOI: 10.1109/JPROC.2003.821915.

[18] P. Tarasak, H. Minn, and V. Bhargava. "Differential modulation for two-user cooperative diversity systems". In: *IEEE Global Telecommunications Conference, 2004. GLOBECOM '04.* Vol. 5. 2004, 3389–3393 Vol.5. DOI: 10.1109/GLOCOM.2004.1378977.

[19] A. Host-Madsen and J. Zhang. "Capacity bounds and power allocation for wireless relay channels". In: *IEEE Transactions on Information Theory* 51.6 (2005), pp. 2020–2040. DOI: 10.1109/TIT.2005.847703.

[20] J. Huang, R. Berry, and M. Honig. "Wireless scheduling with hybrid ARQ". In: *IEEE Transactions on Wireless Communications* 4.6 (2005), pp. 2801–2810. DOI: 10.1109/TWC.2005.858025.

[21] G. Kramer, M. Gastpar, and P. Gupta. "Cooperative strategies and capacity theorems for relay networks". In: *IEEE Transactions on Information Theory* 51.9 (2005), pp. 3037–3063. DOI: 10.1109/TIT.2005.853304.

[22] B. Zhao and M. Valenti. "Practical relay networks: a generalization of hybrid-ARQ". In: *IEEE Journal on Selected Areas in Communications* 23.1 (2005), pp. 7–18. DOI: 10.1109/JSAC.2004.837352.

[23] E. Beres and R. Adve. "On Selection Cooperation in Distributed Networks". In: *2006 40th Annual Conference on Information Sciences and Systems*. 2006, pp. 1056–1061. DOI: 10.1109/CISS.2006.286622.

[24] A. Bletsas et al. "A simple Cooperative diversity method based on network path selection". In: *IEEE Journal on Selected Areas in Communications* 24.3 (2006), pp. 659–672. DOI: 10.1109/JSAC.2005.862417.

[25] J.-F. Cheng. "Coding performance of hybrid ARQ schemes". In: *IEEE Transactions on Communications* 54.6 (2006), pp. 1017–1029. DOI: 10.1109/TCOMM.2006.876846.

[26] J.-T. Wang et al. "A general SFN structure with transmit diversity for TDS-OFDM system". In: *IEEE Transactions on Broadcasting* 52.2 (June 2006), pp. 245–251. ISSN: 0018-9316. DOI: 10.1109/TBC.2006.872988.

[27] S. Yiu, R. Schober, and L. Lampe. "Distributed space-time block coding". In: *IEEE Transactions on Communications* 54.7 (July 2006), pp. 1195–1206. ISSN: 0090-6778. DOI: 10.1109/TCOMM.2006.877947.

[28] A. Alimohammad et al. "A Compact and Accurate Gaussian Variate Generator". In: *IEEE Transactions on Very Large Scale Integration (VLSI) Systems* 16.5 (2008), pp. 517–527. DOI: 10.1109/TVLSI.2008.917552.

[29] A. Bletsas, A. Khisti, and M. Z. Win. "Opportunistic cooperative diversity with feedback and cheap radios". In: *IEEE Transactions on Wireless Communications* 7.5 (2008), pp. 1823–1827. DOI: 10.1109/TWC.2008.070193.

[30] M. Boussif et al. "Interference Based Power Control Performance in LTE Uplink". In: *2008 IEEE International Symposium on Wireless Communication Systems*. 2008, pp. 698–702. DOI: 10.1109/ISWCS.2008.4726146.

[31] A. E. Khandani et al. "Reliability and route diversity in wireless networks". In: *IEEE Transactions on Wireless Communications* 7.12 (2008), pp. 4772–4776. DOI: 10.1109/T-WC.2008.070770.

[32] P. Kyösti et al. "WINNER II channel models". In: *IST-4-027756 WINNER II D1.1.2 V1.2* (Feb. 2008).

[33] A. Simonsson and A. Furuskar. "Uplink Power Control in LTE - Overview and Performance, Subtitle: Principles and Benefits of Utilizing rather than Compensating for SINR Variations". In: *2008 IEEE 68th Vehicular Technology Conference*. 2008, pp. 1–5. DOI: 10.1109/VETECF.2008.317.

[34] R. Tannious and A. Nosratinia. "Spectrally-efficient relay selection with limited feedback". In: *IEEE Journal on Selected Areas in Communications* 26.8 (2008), pp. 1419–1428. DOI: 10.1109/JSAC.2008.081008.

[35] B. Blaszczyszyn, P. Mühlethaler, and Y. Toor. "Maximizing throughput of linear vehicular Ad-hoc NETworks (VANETs) — a stochastic approach". In: *2009 European Wireless Conference*. 2009, pp. 32–36. DOI: 10.1109/EW.2009.5358011.

[36] G. Boudreau et al. "Interference coordination and cancellation for 4G networks". In: *IEEE Communications Magazine* 47.4 (2009), pp. 74–81. DOI: 10.1109/MCOM.2009.4907410.

[37] K. Doppler et al. "Device-to-device communication as an underlay to LTE-advanced networks". In: *IEEE Communications Magazine* 47.12 (2009), pp. 42–49. DOI: 10.1109/MCOM.2009.5350367.

[38] C.-H. Yu et al. "On the Performance of Device-to-Device Underlay Communication with Simple Power Control". In: *VTC Spring 2009 - IEEE 69th Vehicular Technology Conference*. 2009, pp. 1–5. DOI: 10.1109/VETECS.2009.5073734.

[39] P. Heino et al. "CP5-026 WINNER+ D5.3 v1.0 WINNER+ Final Channel Models". In: (Jan. 2010).

[40] M. Zulhasnine, C. Huang, and A. Srinivasan. "Efficient resource allocation for device-to-device communication underlaying LTE network". In: *2010 IEEE 6th International Conference on Wireless and Mobile Computing, Networking and Communications*. 2010, pp. 368–375. DOI: 10.1109/WIMOB.2010.5645039.

[41] N. Baldo et al. "An open source product-oriented LTE network simulator based on ns-3". In: Oct. 2011, pp. 293–298. DOI: 10.1145/2068897.2068948.

[42] D. Lopez-Perez et al. “Enhanced intercell interference coordination challenges in heterogeneous networks”. In: *IEEE Wireless Communications* 18.3 (2011), pp. 22–30. DOI: 10.1109/MWC.2011.5876497.

[43] G. Piro, N. Baldo, and M. Miozzo. “An LTE module for the ns-3 network simulator”. In: *Proceedings of the 4th International ICST Conference on Simulation Tools and Techniques: March 2011* (Jan. 2011). DOI: 10.4108/icst.simutools.2011.245571.

[44] S. Prakash and I. McLoughlin. “Performance of Dual-Hop Multi-Antenna Systems with Fixed Gain Amplify-and-Forward Relay Selection”. In: *IEEE Transactions on Wireless Communications* 10.6 (2011), pp. 1709–1714. DOI: 10.1109/TWC.2011.040411.101415.

[45] D. Lee, G. Y. Li, and S. Tang. “Inter-cell interference coordination for LTE systems”. In: *2012 IEEE Global Communications Conference (GLOBECOM)*. 2012, pp. 4828–4833. DOI: 10.1109/GLOCOM.2012.6503883.

[46] Y. Wang, B. Soret, and K. I. Pedersen. “Sensitivity study of optimal eICIC configurations in different heterogeneous network scenarios”. In: *2012 IEEE International Conference on Communications (ICC)*. 2012, pp. 6792–6796. DOI: 10.1109/ICC.2012.6364885.

[47] Y. Wang and S. Venkatraman. “Uplink power control in LTE heterogeneous networks”. In: *2012 IEEE Globecom Workshops*. 2012, pp. 592–597. DOI: 10.1109/GLOCOMW.2012.6477640.

[48] S. Yiu et al. “Distributed STBC-OFDM and distributed SFBC-OFDM for frequency-selective and time-varying channels”. In: *2012 IEEE Wireless Communications and Networking Conference (WCNC)*. 2012, pp. 251–255. DOI: 10.1109/WCNC.2012.6214222.

[49] M. Mohammadi et al. “Performance Analysis of Generic Amplify-and-Forward Cooperative Networks over Asymmetric Fading Channels”. In: *Wireless Personal Communications* (Sept. 2013). DOI: 10.1007/s11277-013-1000-8.

[50] C. Phillips, D. Sicker, and D. Grunwald. “A Survey of Wireless Path Loss Prediction and Coverage Mapping Methods”. In: *IEEE Communications Surveys and Tutorials* 15.1 (2013), pp. 255–270. DOI: 10.1109/SURV.2012.022412.00172.

[51] B. Bojovic and N. Baldo. “A new channel and QoS aware scheduler to enhance the capacity of voice over LTE systems”. In: *2014 IEEE 11th International Multi-Conference on Systems, Signals Devices (SSD14)*. 2014, pp. 1–6.

[52] E. Dahlman et al. “5G wireless access: requirements and realization”. In: *IEEE Communications Magazine* 52.12 (2014), pp. 42–47. DOI: 10.1109/MCOM.2014.6979985.

[53] B. Soret et al. “Fundamental tradeoffs among reliability, latency and throughput in cellular networks”. In: *IEEE Globecom Workshops*. Dec. 2014. DOI: 10.1109/GLOCOMW.2014.7063628.

[54] J.-C. Guey et al. “On 5G radio access architecture and technology [Industry Perspectives]”. In: *IEEE Wireless Communications* 22.5 (2015), pp. 2–5. DOI: 10.1109/MWC.2015.7306369.

[55] ITU-R. *IMT Vision – Framework and overall objectives of the future development of IMT for 2020 and beyond*. M.2083-0. Sept. 2015.

[56] N. A. Johansson et al. "Radio access for ultra-reliable and low-latency 5G communications". In: *IEEE Int. Conference on Communications Workshops (ICC)*. June 2015, pp. 1184–1189. DOI: 10.1109/ICCW.2015.7247338.

[57] H. Shariatmadari, S. Iraji, and R. Jäntti. "Analysis of transmission methods for ultra-reliable communications". In: *2015 IEEE 26th Annual International Symposium on Personal, Indoor, and Mobile Radio Communications (PIMRC)*. 2015, pp. 2303–2308. DOI: 10.1109/PIMRC.2015.7343682.

[58] B. Soret et al. "Interference coordination for dense wireless networks". In: *IEEE Communications Magazine* 53.1 (2015), pp. 102–109. DOI: 10.1109/MCOM.2015.7010522.

[59] V. N. Swamy et al. "Cooperative communication for high-reliability low-latency wireless control". In: *2015 IEEE International Conference on Communications (ICC)*. 2015, pp. 4380–4386. DOI: 10.1109/ICC.2015.7249012.

[60] Y. Wu et al. "Optimal Power Control for Energy Efficient D2D Communication and Its Distributed Implementation". In: *IEEE Communications Letters* 19.5 (2015), pp. 815–818. DOI: 10.1109/LCOMM.2015.2407871.

[61] O. N. C. Yilmaz et al. "Analysis of ultra-reliable and low-latency 5G communication for a factory automation use case". In: *2015 IEEE International Conference on Communication Workshop (ICCW)*. 2015, pp. 1190–1195. DOI: 10.1109/ICCW.2015.7247339.

[62] M. Boban et al. "Design aspects for 5G V2X physical layer". In: *2016 IEEE Conference on Standards for Communications and Networking (CSCN)*. 2016, pp. 1–7. DOI: 10.1109/CSCN.2016.7785161.

[63] W. Cheng, X. Zhang, and H. Zhang. "Optimal Power Allocation With Statistical QoS Provisioning for D2D and Cellular Communications Over Underlaying Wireless Networks". In: *IEEE Journal on Selected Areas in Communications* 34.1 (2016), pp. 151–162. DOI: 10.1109/JSAC.2015.2476075.

[64] G. Durisi, T. Koch, and P. Popovski. "Toward Massive, Ultrareliable, and Low-Latency Wireless Communication With Short Packets". In: *Proceedings of the IEEE* 104.9 (2016), pp. 1711–1726. DOI: 10.1109/JPROC.2016.2537298.

[65] M. J. Farooq, H. ElSawy, and M.-S. Alouini. "A Stochastic Geometry Model for Multi-Hop Highway Vehicular Communication". In: *IEEE Transactions on Wireless Communications* 15.3 (2016), pp. 2276–2291. DOI: 10.1109/TWC.2015.2501817.

[66] Y. Gao, T. Yang, and B. Hu. "Improving the transmission reliability in smart factory through spatial diversity with ARQ". In: *2016 IEEE/CIC International Conference on Communications in China (ICCC)*. 2016, pp. 1–5. DOI: 10.1109/ICCChina.2016.7636856.

[67] S. R. Khosravirad et al. "Enhanced HARQ Design for 5G Wide Area Technology". In: *2016 IEEE 83rd Vehicular Technology Conference (VTC Spring)*. 2016, pp. 1–5. DOI: 10.1109/VTCSpring.2016.7504237.

[68] K. I. Pedersen et al. "A flexible 5G frame structure design for frequency-division duplex cases". In: *IEEE Communications Magazine* 54.3 (2016), pp. 53–59. DOI: 10.1109/MCOM.2016.7432148.

[69] B. Singh et al. “Ultra-reliable communication in a factory environment for 5G wireless networks: Link level and deployment study”. In: *2016 IEEE 27th Annual International Symposium on Personal, Indoor, and Mobile Radio Communications (PIMRC)*. 2016, pp. 1–5. DOI: 10.1109/PIMRC.2016.7794586.

[70] 3. G. P. P. (3GPP). *LTE: Service requirements for V2X services (Release 14)*. Technical Specification 22.185. Mar. 2017.

[71] 3GPP. *3GPP TSG RAN WG1: R1-1704170*. R1-1704170. Apr. 2017.

[72] A. Abdallah, M. M. Mansour, and A. Chehab. “A Distance-Based Power Control Scheme for D2D Communications Using Stochastic Geometry”. In: *2017 IEEE 86th Vehicular Technology Conference (VTC-Fall)*. 2017, pp. 1–6. DOI: 10.1109/VTCFall.2017.8288050.

[73] S. Ashraf et al. “From Radio Design to System Evaluations for Ultra-Reliable and Low-Latency Communication”. In: *European Wireless 2017; 23th European Wireless Conference*. 2017, pp. 1–8.

[74] B. Aygun et al. “Side-Link Assisted Hybrid Automatic Repeat Request for Ultra-Reliable Low Latency Communications”. In: *WSA 2017; 21th International ITG Workshop on Smart Antennas*. 2017, pp. 1–7.

[75] R. Chen and J. Xu. “Particle swarm optimization based power allocation for D2D underlaying cellular networks”. In: *2017 IEEE 17th International Conference on Communication Technology (ICCT)*. 2017, pp. 503–507. DOI: 10.1109/ICCT.2017.8359687.

[76] B. Di et al. “NOMA-Based Low-Latency and High-Reliable Broadcast Communications for 5G V2X Services”. In: *GLOBECOM 2017 - 2017 IEEE Global Communications Conference*. 2017, pp. 1–6. DOI: 10.1109/GLOCOM.2017.8254830.

[77] C.-P. Li et al. “5G ultra-reliable and low-latency systems design”. In: *2017 European Conference on Networks and Communications (EuCNC)*. June 2017, pp. 1–5. DOI: 10.1109/EuCNC.2017.7980747.

[78] I. Maskulainen et al. “Performance evaluation of adaptive beamforming in 5G-V2X networks”. In: *2017 European Conference on Networks and Communications (EuCNC)*. 2017, pp. 1–5. DOI: 10.1109/EuCNC.2017.7980728.

[79] R. Rouil et al. “Implementation and Validation of an LTE D2D Model for ns-3”. In: June 2017, pp. 55–62. DOI: 10.1145/3067665.3067668.

[80] B. Soret and K. I. Pedersen. “On-Demand Power Boost and Cell Muting for High Reliability and Low Latency in 5G”. In: *2017 IEEE 85th Vehicular Technology Conference (VTC Spring)*. 2017, pp. 1–5. DOI: 10.1109/VTCSpring.2017.8108592.

[81] Z. Wu, F. Zhao, and X. Liu. “Signal space diversity aided dynamic multiplexing for eMBB and URLLC traffics”. In: *2017 3rd IEEE International Conference on Computer and Communications (ICCC)*. 2017, pp. 1396–1400. DOI: 10.1109/CompComm.2017.8322772.

[82] A. Anand, G. De Veciana, and S. Shakkottai. “Joint Scheduling of URLLC and eMBB Traffic in 5G Wireless Networks”. In: *IEEE INFOCOM 2018 - IEEE Conference on Computer Communications*. 2018, pp. 1970–1978. DOI: 10.1109/INFOCOM.2018.8486430.

[83] L. Buccheri et al. "Hybrid retransmission scheme for QoS-defined 5G ultra-reliable low-latency communications". In: *2018 IEEE Wireless Communications and Networking Conference (WCNC)*. 2018, pp. 1–6. DOI: 10.1109/WCNC.2018.8377097.

[84] H. Ji et al. "Ultra-Reliable and Low-Latency Communications in 5G Downlink: Physical Layer Aspects". In: *IEEE Wireless Communications* 25.3 (June 2018), pp. 124–130. ISSN: 1536-1284. DOI: 10.1109/MWC.2018.1700294.

[85] A. Mukherjee. "Energy Efficiency and Delay in 5G Ultra-Reliable Low-Latency Communications System Architectures". In: *IEEE Network* 32.2 (2018), pp. 55–61. DOI: 10.1109/MNET.2018.1700260.

[86] G. Pocovi, K. I. Pedersen, and P. Mogensen. "Joint Link Adaptation and Scheduling for 5G Ultra-Reliable Low-Latency Communications". In: *IEEE Access* 6 (2018), pp. 28912–28922.

[87] P. Popovski et al. "Wireless Access for Ultra-Reliable Low-Latency Communication: Principles and Building Blocks". In: *IEEE Network* 32.2 (Mar. 2018), pp. 16–23. ISSN: 0890-8044. DOI: 10.1109/MNET.2018.1700258.

[88] J. Sachs et al. "5G Radio Network Design for Ultra-Reliable Low-Latency Communication". In: *IEEE Network* 32.2 (Mar. 2018), pp. 24–31. ISSN: 0890-8044. DOI: 10.1109/MNET.2018.1700232.

[89] S. A. A. Shah et al. "5G for Vehicular Communications". In: *IEEE Communications Magazine* 56.1 (Jan. 2018), pp. 111–117. ISSN: 0163-6804. DOI: 10.1109/MCOM.2018.1700467.

[90] T. Soni et al. "Adaptive numerology — A solution to address the demanding QoS in 5G-V2X". In: *2018 IEEE Wireless Communications and Networking Conference (WCNC)*. 2018, pp. 1–6. DOI: 10.1109/WCNC.2018.8377205.

[91] B. Soret et al. "Interference Coordination for 5G New Radio". In: *IEEE Wireless Communications* 25.3 (2018), pp. 131–137. DOI: 10.1109/MWC.2017.1600441.

[92] 3. G. P. P. (3GPP). *5G: Service requirements for next generation new services and markets (Release 15)*. Technical Specification 22.261. Mar. 2019.

[93] 5G-ACIA. *5G for Connected Industries and Automation (Second Edition)*. white Paper. 5G Alliance for Connected Industries and Automation, Feb. 2019.

[94] L. Han et al. "Power Control for Full-Duplex D2D Communications Underlaying Cellular Networks". In: *IEEE Access* 7 (2019), pp. 111858–111865. DOI: 10.1109/ACCESS.2019.2934479.

[95] I. A. Pastushok and N. A. Boikov. "Investigation of Methods for Multiplexing EMBB and URLLC Streams in a Downlink". In: *2019 Wave Electronics and its Application in Information and Telecommunication Systems (WECONF)*. 2019, pp. 1–4. DOI: 10.1109/WECONF.2019.8840593.

[96] M. Schellmann and T. Soni. "Ultra-reliable V2X communication: On the value of user cooperation in the sidelink". In: *2019 European Conference on Networks and Communications (EuCNC)*. 2019, pp. 570–574.

[97] J. Zhang et al. "Machine Learning Based Flexible Transmission Time Interval Scheduling for eMBB and uRLLC Coexistence Scenario". In: *IEEE Access* 7 (2019), pp. 65811–65820. DOI: 10.1109/ACCESS.2019.2917751.

[98] 3. G. P. P. (3GPP). *NR; NR and NG-RAN Overall Description (Release 17) Stage 2*. Technical Specification Group Radio Access Network TS 38.300. Mar. 2020.

[99] 3. G. P. P. (3GPP). *Study on channel model for frequencies from 0.5 to 100 GHz*. TR 38.901. Nov. 2020.

[100] E. Dosti et al. "Ultra Reliable Communication via Optimum Power Allocation for HARQ Retransmission Schemes". In: *IEEE Access* 8 (May 2020), pp. 1–1. DOI: 10.1109/ACCESS.2020.2994277.

[101] H. Dun, F. Ye, and S. Jiao. "A Noval Fast Resource Allocation Scheme for D2D-enabled Cellular Networks". In: *2020 IEEE USNC-CNC-URSI North American Radio Science Meeting (Joint with AP-S Symposium)*. 2020, pp. 91–92. DOI: 10.23919/USNC/URSI49741.2020.9321668.

[102] S. Gengtian et al. "Power Control Based on Multi-Agent Deep Q Network for D2D Communication". In: *2020 International Conference on Artificial Intelligence in Information and Communication (ICAIIC)*. 2020, pp. 257–261. DOI: 10.1109/ICAIIC48513.2020.9065192.

[103] S. Jahan, M. Amin, and M. Islam. "Cooperative Relayed Network under Rayleigh and Nakagami-m Fading Channel". In: *International Journal of Computer Science and Information Security,* 17 (Mar. 2020), pp. 101–108.

[104] C. I. Nwakanma et al. "3GPP Release-16 for Industrial Internet of Things and Mission Critical Communications". In: *2020 International Conference on Information and Communication Technology Convergence (ICTC)*. 2020, pp. 403–406. DOI: 10.1109/ICTC49870.2020.9289520.

[105] Rashmi and P. Kumar. "A new pairing scheme for D2D with cellular users in underlay spectrum sharing". In: *2020 5th International Conference on Computing, Communication and Security (ICCCS)*. 2020, pp. 1–5. DOI: 10.1109/ICCCS49678.2020.9277500.

[106] A. M. Alba, S. Janardhanan, and W. Kellerer. "Enabling Dynamically Centralized RAN Architectures in 5G and Beyond". In: *IEEE Transactions on Network and Service Management* 18.3 (2021), pp. 3509–3526. DOI: 10.1109/TNSM.2021.3071975.

[107] G. Ghatak. "Cooperative Relaying for URLLC in V2X Networks". In: *IEEE Wireless Communications Letters* 10.1 (2021), pp. 97–101. DOI: 10.1109/LWC.2020.3021505.

[108] J. Kilpi, H. Kokkoniemi-Tarkkanen, and M. A. Uusitalo. "Efficient method to validate high reliability of 5G URLLC". In: *2021 IEEE 93rd Vehicular Technology Conference (VTC2021-Spring)*. 2021, pp. 1–6. DOI: 10.1109/VTC2021-Spring51267.2021.9448734.

[109] M. U. A. Siddiqui et al. "Interference Management in 5G and Beyond Network: Requirements, Challenges and Future Directions". In: *IEEE Access* 9 (2021), pp. 68932–68965. DOI: 10.1109/ACCESS.2021.3073543.

[110] T. Soni, M. Schellmann, and A. Knoll. "Sidelink-Assisted URLLC Built on Cooperative Retransmissions With Optimum Power Control". In: *2021 IEEE 32nd Annual International Symposium on Personal, Indoor and Mobile Radio Communications (PIMRC)*. 2021, pp. 1–6. DOI: 10.1109/PIMRC50174.2021.9569334.

[111] W. Sui et al. "Energy-Efficient Resource Allocation With Flexible Frame Structure for Hybrid eMBB and URLLC Services". In: *IEEE Transactions on Green Communications and Networking* 5.1 (2021), pp. 72–83. DOI: 10.1109/TGCN.2020.3028202.

[112] H. Yin, L. Zhang, and S. Roy. "Multiplexing URLLC Traffic Within eMBB Services in 5G NR: Fair Scheduling". In: *IEEE Transactions on Communications* 69.2 (2021), pp. 1080–1093. DOI: 10.1109/TCOMM.2020.3035582.

[113] Y. Prathyusha and T.-L. Sheu. "Coordinated Resource Allocations for eMBB and URLLC in 5G Communication Networks". In: *IEEE Transactions on Vehicular Technology* 71.8 (2022), pp. 8717–8728. DOI: 10.1109/TVT.2022.3176018.

[114] J. Zhang et al. "Intelligent Ultrareliable and Low-Latency Communications: Flexibility and Adaptation". In: *IEEE Internet of Things Journal* 9.17 (2022), pp. 16140–16153. DOI: 10.1109/JIOT.2022.3150490.

[115] 3. G. P. P. (3GPP). *Evolved Universal Terrestrial Radio Access (E-UTRA) and Evolved Universal Terrestrial Radio Access Network (E-UTRAN) Overall description (Release 17) Stage 2*. Technical Specification Group Radio Access Network TS 36.300. Mar. 2023.

[116] T. Soni, M. Schellmann, and A. C. Knoll. "Flipped-Underlay in Power-Efficient Industrial IoT Sidelink-Assisted Communication". In: *IEEE Access* 11 (2023), pp. 134166–134182. DOI: 10.1109/ACCESS.2023.3336409.

[117] 3GPP. *Study on Communication for Automation in Vertical Domains (Release 16)*. Technical Report (TS) 22.804. Version 16.2.0. 3rd Generation Partnership Project (3GPP).

[118] *Infrastructure - ISO 9001/AS9100*. https://www.isaregistrar.com/7-1-3-planning-of-changes-iso-9001-as9100/. Accessed: 2023-08-06.

[119] *Quadriga: The next generation radio channel model*. http://www.quadriga-channel-model.de. Accessed: 2023-08-06.

[120] *V2X in the Connected Car of the Future, 2018*. https://www.qorvo.com/design-hub/blog/v2x-in-the-connected-car-of-the-future. Accessed: 2023-08-06.